Identification of Novel Drug Combinations for Haematological Malignancies

---

A thesis submitted to the National University of Ireland in fulfilment of the requirement for the degree of

Doctor of Philosophy

by

Mairéad Reidy

School of Natural Sciences, National University of Ireland Galway

Thesis Supervisors:

Dr. Eva Szegezdi, Prof. Afshin Samali and Dr.Adrienne Gorman

This work is dedicated in the loving memory of my dearest grandmothers Ann and Mary.

Table of Contents

Abbreviations

7-AAD	7-aminoactinomycin D
8-OH-DPAT	8-Hydroxy-DPAT
ABC	Activated B Cell
AML	Acute Myeloid Leukaemia
ATF4	Activating Transcription Factor 4
ATP	Adenosine Triphosphate
Bcl-2	B-cell lymphoma-2
BH	Bcl-2 homology
BM	Bone Marrow
CAND1	Cullin Associated and Neddylation Dissociated 1
CARD	Caspase Recruitment Domain
c-C3	Cleaved Caspase 3
c/EBPα	CCAAT/enhancer-binding protein alpha
CI	Combination Index
cIAP	cellular IAP
CLP	Common Lymphoid Progenitor
CN	Cytogenetically Normal
CMP	Common Myeloid Progenitors

Abbreviations

CRL	Cullin Ring Ligase
CSN	COP9 Signalosome
DAPK1	Death-associated protein kinase 1
DD	Death Domains
DED	Death Effector Domain
DISC	Death Inducing Signalling Complex
DLBCL	Diffuse Large B Cell Lymphoma
DR3	Death Receptor 3
DUB	Deubiquitinating enzymes
E6-AP	E6-associated protein
EDAR	Ectodysplasin A Receptor
ELISA	Enzyme-linked immunosorbent assay
ERAD	Endoplasmic Reticulum-Associated Degradation
ERK	Extracellular Regulated Kinase
ETP	Early T Lineage
FADD	Fas-associated Death Domain
FLT3-ITD	Fms-related tyrosine kinase 3-Internal Tandem Duplications
GC	Germinal Centre
GMP	Granulocyte-Macrophage Progenitors

HECT	Homologous to the E6-AP Carboxyl Terminus
HSC	Hematopoietic Stem Cell
IAP	Inhibitor of Apoptosis Protein
IkBs	Inhibitor of Kappa B
IP	Intraperitoneal
JNK	Jun NH2 terminal kinases
LIC	Leukemic Initiating Cell
LSC	Leukemic Stem Cell
MAPK	Mitogen Activated Protein Kinase
MEP	Megakaryocyte Erythrocyte Progenitors
MDS	Myelodysplastic Syndrome
MGUS	Monoclonal Gammopathy of Undetermined Significance
MM	Multiple Myeloma
MPD	Myeloproliferative Disease
NAE	NEDD8 Activating Enzyme
NEDD8	Neural precursor cell expressed, developmentally down-regulated 8
NF-κB	Nuclear factor kappa-light-chain-enhancer of activated B cells
NHL	Non-Hodgkins Lymphoma
NPM	Nucleophosmin

Nrf2	Nuclear factor-like 2
OPG	Osteoprotegerin
PARP	Poly (ADP-ribose) polymerase
PB	Peripheal Blood
RING	Really Interesting New Gene
SC	Subcutaneous
SCF	SKP1, Cul1, and F-box
SCID	Severe combined immunodeficiency
SIM	Substrate Interacting Motif
SMAC	Second Mitochondrial Activator of Caspases
SUMO	Small Ubiquitin-like Modifier
TMRE	Tetramethylrhodamine ethyl ester
TNF	Tumour Necrosis Factor
TNFR1	TNF receptor 1
TRADD	TNFR-associated Death Domain
TRAIL	TNF-related apoptosis-inducing ligand
TRAILR1	TNF-related apoptosis-inducing ligand receptor 1
UAE	Ubiquitin Activating Enzyme
Ub	Ubiquitin

Abbreviations

UBC	Ubiquitin Conjugating Catalytic
UBL	Ubiquitin-like protein
UPS	Ubiquitin Proteasome System
XIAP	X-linked Inhiitor of Apoptosis
WHO	World Health Organisation

Declaration of Author

The work presented in Chapter 3 was in collaboration with the group of Prof. Paul Murphy at NUIG. The compounds were generated within this group. In addition the data generated for Table 3.1 was by this group. The remainder of the work, including all of the figures in this chapter were completed by myself.

The *in vivo* work presented in Chapter 4 was done in part with a collaboration with Millennium Pharmaceuticals. All *in vivo* work was carried out at Millennium Pharmaceuticals. Raw data and samples were delivered to us for analysis by western blotting and ELISA. (Exception: Figure 3.9 (C) – MLN4924 ELISA which was carried out by Millennium Pharmaceuticals).

Abstract

TNF-related apoptosis ligand (TRAIL) is a tumour selective cytokine with potential anti-cancer activity which is currently in clinical trials. Haematological malignancies along with several other cancers have showed varied sensitivity to TRAIL treatment. In vitro and in vivo studies have shown that TRAIL-resistant tumour cells can be sensitised to TRAIL by various chemotherapeutic agents. This has opened up new possibilities for combination therapies. Proteasome inhibitors have previously been used in this way.

MLN4924 is an investigational inhibitor of NEDD8 activating enzyme (NAE), which is part of the ubiquitin proteasome pathway. MLN4924 is currently in Phase 1 trials (Millennium Pharmaceuticals, Inc.). MLN4924 binds to NAE and forms an MLN4924-NEDD8 adduct in place of an NEDD8 adenylate thus locking the enzyme in an inactive state. As a consequence, MLN4924 inhibits the NEDD8-dependent activation of a subset of ubiquitin E3 ligases known as cullin ring ligases (CRLs). When CRL neddylation is disrupted, so is the ubiquitin-dependent turnover of CRL substrates, many of which have important roles in cellular processes associated with cancer cell growth and survival pathways including DNA replication and NFkB activity. Targeting the activity of a specific subset of E3 ligases is particularly attractive because there is the potential to selectively block the degradation of certain cellular proteins and possibly avoid unwanted effects on other proteins.

We sought to investigate the apoptotic effect MLN4924 in combination with TRAIL may have in multiple myeloma (MM), acute myeloid leukaemia (AML), and diffuse large B cell lymphoma (DLBCL) cell lines.

It emerged that MLN4924 and TRAIL have a synergistic effect in a number of AML and MM cell lines. Examples of combination index values obtained for these cell lines include AML2-0.07; MOLM13-0.69; ML1-0.55.

In an attempt to identify the mechanism of action we found that MLN4924 induces the expression of Bim and Noxa, pro-apoptotic, BH3-only members of the Bcl-2 protein family. MLN4924 did not significantly affect the expression of apoptotic regulators acting at the TRAIL death receptors, including c-FLIP, pro-caspase-8, cIAP1/2, DR4, DR5,

DcR1 or DcR2. Through study of the known transcription factors regulated after MLN4924 treatment, it was found that treatment with MLN4924 led to the induction of p53 and C/EBPα in OCI AML2 cells. Inhibition of p53 action with Nutlin3 could sensitise the AML cells to TRAIL-induced apoptosis. Silencing of c/EBPα partly reversed the synergism observed between MLN4924 and TRAIL thus identifying it as a key player in the mechanism of sensitisation in OCI AML2 cells. In addition we have observed that p53 and c/EBPα most likely behave in a feedback loop fashion.

OCI-M2 xenografts treated with a biweekly dose of MLN4924 (on days 1 and 4, each week for 3 weeks) combined with daily dosage of recombinant human TRAIL (days 1-5 each week for 3 weeks) resulted in very significant reduction in tumour volume.

In conclusion, this study shows that MLN4924 can sensitise AML and potentially MM cells to TRAIL induced apoptosis to trigger very robust anti-tumour effects by increasing c/EBPα and p53 levels.

An additional study (Chapter 4) focused on examining the apoptotic effect of a novel compound on AML cells. This compound was generated by the chemistry department at NUIG. It induces apoptosis in AML cells whilst sparing normal cells. We have identified the serotonin receptors as a possible mechanism through which this compound can induce apoptosis.

Chapter 1

Introduction

General Introduction

Cancer cells depend on signals that can promote cell cycle progression. The ubiquitin proteasome system plays a pivotal role in controlling the sequence of events of cell division. Cancer cells also depend on signals which can prevent programmed cell death. Programmed cell death would occur otherwise in response to cumulative, aberrant stress. Both of these are regulated by the ubiquitin proteasome system. This makes this pathway a potential and explorable pathway for therapeutic intervention. This chapter discusses this in relation to haematological malignancies as they have high ubiquitinitation activity.

1.1 Haematological Malignancies

The haematological malignancies are a diverse group of neoplastic diseases. They are tumours which affect the blood, bone marrow and lymph nodes. They currently represent the fifth most common cancer in the UK (Gounaris-Shannon and Chevassut 2013).

The classification system of haematological cancers has changed a lot over the years. It has moved from a system being based mainly on morphology to a system based on clinical features, morphology, immunophenotyping and molecular genetic data. The current classification system is known as the World Health Organisation (WHO) Classification. It was established in 2001 and was again revised in 2008. Haematological malignancies can be broadly divided into one of three categories – i) myeloid neoplasms, ii) aggressive B cell lymphomas and iii) plasma cell neoplasms. The WHO classification places a large emphasis on cell lineage. Haematological malignancies can arise from a myeloid or a lymphoid origin which are generated from hematopoietic stem cells (Kondo, 2010). These two lineages are separable at the progenitor level (Figure 1.1). Common lymphoid progenitors (CLPs) can differentiate into T, B and natural killer (NK), cells whereas common myeloid progenitors (CMPs) can differentiate into erythrocytes, granulocytes, megakaryocytes (precursors of platelets) and macrophages (Laiosa, Stadtfeld et al. 2006) . Haematological malignancies commonly associated with the myeloid lineage include acute myeloid

leukaemia (AML) and chronic myeloid leukaemia (CML). On the other hand, malignancies associated with the lymphoid lineage include lymphomas, myeloma and lymphocytic leukaemia.

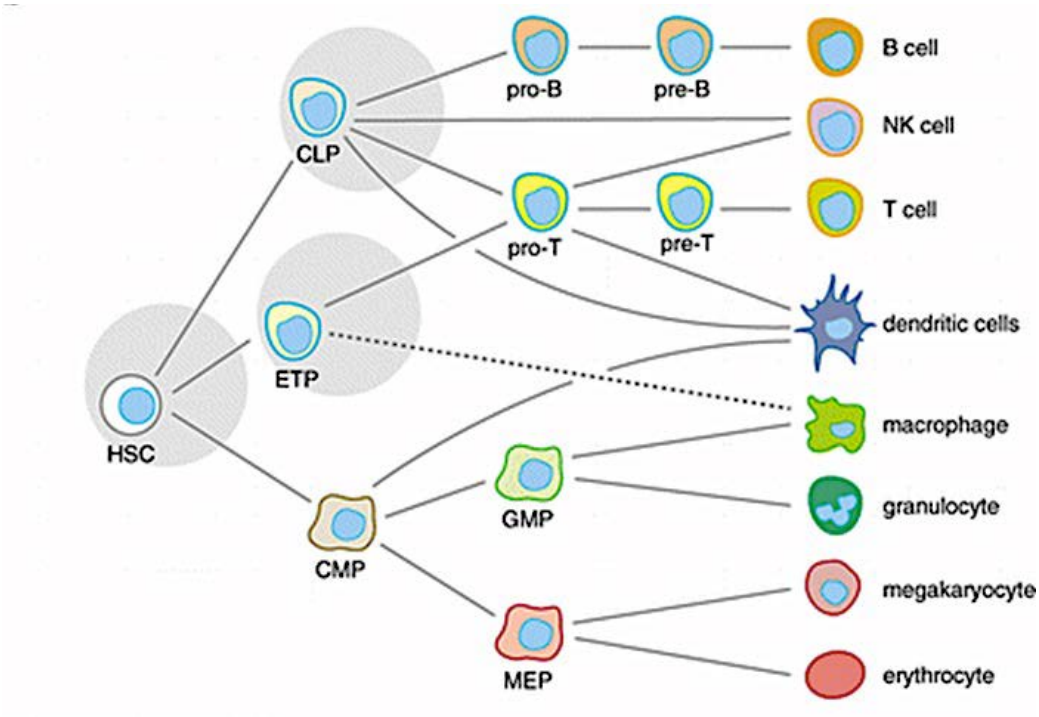

Figure 1.1 **Cell lineages derived from hematopoietic stem cells (HSCs)** (Laiosa, Stadtfeld et al. 2006)

Lineage tree showing areas where branching can occur. HSCs can differentiate into common lymphoid progenitors (CLPs), early T lineage progenitors (ETPs) and common myeloid progenitors (CMPs). CLPs and ETPs give rise to early B and T cells respectively which can then differentiate further into more cells. CMPs give rise to two more progenitors – granulocyte-macrophage progenitors (GMPs) and megakaryocyte-erythrocyte progenitors (MEPs) generating GM and MegE cells respectively.

For the purpose of this thesis only those malignancies that are relevant to work discussed later will be mentioned here. These include AML, multiple myeloma (MM) and diffuse large B cell lymphomas (DLBCL).

1.1.1 Acute Myeloid Leukaemia

AML is the most common acute leukaemia in adults. AML is a cancer of the myeloid lineage where leukaemic cells or 'blasts' are unable to differentiate beyond a certain stage of differentiation. This results in malignant clonal proliferation of these undifferentiated cells in the bone marrow and peripheral blood. These cells exhibit a severe block in their ability to differentiate into mature granulocytes or macrophages (Conway O'Brien, Prideaux et al. 2014).

The current five-year survival rates of patients under age 60 who receive intensive chemotherapy for AML range from 30% to over 40%. Older patients with AML who receive intensive chemotherapy have a notably worse prognosis; with a 5-year survival rate of about 15%. There are several reasons for this. Cytotoxic drug toxicity is increased in the elderly. In addition, older patients more commonly have particular risk factors for a bad outcome, including poor risk cytogenetic abnormalities and overexpression of genes associated with drug resistance. Aside from all of these factors, age itself is an independent prognostic factor in AML (Krug et al, 2011).

AML is frequently associated with chromosomal translocations which results in loss of function mutations in transcription factors required for normal hematopoietic development. This results in fusion proteins that include AML1/ETO (t{8;21}), CBFβ/SMMHC (inv{16}) and TEL/AML1 (t{12;21}) (Keeshan, 2006}. Mutations in transcription factors such as PU.1, c/EBPα, AML1 and GATA-1 are also associated with AML, as are other types of oncogenic perturbations that lead to functional inactivation of critical transcription factors. Recurrent involvement of a limited set of transcription factors suggests that disruption of these genes is rate limiting for leukemia development (Keeshan, 2006).

Loss of function mutations in transcription factors is not sufficient to cause AML. Evidence indicates that activating mutations in the hematopoietic tyrosine kinases FMS-like tyrosine kinase-3 (FLT3) and c-KIT, and in N-RAS and K-RAS, confer proliferative advantage to hematopoietic progenitors and cooperate with loss-of-function mutations in hematopoietic transcription factors to cause an AML phenotype (Kelly, 2002}.

Myeloproliferative disease (MPD) and myelodysplastic syndrome (MDS) are also classed as myeloid cancers and have the potential to transform into AML. MPD is characterized as a chronic leukaemia with mature cells in both the peripheral blood and the bone marrow. MDS has one or more cytopenias in the peripheral blood (Sheehan, 2011, Chevassut et al, 2014).

The outcome of patients diagnosed with AML is dismal with an overall survival rate of approximately 25%. Many patients with AML are classed into low, intermediate or high risk groups based on cytogenetic information. However, nearly half of all AML patients are cytogenetically normal (CN). Deregulated transcriptional pathways feature prominently in the genetic etiology of AML. Pharmacological targeting of transcriptional regulatory proteins represents a validated approach for undermining the driver oncogenes in AML.

The additional use of molecular mutational analysis is now being used to direct therapy and these molecular features are also being used as a target for a new generation of small molecule inhibitors (Burnett, Wetzler et al. 2011).

Current treatments for AML usually involve chemotherapy alongside an anthracycline/cytarabine combination (Roboz, Wissa et al. 2012). Treatments have changed little over the past few decades and it is thought that a combination of chemotherapeutics with molecular targeted agents holds a lot of promise for the future of AML.

Compounds containing macrocyclic ring structures are capable of extremely potent biological activity and specificity. This can be clearly illustrated by the exquisite biological activity of many macrocyclic natural products that has been harnessed by medicinal chemists to provide chemotherapy for a broad range of conditions. Currently macrocyclic structures account for over 100 approved drugs covering examples of antibiotic, immunosuppressant and anticancerchemotherapeutics.

There are a number of ways that structural diversity can be incorporated into a compound collection; however, variation of the molecular scaffold is widely thought to be the most important. Compounds based on macrocyclic scaffolds are underrepresented in screening collections and consequently not sufficiently investigated to date in drug discovery or chemical biology. In chapter 4 we investigate

the effect of macrocyclic compounds in haematological malignant cell lines, particularly in AML.

1.1.2 Multiple Myeloma

MM is of lymphoid origin. It is a B-cell malignancy characterised by a monoclonal expansion and accumulation of abnormal plasma cells in the bone marrow (Dimopoulos and Terpos 2010). Myeloma comprises approximately 1% of all cancers. It is the second most common haematological malignancy after lymphomas.

The myeloma cell is a long-lived plasma cell, which has been exposed to antigen having undergone the B-cell maturation processes. Maturation of normal B-cell precursors to mature plasma cells involves rearrangement of the Ig genes with subsequent somatic mutation of the variable (V) region {Dimopoulos, 2010}. A myeloma protein is an abnormal antibody fragment that is produced in excess by these abnormal plasma cells. This protein is commonly referred to as an M protein. A hallmark of multiple myeloma is high levels of this protein in the blood.

In almost all cases multiple myeloma can be preceded by monoclonal gammopathy of undetermined significance (MGUS). MGUS is characterised by an abnormal level of M protein in the blood. MGUS is associated with a lifelong risk of progression to multiple myeloma or related disorders. The rate of progression of MGUS to MM or related malignancy is 1% per year {Rajkumar, 2006}.

Interaction between the bone marrow microenvironment and myeloma cells is essential for myeloma cell survival. Advances have been made in understanding the biology of MM through the study of the bone marrow microenvironment. Indeed, the bone marrow niche appears to play an important role in differentiation, migration, proliferation, survival, and drug resistance of the malignant plasma cells providing the preclinical evidences for targeting MM cells and bone marrow stromal cells (BMSC) as an antitumor strategy in this disease {Manier, 2012}.

Patients can have asymptomatic myeloma and remain stable for a long time without any treatment. Only symptomatic MM is treated. Two classes of drugs form the backbone of how MM is treated. The first of these classes is proteasome inhibitors.

These include bortezomib (Velcade), which can bind the 26S proteasome preventing protein degradation, and Carfilzomib (Kyprolis) which binds the 26S proteasome more selectively than Bortezomib. To date Carfilzomib has been reported to have an improved safety profile over Bortezomib. The second class of drugs is immunomodulatory drugs. The best known of these is Thalidomide which can cause cell cycle arrest and induce apoptosis (Katsnelson, 2012).

Although treatments in MM have improved the malignancy remains largely resistant (de la Puente, Muz et al. 2014). A recent study that involved parallel sequencing of paired tumour/normal samples on 203 MM patients identified significantly mutated genes and copy number alteration and discovered putative tumour suppressor genes. Frequent mutations were discovered in KRAS, NRAS, BRAF, TP53, FAM46C and DIS3 (Lohr, Stojanov et al. 2014). Multiple mutations were found within the same pathway and mutations were also found to exist in subclonal populations. Therefore therapy targeting a mutation that is only present in a certain population of cells will lead to limited clinical benefit. This highlights the need for a more effective therapy which could include combination treatments.

1.1.3 Diffuse Large B cell Lymphoma (DLBCL)

Diffuse Large B Cell Lymphoma (DLBCL) is the most common lymphoid malignancy in adults. It accounts for 31% of all Non-Hodgkins Lymphoma (NHL) in western countries. DLBCL is characterised by large cells with vesicular nuclei, prominent nucleoli, basophilic cytoplasm and usually a high proliferation rate (Martelli, Ferreri et al. 2013). DLBCL derives from a mature B cell that has experienced the germinal centre (GC) reaction. Germinal centres are sites within lymph nodes where mature B lymphocytes rapidly proliferate, differentiate and mutate their antibodies. DLBCLs have been divided into subgroups based on cells of origin. Activated B cell-like (ABC)-DLBCL arise from post-germinal centre B cells that are arrested during plasmablastic differentiation. These tumours downregulate the GC-specific program, concomitant with activation of NF-κB and BCR signaling pathways, and upregulate genes required for plasma cell differentiation (Pasqualucci and Dalla-Favera 2014).

DLBCL is curable even in advanced stages, however one-third of patients do not achieve cure with initial therapy (Wilson et al, 2014). Some mutational changes such as bcl-6, bcl-2, p53 and c-myc are associated with poor outcomes (Briere et al, 2013). The standard treatment of DLBCL is rituximab, cyclophosphamide, doxorubicin, vincristine and prednisone (R-CHOP) (Cultrera and Dalia 2012).

1.2 Ubiquitin Proteasome System

The level of proteins in cells are determined not only by rate of synthesis but also by rate of degradation. The degradation of proteins is widely varied. Different rates of protein degradation are an important aspect of cell regulation. Many rapidly degraded proteins function as regulatory molecules, such as transcription factors. The rapid turnover of these proteins is necessary to allow their levels to change quickly in response to external stimuli. Faulty or damaged proteins are recognized and rapidly degraded within cells, thereby eliminating the consequences of mistakes made during protein synthesis. Two major pathways mediate protein degradation - the ubiquitin-proteasome pathway and lysosomal proteolysis.

Lysosomal proteolysis involves the uptake of proteins into the lysosome by endocytosis where they are degraded. The lysosome contains a number of digestive enzymes including several proteases {Lecker, 2006}. Some proteins are degraded in the lysosome after being engulfed in autophagic vacuoles that fuse with lysosomes.

The major pathway of degradation, the ubiquitin proteasome system (UPS) is responsible for the regulated degradation of intracellular proteins with important roles in a broad array of cellular functions. Among UPS substrates are proteins involved in cell cycle regulation, cellular growth and proliferation, intracellular signalling, DNA repair, membrane receptor regulation, and pro-apoptotic and anti-apoptotic signalling (Soucy, Dick et al. 2010). Balanced protein synthesis and degradation maintain normal healthy cellular function and failure to maintain protein homeostasis within the cell can lead to unrestrained cellular proliferation and/or failure to undergo programmed cell death, which can lead to the development of cancer and other diseases (Sarikas, Hartmann et al. 2011).

Approximately 80% of intracellular proteins are processed by the UPS (Crawford and Irvine 2013). The UPS is a selective pathway in which a substrate is first tagged with a

chain of ubiquitin and the resulting modified protein is then recognised by the 26S proteasome, where proteolysis of the protein takes place (Sarikas, Hartmann et al. 2011).

1.2.1 Ubiquitin

Ubiquitin itself is a highly stable, 76 amino acid protein which is highly conserved (Figure 1.2). Ubiquitin forms a compact globular structure with an exposed C- terminal tail that can be covalently linked to other proteins (Husnjak and Dikic 2012). The linkage of ubiquitin to the target protein, or itself, is through a bond between the carboxyl-terminal glycine on ubiquitin and an internal lysine on the substrate (Wang and Maldonado 2006). Molecules other than ubiquitin have been identified to confer similar modes of functional protein modification and are referred to as ubiquitin-like proteins {Herrmann, 2007}. These include, for example, NEDD8 and SUMO. This will be discussed in more detail further on in Section 1.2.

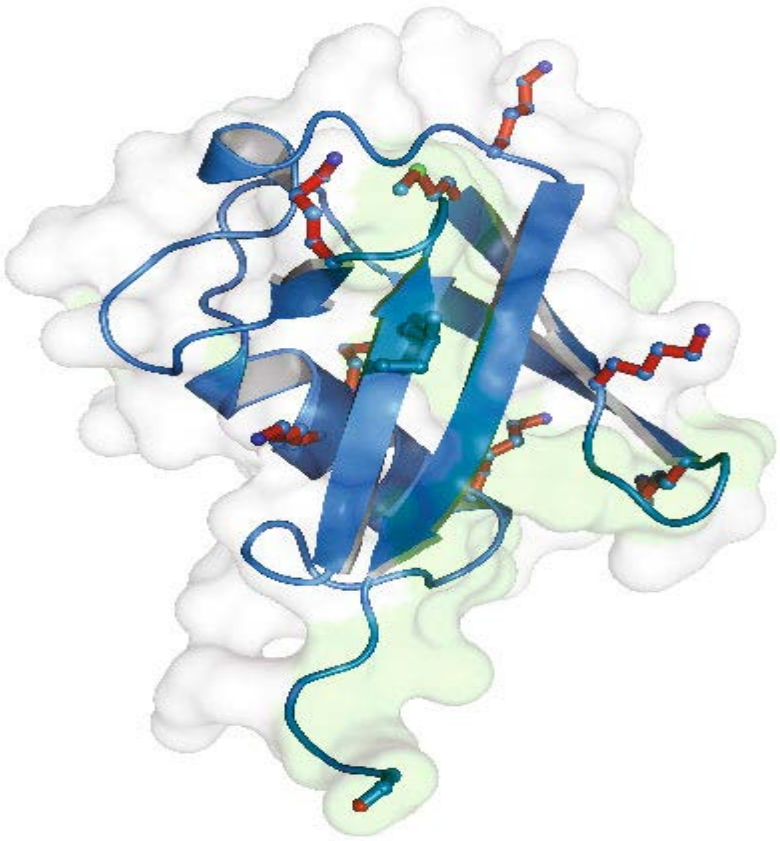

Figure 1.2 **The structure of ubiquitin (Dikic and Robertson 2012)**

Ubiquitin is a small, compact protein. The seven lysines that can be linked to the terminal glycine of another ubiquitin molecule to form poly-ubiquitin chains are coloured red. The green shading indicates the hydrophobic patch through which ubiquitin interacts with specific ubiquitin-binding proteins.

Ubiquitin contains seven different acceptor lysine residues: K6, K11, K27, K29, K33, K48 and K63. All of these can be conjugated to another ubiquitin to form a polyubiquitination chain. Polyubiquitin chains synthesised through different lysine linkages gives rise to ubiquitin chains of different topologies, lengths and functional outcomes (Hoeller and Dikic 2009). The ability to generate diverse substrate-ubiquitin structures is important for targeting proteins to different fates as outlined in Figure 1.3. For example, K48 and K11 linked polyubiquitin chains usually target proteins for proteasomal degradation, whereas K63 polyubiquitin chains and monoubiquitination regulate cellular functions such as protein kinase activation, gene expression, DNA repair, membrane trafficking and chromatin remodelling, largely through proteasome-independent mechanisms (Wu, Liu et al. 2012).

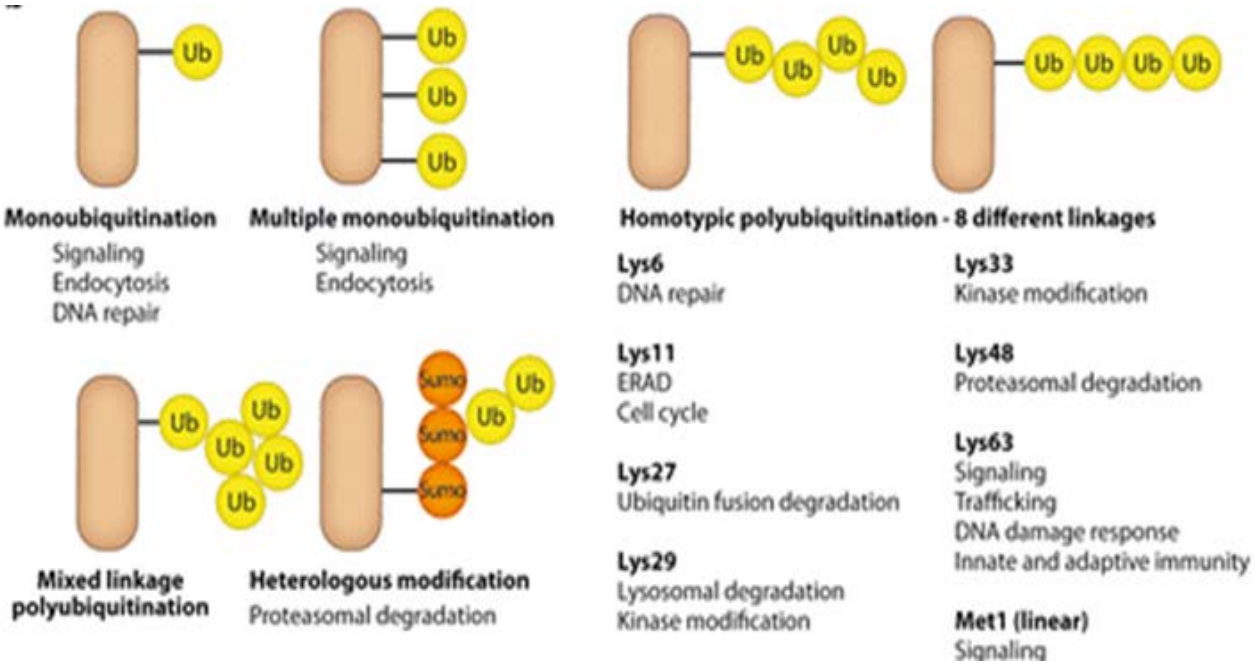

Figure 1.3 **Different modes of ubiquitination lead to different substrate fates (Dikic et al, 2012)**

The versatility of ubiquitin in regulating different processes is derived from its ability to be conjugated as a monomer on one (monoubiquitination) or more substrate lysines (multiubiquitination) or as a polymer (polyubiquitination) by the addition of ubiquitins to each other through lysine residues.
Abbreviations: ERAD, endoplasmicreticulum-associated degradation; SUMO, small ubiquitin-like modifier (Sadowski and Sarcevic 2010; Dikic and Robertson 2012).

The process of protein degradation by the UPS involves two successive steps. The first step being ubiquitination which involves the attachment of ubiquitin to the substrate targeting it for degradation and the second step involves proteasomal degradation by the proteasome. Both steps are described below.

1.2.2 Ubiquitination

The attachment of ubiquitin to a substrate requires the consecutive actions of three classes of enzymes, a process referred to as ubiquitination. Ubiquitin can be covalently attached to target proteins as a single moiety (monoubiquitin), as multiple single moieties (multiple monoubiquitin), as chains coupled through the same lysine residue in ubiquitin (homotypic polyubiquitin), as mixed chains linked through different lysine

residues in ubiquitin (branched polyubiquitin) or as head-to-tail bound ubiquitin moieties (linear polyubiquitin) {Dikic, 2009}.

The first step in ubiquitination involves the activation of ubiquitin by E1 enzymes. There are only two known human E1 enzymes, UBE1, the primary E1 in eukaryotes and the more recently described UBE1L2 (Stintzing and Lenz 2014). The ubiquitin activating E1 enzyme adds an energy rich thio-ester bond at the C-terminal end of ubiquitin. This is an adenosine triphosphate (ATP)-dependent reaction.

In the second step, the activated ubiquitin is transferred from the E1 to an ubiquitin-conjugating enzyme, E2. About 50 E2 enzymes have been identified. The central functional motif is a ubiquitin-conjugating catalytic (UBC) fold. The UBC fold displays a catalytic cysteine residue that, together with the thioester bond of the activated ubiquitin, forms a high-energetic conjugate. E2 enzymes define the position of ubiquitination (e.g., K48 vs. K63) and thus as a consequence, generally determine the destiny of the protein substrate.
Ubiquitin-conjugating enzymes (E2) are capable of transferring the activated ubiquitin onto a ubiquitin ligase (E3) enzyme–substrate complex. After the linkage of ubiquitin to the protein substrate, a polyubiquitin chain is formed in which the C-terminus of each ubiquitin is linked to an amino group of a specific lysine residue of the previous ubiquitin. Although generally ubiquitination involves linkage through lysine, it has also been discovered that ubiquitin chains can be formed between the carboxy-terminal glycine of one ubiquitin and the amino terminal methionine of another. Linear ubiquitin chains are thus formed and in this case it is the E3 (a complex known as LUBAC) which decides the linkage (Walczak, Iwai et al, 2012).

E3 ligases are a diverse group of proteins (>600) with distinct motifs. The high specificity and selectivity of the UPS system lies in the diversity of different ubiquitin-protein ligase E3s that can recognise a specific substrate (Wang and Malonado 2010).

Following multiple cycles the polyubiquitinated substrate is recognised and degraded by the 26S proteasome (Figure 1.4).

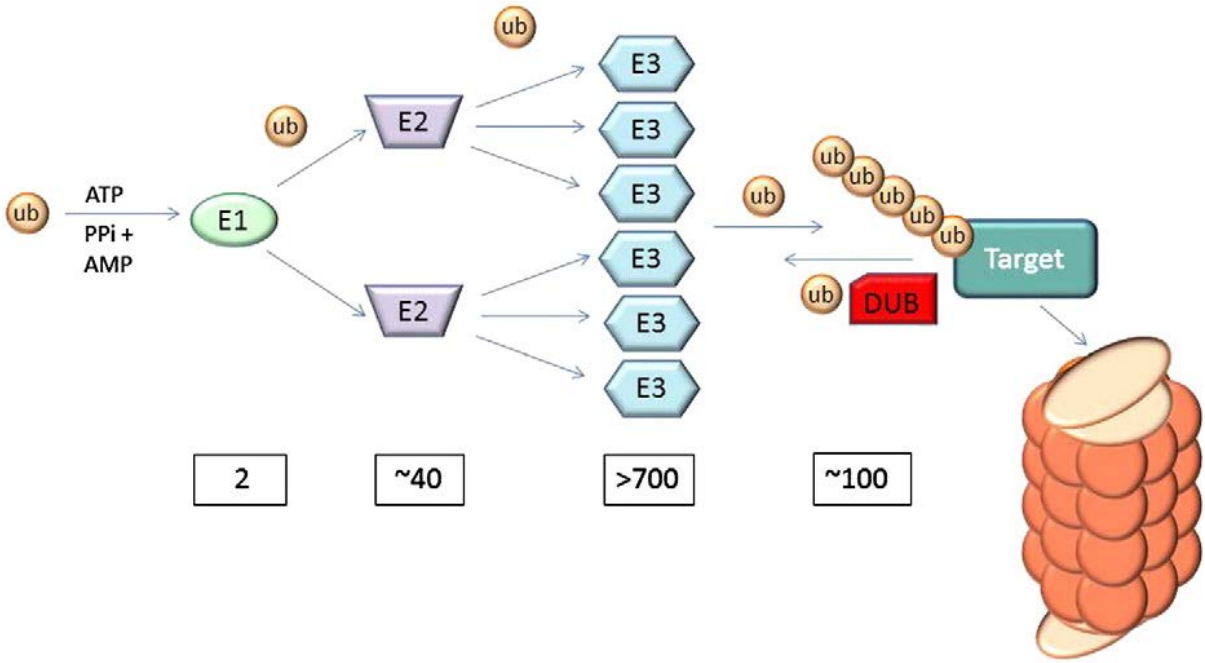

Figure 1.4 **The ubiquitin proteasome system (Crawford and Irvine 2013)**

An E1 ubiquitin-activating enzyme binds ubiquitin (Ub) which is then transferred to an E2 ubiquitin-conjugating enzyme. An E3 ubiquitin ligase subsequently recruits the target protein and mediates the transfer of ubiquitin to the target protein.

1.2.3 Proteasomal Degradation

As mentioned previously, degradation of a protein by the UPS requires two steps, ubiquitination and proteasome degradation. Ubiquitinated proteins, polyubiquitinated with K48 Ubiquitin linkages are targeted for proteolysis are recognised by proteasomes. At the heart of this system is the 26S proteasome which functions as the key enzyme for non-lysosomal protein degradation. Proteasomal degradation removes denatured, misfolded, damaged or improperly translated proteins from cells as well as regulating the level of proteins such as cyclins and transcription factors (Wang and Maldonado 2006). The 26S proteasome is a large complex which can be divided into two smaller complexes, the 20S catalytic core and the 19S regulatory particle, which appears to be responsible for recognising, unfolding, and translocating the polyubiquitinated substrates into the 20S proteasome, where they are degraded (Berko, Tabachnick-Cherny et al. 2012). The proteolytic activities are located within this 20S structure which consists of four stacked rings arranged around an inner catalytic chamber. Each of the outer rings has seven polypeptide α subunits which act as the gates through which proteasome substrates can enter. The two inner rings

consist of seven β subunits. The β-1, 2 and 5 subunits contain the postglutamyl peptidyl hydrolytic-like, tryptic-like, and chymotryptic-like proteolytic activities of the proteasome, respectively (Voorhees et al. 2006). Following its degradation a protein is released from the proteasome as oligopeptides.

1.2.4 Ubiquitin – like proteins

Although the UAE-ubiquitin pathway is the best characterised, a number of homologous enzyme cascades have been described for another eight different classes of ubiquitin-like proteins (UBLs). Each cascade is initiated by a unique E1 enzyme. UBLs and their E1s include **NEDD8** (with NEDD8 activating enzyme (NAE)), **SUMO-1,-2 and -3** (SUMO activating enzyme, SAE), **ATG8, ATG12** (ATG7 for both), **ISG15** (Uba7), **Urm1** (Uba4), **Ufm1** (Uba5) and **FAT10** (Uba6) (Soucy, Dick et al. 2010).

SUMO has been quite well characterised in comparison to other UBLs. It seems to be mainly involved in the regulation of nuclear processes, such as DNA replication, DNA damage repair and transcriptional repression. It differs from the UAE-ubiquitination pathway in that it uses a single E2 enzyme, UBC9. This enzyme is overexpressed in several human tumours and is an attractive target for therapeutic intervention. Several approaches to target UBC9 are in experimental phases, including inhibition of the active site and blocking its binding to target proteins (Dikic and Robertson 2012).

Each UBL is structurally related to ubiquitin and each UBL pathway shares features with the UAE-ubiquitin pathway, however each pathway is associated with different functions. For example, NEDD8 plays an important role in the activation of the cullin-ring E3 ligases by its covalent attachment to the catalytic core of cullin ring ligases (CRLs).

1.2.5 Deubiquitinating Enzymes

The activity of the enzymes of the ubiquitin pathway can be counterbalanced by the actions of deubiquitinating enzymes (DUBs). These remove the ubiquitin from the targeted protein by cleaving the isopeptide bond between the ubiquitin and the substrate (Pou et al, 2013). DUBs can be divided into six classes. These include

ubiquitin specific proteases, ubiquitin C-terminal hydrolases, Machado-Joseph disease protein domain proteases, ovarian tumour domain containing proteases, JAB1/MPN/MOV34 (JAMMs) and monocytic chemotactic protein-induced protein (Komander, Clague et al. 2009). The ubiquitin proteases are the largest subclass of DUBs with over 60 members.

The general roles of DUBs include precursor processing, rescue from degradation, removal of non-degradative ubiquitin signal, recycling, disassembly of ubiquitin chains allowing recycled ubiquitin to re-enter the ubiquitin pool and editing of udiquitin chains, exchanging one type of ubiquitin signal for another (Komander, Clague et al. 2009).

Different subclasses of DUBs have different preferences towards the type of poly-ubiquitin linkages they act on. There are three DUBs which are associated with the 19s regulatory subunit of the proteasome. These are UCH37, USP14 and Rpn11 which belong to the Ubiquitin C-terminal hydrolase, Ubiquitin specific protease and JAMM classes, respectively. Rpn11 cleaves K63-linked polyubiquitination whereas UCH37 cleaves K48-linked. Rpn11 promotes substrate degradation. USP14 and UCH37-mediated deubiquitination suppresses substrate degradation (Shen, Schmitt et al. 2013).

1.3 Targeting the UPS in haematological malignancies

As mentioned previously, many proteins which are regulated by ubiquitination are involved in controlling cellular processes relevant to tumorigenesis, such as cell-cycle progression, apoptosis, receptor downregulation and gene transcription. The ubiquitin-proteasome system therefore offers several possibilities for therapeutic intervention.

1.3.1 E1 Activating Enzymes

Along with high levels of proteasome activity, leukemic cells also have increased levels of ubiquitination. For this reason, it is thought that blocking ubiquitination at the E1 enzyme, which is the initial step, may be of therapeutic benefit (Schimmer et al, 2010). Inhibitors of E1 enzymes are designed to interfere with the thioster bond which is necessary for the activation of ubiquitin. The compound PYR-41 was originally

identified as an inhibitor of p53 but was subsequently discovered to act by blocking the ubiquitin-thioster bond (Crawford and Irvine 2013). A structurally related compound to PYR-41, known as PPZD-4409, has demonstrated preferential cytoxicity to malignant cells and primary patient cells over normal cells. It has also demonstrated to have an anti-tumour effect in in vivo models of leukaemia (Shen, Schmitt et al. 2013).

1.3.2 E2 Conjugating Enzymes

Approximately forty E2 conjugating enzymes have been identified. E2 enzymes receive the activated ubiquitin from the E1 enzyme and catalyse its transfer to a substrate protein together with an E3 ligase. E2s are the main determinant for selecting the lysine linkage site of ubiquitin, thereby determining the fate of the ubiquitinated protein. An E2 inhibitor, NSC697923, has recently been identified that acts on the E2 UBC13 to suppress the activation of NFkB (Crawford and Irvine 2013). Constitutive activation of NFkB is associated with DLBCL and this compound has been shown to inhibit growth and survival of DLBCL cell lines *in vitro* (Pulvino, Liang et al. 2012).

1.3.3 E3 Ligases

Other components of the ubiquitin proteasome system have also been looked at as possible therapeutic targets. The E3 ligases are considered to be the most important components of the ubiquitin conjugation machinery as they bind directly to their target proteins and so have substrate specificity. They recognise both the substrate protein and an E2 ubiquitin conjugating enzyme. Thus they represent a class of "drugable" targets for pharmaceutical intervention.

E3 ligases are a diverse group of enzymes which can be classified into three families based on their domain structure and substrate recognition. These include:

1) N-end rule ubiquitin ligases: N-end rule ligases target protein substrates which have a specific destabilising N-terminal residues including Arg, Lys, His (type1) and Phe, Tyr, Trp, Leu, Ile (type 2). An example of protein degradation by the N-end rule ligases is DIAP, a Drosophila inhibitor of apoptosis protein (Sun 2003).

2) HECT E3 ligases: HECT-type E3 ligases are characterised by a Homologous to the E6-AP Carboxyl Terminus (HECT) domain that forms a thioester intermediate with ubiquitin as a prerequisite for ubiquitin transfer to the substrate protein. The first family member is E6-AP (E6-associated protein) that together with oncoprotein E6 promotes p53 ubiquitination and degradation (Sarikas, Hartmann et al. 2011).

3) RING family ligases: RING-type E3 ligases use RING (really interesting new gene) zinc finger domains to recruit and activate an ubiquitin-charged E2 enzyme for direct ubiquitin transfer to the substrate. RING finger domains have a characteristic architecture of three β strands, one α-helical domain and two free loops that are arranged by Zn^{+} ions. The loops are stabilised by a cluster of cysteine residues and up to two histidines (Sarikas, Hartmann et al. 2011). The majority of E3 ligases belong to this class. Of all the RING proteins expressed in human cells, the cullin ring ubiquitin ligases (CRLs) represent the largest known category.

1.3.3.1 Cullin Ring Ligases

Human cells express seven different cullins that each nucleates a multisubunit ubiquitin ligase. Each cullin forms a distinct class of CRL complex, with distinct adaptors and/or substrate recognition subunits. The catalytic core, however, is common to all CRLs. Substrate receptors are generally linked to the catalytic core through adaptor proteins. Numerous substrate receptors can be recruited to each CRL core which increases the diversity of proteins that can be targeted for ubiquitination. The diversity of proteins that can be targeted is further increased by post-translational modification, which is often required for substrates to be recognised by CRLs.

The ability of CRLs to target numerous substrates can thus have an impact on a range of biological processes, including cell growth, development, signal transduction, transcriptional control, genomic integrity and thus tumour suppression (Sarikas, Hartmann et al. 2011). CRL substrates with important roles in cancer include p27, c-MYC, c-JUN, mTOR, CDT1 and HIF1α (Soucy, Smith et al, 2009). Dysfunction of CRL activities has been associated with oncogenic transformation. Thus, targeting CRLs is an emerging frontier in rational drug design.

The cullin-ring ligase model was initially established by SCF/Cul1 which is shown in Figure 1.5 and this can now be extended to a family of CRLs. The cullin protein family is characterised by the presence of a distinct globular C-terminal domain and a series of three N-terminal repeats of a five-helix bundle. It is at the N terminal end that the adaptor protein and the F box protein binds. It is well established that it is the F box that determines substrate specificity of the SCF complex (Jia and Sun 2011). The C-terminal domain binds the RING protein and NEDD8. The RING protein in turn recruits E2 ubiquitin conjugating enzymes and activates the transfer of ubiquitin from E2 to the substrate.

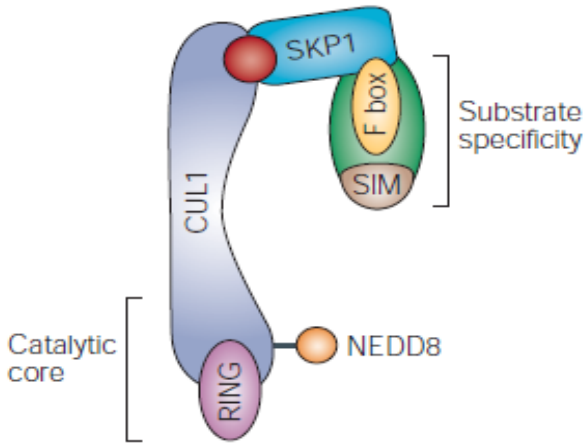

Figure 1.5 **Structure of SCF/Cul1 which provides the basis for the structure of the remaining cullin family (Petroski and Deshaies 2005)**

SCF consists of SKP1, Cul1, an F-box protein that confers substrate specificity and a RING protein that is also known as HRT1, RBX1 or ROC1. SKP1 is an adaptor protein which is divided into two domains: an N-terminal segment that binds Cul1 and a C-terminal region that binds the F-box motif of substrate receptors. Abbreviations: Substrate Interacting Motif (SIM), SKP1, Cul1, and F-box (SCF)

A key and common feature of CRLs is that a NEDD8-modification is required for their activation. NEDD8 is an ubiquitin-like protein which is conjugated as a single molecule to a Lys residue in all cullin-family members. NEDD8 activation and conjugation to cullin proteins is catalysed via an enzymatic cascade that is homologous to

ubiquitination involving ATP, NEDD8's E1 (NEDD8 activating enzyme (NAE)) and E2 (Ubc12). This process is referred to as NEDDylation.

As with ubiquitination, NEDDylation is initiated by an E1 ligase, NEDD8 Activating Enzyme (NAE). NAE first uses ATP to form a NEDD8 adenylate and then transfers NEDD8 from the adenyl group to a specific cysteine within NAE forming an activated NAE-NEDD8 thio-ester. The activated NEDD8 is then transferred to the active site cysteine of Ubc12. Finally, NEDD8 is conjugated to a conserved lysine near the C-terminal end of the cullin protein. This last step is mediated by the NEDD8 E3 ligase.

The NEDDylation process is also highly regulated. NEDD8, which is attached to cullins is detached (deneddylation) by the isopeptidase activity of the metalloprotease CSN5/Jab1 subunit of the COP9 signalosome (CSN). CSN also binds to a de-ubiquitinase enzyme UBP12 that protects the CRL from self-ubiquitination. In addition, CRL is also regulated by Cullin-associated and neddylation-dissociated-1 (CAND1) which inhibits the E3 ligase activity of CRLs by binding to all cullins in their un-neddylated forms (Sarikas, Hartmann et al, 2011). CAND1 competes with SKP1 for binding to Cul1 and only binds Cul1 molecules that are not conjugated to NEDD8. CAND1 can be disassociated from Cul1 by either the conjugation of NEDD8 or the simultaneous presence of SKP1 plus high concentrations of ATP. This regulation is depicted in Figure 1.6. Cycles of NEDD8 attachment and removal might be important in the regulation of cullin-RING ligase activity (Petroski and Deshaies 2005).

Given that NEDD8 modification is necessary for CRL activation it represents an attractive therapeutic target. Hence the appeal that is surrounding the compound MLN4923. MLN4924 is a mechanism based inhibitor of NAE. NAE catalyses the formation of a NEDD8-MLN4924 inhibitor adduct in situ. This adduct resembles adenylated NEDD8. It binds tightly to the adenylation site but cannot be used to form the thio-ester, and thus locks the enzyme in an inactive state.

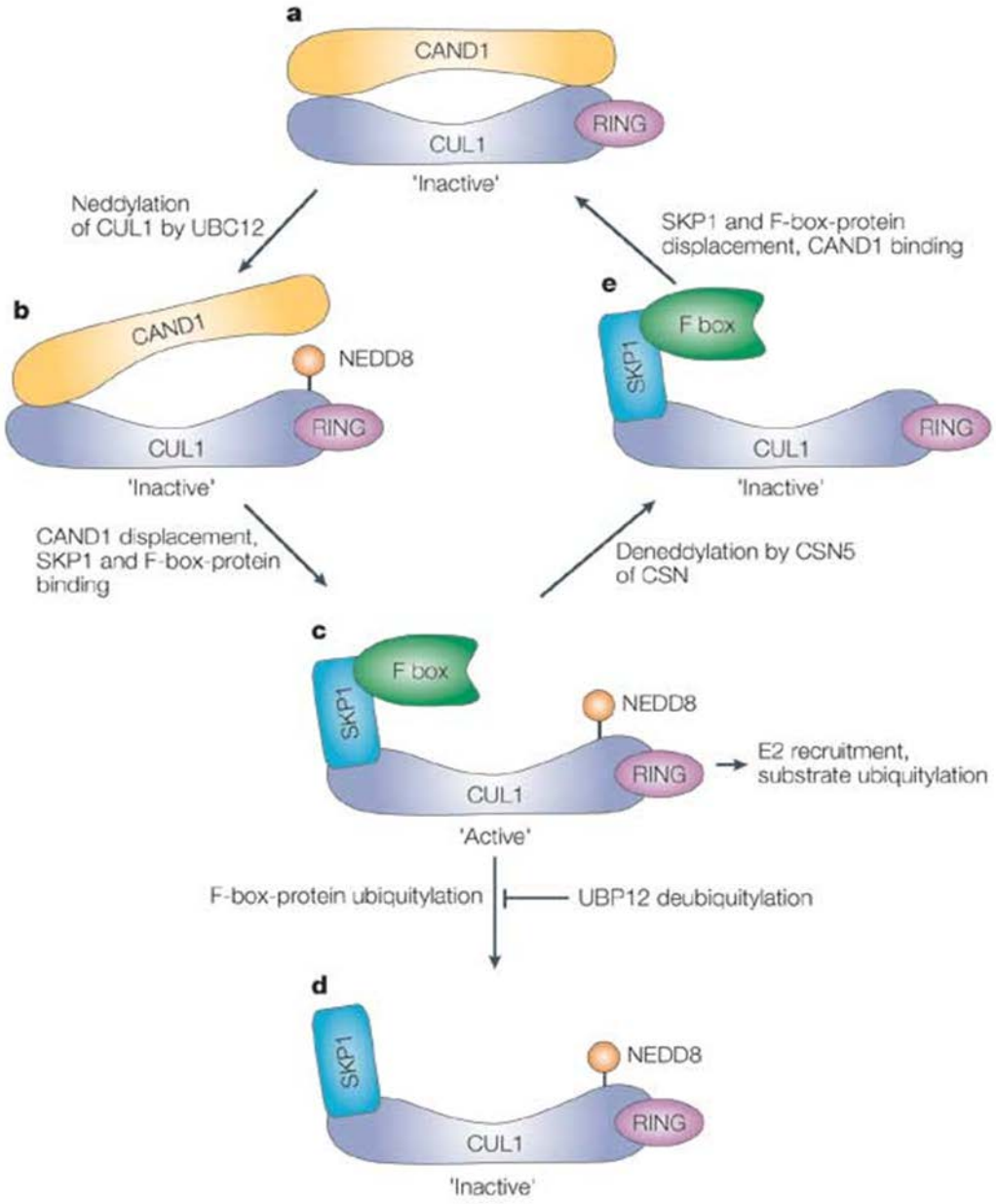

Figure 1.6 **MLN4924 disrupts NEDDylation which is regulated by the COP9 signalosome and CAND1 (Petroski and Deshaies 2005)**

As with ubiquitination, neddylation covalently attaches NEDD8 to a lysine residue of a target protein. It is catalyzed by NEDD8-activating enzyme (NAE), conjugating enzyme (Ubc12), and cullin-ring ligases. Cullin neddylation displaces cullin-associated NEDD8-dissociated protein 1 (CAND1), which triggers the assembly of an active CRL complex and brings the adaptor-bound substrate to a close proximity to Ub-charged E2 and allows efficient transfer of the Ub from E2 to the substrate. Deneddylation counters neddylation and is done by deneddylases. The COP9 signalosome (CSN) is the deneddylase responsible for cullin deneddylation. Cullin deneddylation triggers the disassembly of the CRL-substrate complex, releases ubiquitinated substrates, and recycles NEDD8.

1.3.4 Proteasome

Defects in the proteasome have not been linked to cancer development, which may suggest that cancer cells use the proteasome to their benefit. This is evident in particular with the pro-oncogenic NF-kappaB pathway. High NF-κB activity has been associated with many cancer types, including AML. NF-κB is retained in an inactive state by their binding to inhibitors of NF-κB proteins (IkBs). In order to be freed from this inhibition IkBs need to be phosphorylated, which induces their polyubiquitination and proteasomal degradation. Bortezomib is a boron-containing molecule that reversibly inhibits the proteasome by binding to the threonine residue of subunit of the 26S proteasome and inhibiting its chymotryptic activity Field-Smith, Morgan et al. 2006). The therapeutic value of targeting the proteasome has been validated with Bortezomib (Velcade). Bortezomib was found to downregulate NF-κB signalling by blocking the proteasomal degradation of IkBs. Downregulation of NF-κB reduced the expression of pro-inflammatory response genes and upregulated the cyclin-dependent kinase inhibitors p21 and p27, resulting in increased apoptosis in tumour cells (Hoeller and Dikic 2009).

Bortezomib has been approved by the Food and Drug Administration (2003) as a drug for the treatment of multiple myeloma and mantle cell lymphoma. Proteasome inhibitors have also been used as a method of sensitizing cancer cells to other agents. A new generation of proteasome inhibitors including Salinosporamide and Carfilzomib appear to be more effective than Bortezomib, as their mechanism of action differs; both Salinosporamide and Carfilzomib bind to the proteasome irreversibly (Berko, Tabachnick-Cherny et al. 2012).

1.4 Apoptosis

In 1972 the term “apoptosis” was used for the first time to describe a form of cell death which was associated with certain morphological features. Such features included membrane blebbing, cell shrinkage, chromatin condensation and cellular fragmentation into apoptotic bodies. These apoptotic bodies are recognised and engulfed by surrounding cells and phagocytes.

The central event in apoptotic cell death is the activation of caspases. Caspases (which are so-named as they are cysteine proteases that cleave after an aspartate residue in their substrate) are a conserved family of enzymes that irreversibly commit a cell to die. Although the first mammalian caspase to be identified (caspase-1) has a primary role in inflammation, seven of the fourteen known mammalian caspases play a role in apoptosis (Takatoku, Noborio-Hatano et al. 2004). Caspases exist in the cell as inactive zymogen precursors composed of a prodomain followed by a large and a small subunit which after proteolytic processing, fold into an active caspase able to specifically cleave a variety of cellular substrates, leading to the apoptotic phenotype (Schneider and Tschopp 2000). Two prodomains have been identified which include the caspase recruitment domain (CARD) and the death effector domain (DED). These domains typically facilitate interactions with proteins with the same domains (Logue and Martin 2008).

Apoptotic caspases can be divided into initiator (caspase-2, -8, -9 and -10) and executioner caspases (caspase -3, -6, -7). Initiator caspases are able to auto-activate and initiate the proteolytic processing of other caspases. Effectors caspases are activated by other caspase molecules and they cleave the vast majority of substrates during apoptosis. In mammalian cells caspases can be activated by either the intrinsic or the extrinsic pathway which are outlined below and depicted in Figure 1.7.

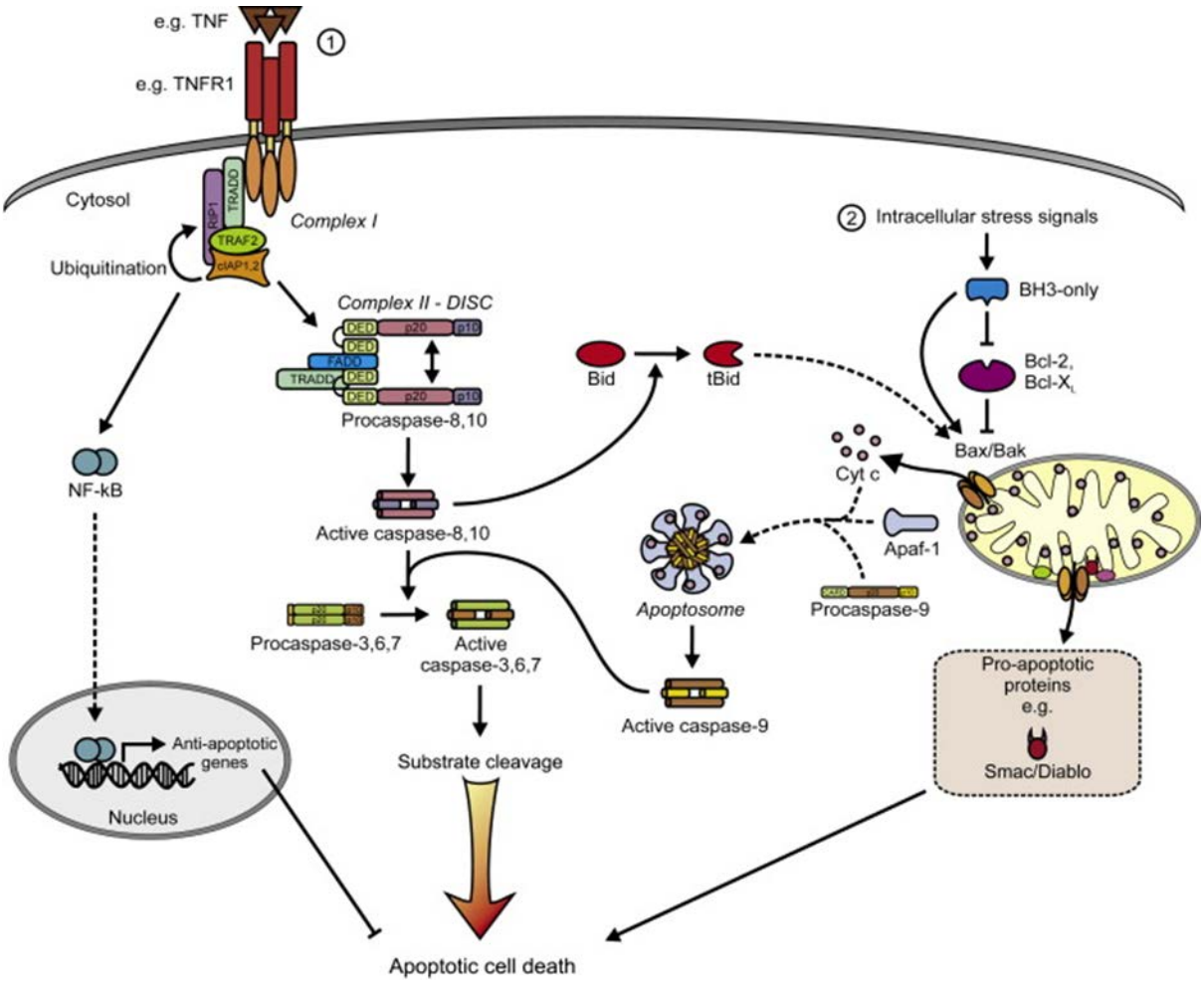

Figure 1.7 **Apoptosis can occur through either 1) the extrinsic pathway or 2) the intrinsic pathway.**

Death ligands, such as TRAIL or TNFα engage their respective receptors leading to the formation of the death-inducing signalling complex (DISC). DISC recruitment leads to the activation of caspase 8 and the subsequent activation of effector caspases 3 and 7. The intrinsic pathway can be activated by chemotherapeutic agents, irradiation or growth factor withdrawal, leading to the activation of Bcl-2 family members. Consequent disruption of mitochondrial integrity causes the release of cytochrome c and second mitochondrial activator of caspases (SMAC) and apoptosome-dependent activation of caspase 9. This leads to the activation of caspases 3 and 7 and, ultimately, to apoptosis.

1.3.1 Death Receptor Pathway

The extrinsic pathway of apoptosis is induced through stimulation of the death receptors. Eight death receptors have been identified, all of which belong to the tumour necrosis factor (TNF) family. These include TNF receptor 1 (TNFR1), CD95, death receptor 3 (DR3), TNF-related apoptosis-inducing ligand receptor 1

(TRAILR1/DR4), TRAILR2/DR5, DR6, ectodysplasin A receptor (EDAR) and the p75 neurotrophin receptor (p75) (Sessler, Healy et al. 2013).

The most understood of these receptors include TNFR1, Fas and TRAIL-R. Signalling by these receptors can lead to a variety of cellular responses including apoptosis, cell proliferation and differentiation (Vandenabeele et al, 2009). Apoptosis is induced by formation of the death inducing signalling complex (DISC) following activation of Fas and TRAIL receptors. DISC components are held together by homotypic protein-protein interactions between death domains (DDs) and death effector domains (DEDs), i.e. a death domain of one protein binds to a death domain of another protein and likewise for death effector domains.

In this complex, Fas-associated death domain (FADD) which has both a DD and a DED can be recruited to the death domain of the receptor and in turn recruits the initiator caspases-8 and/or -10 through homotypic death effector domain interactions.

In contrast to signalling induced by Fas and TRAIL receptors which lead to formation of the DISC, TNFR1 leads to the formation of complex I which is composed of TNFR1, TNFR-associated death domain (TRADD), TRAF2, RIP1, cIAP1 and cIAP2. Endocytosis of complex I is followed by formation of complex II which includes TRADD, FADD and caspase-8 and/or -10. Activation of the initiator caspases -8 and -10 leads to the activation of executioner caspases and these enzymes carry out much of the proteolysis that is seen during the demolition stage of apoptosis (Vanden Berghe, Linkermann et al. 2014).

1.3.2 Intrinsic Pathway

The intrinsic pathway can be activated by various stimuli such as DNA damage and cytotoxic insults. The intrinsic pathway acts through the mitochondria and the integrity of the mitochondria is regulated by proteins of the B-cell lymphoma-2 (Bcl-2) family.

This protein family is composed of those that inhibit apoptosis and those that promote apoptosis. They have traditionally been classified according to their Bcl-2 homology (BH) motifs. These include **1)** multi-domain anti-apoptotic proteins (BH1-BH4), **2)**

multi-domain pro-apoptotic proteins (BH1-BH3), and **3)** BH3-only proteins (Hardwick and Youle 2009).

The anti-apoptotic proteins contain four BH domains and include Mcl-1, Bcl2-A1, Bcl-2, Bcl-XL and Bcl-W. They typically have transmembrane domains which allow them to associate with the membrane (Borner, 2003). These proteins block apoptosis by preventing the BH3-only proteins from promoting the oligomerization of the pro-apoptotic Bcl-2 proteins, which would cause cytochrome C release. Pro-apoptotic Bcl-2 proteins on the other hand lack the BH4 domain and promote apoptosis by forming pores in outer mitochondrial membranes. This class is composed of Bak, Bax and Bok. The BH3-only family is made up of eight members (BID, BAD, BIM, BIK, BMF, NOXA, PUMA and HRK) all of which promote apoptosis when overexpressed (Martin et al, 2008). Both BIM and NOXA can be transcriptionally upregulated by p53. p53 is a tumour suppressor protein that can inhibit cell growth by inducing apoptosis, senescence, cell cycle arrest and more recently cell metabolism (Muller and Vousden 2014). DNA damage therefore results in increased synthesis of these proteins in a p53-dependent manner.

BH3-only proteins are generally inactive under normal conditions. When activated they serve to activate the larger pro-apoptotic proteins such as Bax and Bak.

Activation of the intrinsic pathway leads to BH3-only protein activation. BH3-only protein activation above a certain threshold overcomes the inhibitory effect of the anti-apoptotic Bcl-2 family members. The assembly of BAK-BAX oligomers is promoted, leading to their oligomerization and formation of a channel through which cytochrome *c* can be released (Vanden Berghe, Linkermann et al. 2014). Central to this pathway is the formation of the apoptosome, a caspase-9 activating complex. Cytochrome *c* together with ATP and Apaf-1 recruit caspase-9 to activate it (Sprick and Walczak 2004). Activated caspase-9 can then lead to activation of the executioner caspases -3, -6 and -7.

1.5 TRAIL

TNF related apoptosis inducing ligand (TRAIL/Apo2L) has the ability to induce apoptosis in transformed cells but not in healthy cells. Resistance in non-transformed cells has

been shown to be due to cFlip, anti-apoptotic Bcl-2 proteins and XIAP, all independently (Dijk et al, 2013). Whilst this is remarkable a lot of cells, including primary cells are resistant to TRAIL-induced apoptosis. TRAIL also has the ability to trigger non-apoptotic signalling pathways which can promote survival of malignant cells. This section discusses how TRAIL can induce apoptosis, mechanisms by which cells are resistant to TRAIL, the link between TRAIL and ubiquitination and finally the current status of TRAIL in a clinical setting.

1.5.1 TRAIL-induced apoptosis

TRAIL has the ability to bind to four membrane bound receptors and one soluble receptor, osteoprotegerin (OPG). The four membrane bound receptors include TRAIL-R1 (DR4), TRAIL-R2 (DR5), TRAIL-R3 (DcR1) and TRAIL-R4 (DcR2). Of these receptors two are capable of inducing apoptosis, DR4 and DR5. DR4 and DR5 both contain cysteine rich domains (CRD) in their extracellular region, the first of which is a highly conserved incomplete CRD, with complete CRDs 2 and 3 being important for ligand binding (Cha et al, 1999). DR4 and DR5 also both contain death domains through which they can induce apoptosis. Upon TRAIL binding to its receptor DR4 and/or DR5 the receptors undergo trimerization and recruit the adaptor protein FADD through its death domain to the death domains located on the receptors. FADD then in turn recruits through its DED pro-caspase 8/10 to this death inducing signalling complex (DISC). These caspases also contain DEDs which allows for this homotypic interaction with FADD. The caspases then become activated at the DISC. Caspase 8 is the apoptosis-initiating caspase at the DISC and becomes fully activated through auto-catalytic cleavage and formation of homodimers. With release of active homodimers from the DISC, caspase 8 cleaves and activates downstream substrates of the apoptotic pathway (Lemke, von Karstedt et al. 2014). This mechanism of TRAIL-induced apoptosis is depicted in Chapter 4 (Figure 3.2).

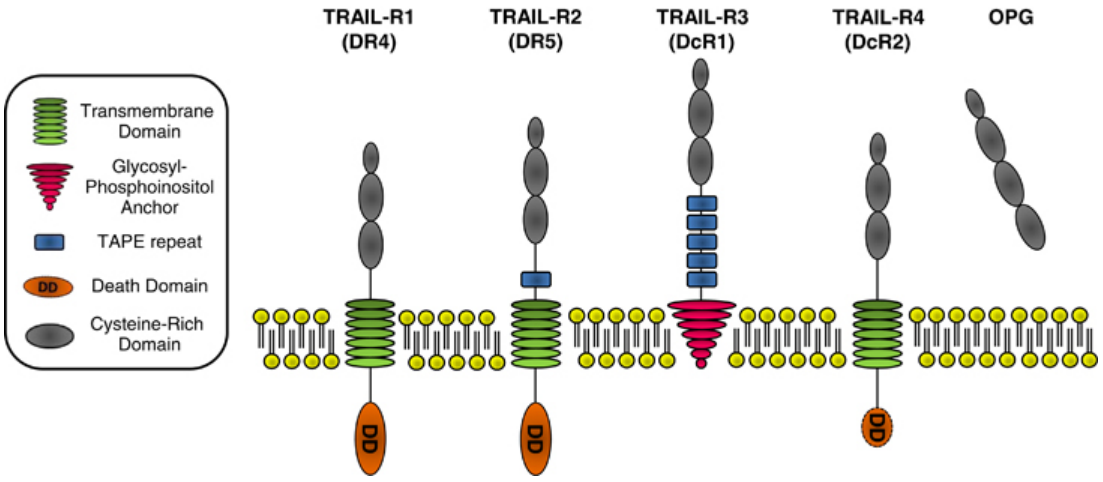

Figure 1.8 **Schematic of the five TRAIL receptors** (Lemke, von Karstedt et al. 2014**)**

TRAIL can bind to five different receptors, four membrane-bound and one soluble receptor. Two of these membrane receptors, TRAIL-R1/death receptor 4 (DR4) and TRAIL-R2/death receptor 5 (DR5), contain a death domain through which TRAIL can transmit an apoptotic signal. The other two membrane receptors, TRAIL-R3/decoy receptor 1 (DcR1) and TRAIL-R4/decoy receptor 2 (DcR2), can also bind TRAIL, but act as antagonistic/receptors, lacking the death domain. In addition to these four membrane receptors, a fifth soluble antagonistic receptor, osteoprotegerin (OPG) can also bind TRAIL.

In contrast to DR4 and DR5, the TRAIL receptors DcR1, DcR2 and OPG have been reported to impair the ability of TRAIL to induce apoptosis. DcR1 is a glycosyl-phosphatidyl-inositol-anchored receptor lacking an intracellular domain and DcR2 contains a truncated non-functional domain in its intracellular domain thus while capable of binding TRAIL they are incapable of inducing apoptosis. In this manner they can compete with the TRAIL receptors containing DDs for TRAIL binding. DcR2 has been reported to impair TRAIL-induced apoptosis by triggering anti-apoptotic signalling pathways including NF-κB and Akt (Degli-Esposti, Dougall et al. 1997; Jennewein, Karl et al. 2012). Decoy receptor expression has also been correlated with cancers (Sheikh, Huang et al. 1999).

1.5.2 Resistance to TRAIL-induced apoptosis

Resistance to TRAIL-induced apoptosis can occur at different stages of the TRAIL apoptotic pathway. cFLIP for example contains two DEDs that are very similar to the

DEDs on caspase 8 and thus compete with caspase 8 for binding to the DISC. In this manner they inhibit the pro-apoptotic activity of the DISC. Three common splice variants of cFLIP exist. These are cFLIP-long (cFLIPL), cFLIP-short (cFLIPS) and cFLIP-raji (cFLIPR) (Krueger, Baumann et al. 2001). All three variants contain two N terminal DEDs. cFLIPS and cFLIPR contain short C terminal domains whereas cFLIPL contains a long C terminal domain. It is cFLIPS and cFLIPR which compete for binding to FADD at the DISC. When cFLIPL is expressed at high levels it acts in an anti-apoptotic manner similar to the other two variants. At low levels it can enhance apoptosis by promoting the recruitment of pro-caspase-8 to the DISC.

The inhibitors of apoptosis proteins (IAPs) have also been frequently associated with resistance to TRAIL-induced apoptosis. This family includes X-linked Inhiitor of Apoptosis (XIAP), cellular IAP (cIAP) 1 and 2. This family are characterised by containing at least one baculovirus repeat (BIR) domain. XIAP can prevent activation of caspase-3, -7 and -9 by binding them directly through its BIR domains. cIAP1 and cIAP2 can also bind caspases but cannot efficiently inhibit them (Shiozaki, Chai et al. 2003). It is thought that they exert their anti-apoptotic activity by promoting the degradation of caspases. XIAP along with the cIAPs have E3 ligase activity via their RING domain which enables them to ubiquitinate proteins. Through ubiquitination the IAPs have also been linked to cell survival pathways such as NF-κB signalling.

The balance of pro- and anti-apoptotic Bcl2 family members can also play a role in cells having resistance to TRAIL-induced apoptosis. Alterations in the balance, for example increased expression of anti-apoptotic member Mcl-1 can cause a cell to become resistant to TRAIL treatment.

Resistance to the apoptosis inducing effect of TRAIL is frequently encountered in tumour cells but can often be bypassed with combination treatments.

1.5.3 Ubiquitin and TRAIL

Following its release from the DISC, caspase 8 is fully active and can engage with executioner caspases. It has been reported that death receptor ligation can induce polyubiquitination of caspase 8 and that it can do this by recruiting the E3 ligase, Cullin

3 to the DISC. The ubiquitin binding protein, p62 promoted stabilisation of caspase 8, thereby leading to DISC activation and cell death (Jin, Li et al, 2009).

It has also been shown that tumour necrosis factor receptor-associated factor 2 (Traf2) can interact with the DISC downstream of Cullin 3 and can mediate the polyubiquitination of the catalytic domain of caspase 8. This leads to the proteasomal degradation of caspase 8 limiting DISC activity (Gonzalvez, Lawrence et al. 2012). A depletion of TRAF-2 would thus lower the signal threshold for DR-mediated apoptosis, altering cell survival vs cell death. Overall the DISC is highly regulated and ubiquitination certainly plays a role in this (Lemke, von Karstedt et al. 2014).

1.5.4 Non-Apoptotic TRAIL Signalling

In addition to apoptosis TRAIL can also induce non-apoptotic signalling pathways. These include the NF-κB pathway, mitogen activated protein kinases (MAPK), Src and PI3 kinase pathways (Lemke, von Karstedt et al. 2014). Activation of these pathways can promote cancer itself through promoting migration and invasion of malignant cells Ishimura, Isomoto et al. 2006). A recent review on TRAIL highlighted a study showing that TRAIL treatment could stimulate the invasion of colorectal cancer cells in a K-Ras dependent manner. Loss of mutant K-Ras could switch the receptors back into apoptosis mode (Hoogwater, Nijkamp et al. 2010).

DR4 and DR5 have been found to activate NF-κB in a TRADD and RIP-1 dependent manner. NEMO is also part of this complex and can recruit IKKα/β to the complex. This results in the phosphorylation and proteasomal degradation of IkB leading to the release and accumulation of NF-κB. NF-κB is then free to translocate to the nucleus where it can activate the transcription of a number of genes (Plantivaux, Szegezdi et al. 2009). These can include anti-apoptotic genes such as Mcl-1 and cFlip.

Six groups of MAPKs exist. These include extracellular regulated kinases (ERK1/2), Jun NH2 terminal kinases (JNK1/2/3), p38 (p38 a/b/g/d), ERK7/8, ERK3/4 and ERK5 (Azijli, Weyhenmeyer et al. 2013). TRAIL can activate MAPKs in cancer cells mostly leading to promotion of cell proliferation and cell survival signalling.

1.5.5 Therapeutic Value of TRAIL

TRAIL targeting strategies can be divided into two categories. These are recombinant human TRAIL and monoclonal antibodies against DR4 and DR5. Targeting both DR4 and DR5 using recombinant TRAIL may induce a greater death signal than targeting a single receptor with a monoclonal antibody. However the presence of the decoy receptors could alleviate some of its apoptosis activity. Monoclonal antibodies have been shown to be effective therapeutically as they can target specific antigens and they also have a much longer half-life than recombinant human TRAIL ligands (Azijli, Weyhenmeyer et al. 2013). The half-life of recombinant TRAIL is hours whereas the half-life of antibodies is from several days to weeks (Lemke, von Karstedt et al. 2014).

Dulanerim is recombinant TRAIL that was developed for use in a clinical setting. It has so far shown to be well tolerated. It has been entered into two randomised controlled trials. The first is with non-small lung cancer in combination with chemotherapy and chemotherapy alone. The second one was in non-Hodgkins lymphoma which compared rituximab alone to a combination of rituximab and dulanerim. Neither study revealed a great anticancer effect.

A number of human DR4 and DR5 monoclonal antibodies are now in Phase-I-II clinical trials in adults including mapatumumab and lexatumumab. As with Dulanerim monoclonal antibodies can be tolerated quite well but have a minimal anticancer effect (Lemke, von Karstedt et al. 2014). The use of more active treatments targeting TRAIL is likely to produce greater activity in cancer cells that are already susceptible to TRAIL-induced apoptosis which highlights the importance of TRAIL in combination with chemotherapeutic agents.

Chapter 2.

Materials and Methods

2.1 Materials

2.1.1 Suppliers

Abcam, Cambridge, CB4 0FL, UK

Affymetrix/eBioscience Ltd., Hatfield, AL10 9NA, UK

BD Biosciences-Pharmingen, San Diego, CA 92121, USA

Calbiochem, Nottingham, NG9 2JR

Cell Signalling Technology (CST), Inc., Beverley, MA 01915, USA

Enzo Life Sciences Ltd., Exeter EX2 8NL, United Kingdom

Fisher Scientific Ireland, Dublin 15, Ireland

Invitrogen, Crofton Rd., Dun Laoghaire, Dublin, Ireland

Jackson ImmunResearch Ltd., Suffolk, CB8 7SY, UK

Medray Imaging Systems, Baldonnell Business Park, Dublin 22, Ireland

Merck Millipore, Billerica, MA 01821, USA

New England Biolabs (NEB), Ipswich, MA01938-2723, UK

Pierce, Subsidiary of Thermo Scientific Ltd, Rockford, IL 61105 USA

Promega, Mulhuddart, Dublin 15, Ireland

R&D systems, Abingdon, OX14 3NB, UK

Santa Cruz Biotechnologies (SantaCruz), Inc., Santa Cruz, CA 95060, USA

Sigma-Aldrich Ireland, Dublin, Ireland

Vector Laboratories Inc, Burlington, CA 94010, USA

All chemicals were obtained from Sigma-Aldrich unless otherwise stated

2.2 Methods

2.2.1 Cell Culture techniques

A summary of the cell lines used is illustrated in Table 2.1. All cell lines were maintained in growth medium supplemented with heat inactivated fetal bovine serum (FBS), 50 U/ml penicillin and 50 U/ml streptomycin (All growth media and supplements were obtained from Sigma-Aldrich). All cell lines were maintained at 37 ^{o}C in a humidified atmosphere of 5% CO_2. When cells reached a confluence of 85-90% they were subcultured at the seeding density described below in Table 2.1.

OCI-AML2, OCI-AML3, MOLM-13, HL-60 and ML-1 are all AML cell lines. MMIR, MMIS and KMS18 are MM cell lines while OCI-LY1, OCI-LY7, OCI-LY10, SU-DHL-6 and RIVA are all DLBCL cell lines.

Table 2.1 **Cell lines and culturing conditions**

Cell Line	Seeding density cells/cm^2	Seeding density cells/ml	Growth media	Serum	Subculture	Cell type	Known Mutations
HS-5	4 x 10^4	-	High glucose Dulbecco's Modified Eagle Medium (DMEM)	10% FBS	72 h	Human Fibroblasts	
HEK293T	4 x 10^4	-	High glucose DMEM	10% FBS	72 h	Epithelial kidney	
OCI-AML2	-	3 x 10^5	Minimum Essential Medium (MEM)	10% FBS + 1mM sodium pyruvate+ 1% non-essential amino acids	48 h	AML	DNMT3A

OCI-AML3	-	3 x 10^5	Roswell Park Memorial Institute Medium (RPMI)	10% FBS+ 1mM sodium pyruvate	48 h	AML	NPM1, DNMT3A
MOLM-13	-	3 x 10^5	RPMI	10% FBS+ 1mM sodium pyruvate	48 h	AML	CBL
ML-1	-	3 x 10^5	RPMI	10% FBS+ 1mM sodium pyruvate	48 h	AML	FLT3-NPM1
HL-60	-	3 x 10^5	RPMI	10% FBS+ 1mM sodium pyruvate	48 h	AML	NRAS, p53 gene deletion
KMS18	-	5 x 10^5	RPMI	10% FBS	72 h	MM	
MMIR	-	5 x 10^5	RPMI	10% FBS	72 h	MM	
MMIS	-	5 x 10^5	RPMI	10% FBS	72 h	MM	
OCI-LY1	-	3 x 10^5	Iscove's Modified Dulbecco's Medium (IMDM)	10% FBS	72 h	DLBCL	
OCI-LY7	-	3 x 10^5	IMDM	10% FBS	72 h	DLBCL	
OCI-LY10	-	3 x 10^5	IMDM	10% FBS	72 h	DLBCL	
RIVA	-	3 x 10^5	RPMI	10% FBS	72 h	DLBCL	
SU-DHL-6	-	3 x 10^5	RPMI	10% FBS	72 h	DLBCL	

2.2.2 Clonogenic Assay

OCI-AML2 cells were treated as described with MLN4924 (Millennium Pharmaceuticals, Inc) and TRAIL for 24 h. Following treatments, cells were reseeded into methylcellulose at a density of 5 x 10^4 cells/ml and allowed to proliferate for 10 days. Images were taken of colonies in the plates and these images were then used for counting.

To prepare the methylcellulose solution, 0.6 g of methylcellulose was added to 25 ml of IMDM medium which was heated to 60 ^oC. Once dissolved 25 ml of IMDM medium at room temperature was added. The solution was rotated for 2 h at 4 ^oC. Finally the solution was centrifuged at 5,000 x g for 2 h at room temperature.

2.2.3 Ficoll Separation

For isolation of mono-nuclear cells AML bone marrow and peripheral blood samples were diluted in Hank's Balanced Salt Solution (blood sample: 2-fold and bone marrow sample: 4-fold). The AML sample was layered on top of Ficoll-Paque Plus (GE Healthcare; Fisher Scientific) at a 2:1 ratio. After spinning tubes at 1,200 rpm for 20 minutes the buffy layer was removed, washed in Hanks and cryopreserved in 10% dimethyl sulfoxide (DMSO) freezing medium (5 x 10^6). Primary AML cells were cultured in MEM with 10% FBS.

2.2.4 Co-culture

For co-culture experiments, HS5-GFP (HS5 cells were transduced with a GFP lentiviral vector as per section 2.2.16) cells were plated at 5 × 10^4 cells/well in a 24 well/plate and incubated for 48 h. After incubation, AML cells were plated at 5 × 10^5 cell/mL (0.5 mL/well) in presence/absence of HS5-GFP. The cells were then incubated for 24 h before being treated with relevant drugs for a further 24 h or 48 h.

2.2.5 CD34/38 staining

Cells were seeded at 3 x 10^5/ml for 24 h prior to treatments. Following completion of treatment cells were collected in eppendorfs, supernatant decanted and resuspended

in 50µl of FACS buffer (1% BSA in PBS). For each sample 10 µl of anti-CD34-PE (BD Biosciences; PE Mouse Anti-Human CD34 555822) and 2.5 µl of anti-CD38-APC-H7 (BD Bioscience; APC-H7 Mouse Anti-Human CD38 656646) was added and incubated for 40 minutes at room temperature, protected from light. 1 ml of FACS buffer was added to each sample and centrifuged for 5 minutes at 1,200 rpm. Supernatant was removed, pellets resuspended in 500 µl of FACS buffer and analysed by flow cytometry.

2.2.6 7-Amino-actinomycin D (7-AAD) staining

Cells were seeded at 3 x 10^5/ml for 24h prior to treatments. On completion of treatments cells were transferred to eppendorfs, centrifuged at 1,200 rpm and pellets resuspended in FACS buffer with 5 µl of 7-AAD (concentration: 1 mg/ml; Affymetrix/eBioscience). Samples were incubated for 20 minutes at room temperature, protected from light before being analysed by flow cytometry.

2.2.7 MTT assay

Cell viability was monitored using 3-(4, 5-dimethylthiazolyl)-2, 5-diphenyl tetrazolium bromide (MTT) assay. Cells were seeded into a 96 well plate and left for 24 h prior to treatments. After treatment, MTT (0.5 mg/ml) was added to cells and incubated for 3 h at 37^{o}C. The reaction was stopped by addition of an MTT stop solution of 20% Sodium dodecyl sulfate (SDS) in 40% dimethyl formamide. The purple formazan precipitate generated was allowed to dissolve for 1 h on an orbital shaker. The colour intensity was measured at 550 nm on a Wallac Victor 1420 Multilabel counter (PerkinElmer Life Sciences, Waltham, MA, USA). Cell viability was expressed relative to the absorbance of untreated cells, which was taken as 100% viable.

2.2.8 TMRE staining

Cells were seeded into a 24 well plate at the density outlined in Table 2.1 and allowed to adhere overnight. The cells were then treated as desired and harvested by trypsinisation as described in Section 2.2.11.

2 mM of tetramethylrhodamine (TMRE; BD Biosciences) was added and the cells were resuspended gently. The cells were then incubated in the dark for 30 min and measured by flow cytometry using the BD FACSCanto on channel PerCP and PE. All analysis was carried out using Cyflogic software.

2.2.9 Annexin V staining of suspension cells

For Annexin V staining cells were seeded into a 24 well plate and left for 24 h before treatments. Following treatments 10^5 cells were collected by centrifugation at 350 xg and incubated with Annexin-V-FITC in calcium buffer (10 mM HEPES/NaOH, pH 7.4, 140 mM NaCl and 2.5 mM $CaCl_2$) for 15 min on ice in the dark. Cells were washed in calcium buffer before measuring the FITC fluorescence intensity on the individual cells on a FacsCanto flow cytometer (Becton Dickinson, Franklin Lakes, NJ, USA). Analysis was performed using FACS Diva software (Becton Dickinson).

2.2.10 Haematoxyin + Eosin staining

After treatments, cells were spun onto microscope slides, fixed in methanol for 5 minutes at room temperature and were stained by immersion into Harris haematoxylin solution (Sigma-Aldrich) for 5 minutes followed by 1 minute immersion in Eosin Y (Sigma-Aldrich). The slides were let to airdry and then mounted for microscopy using DPX Mountant (Sigma-Aldrich). Phase contrast images were taken from 15 randomly chosen areas per sample using 400 fold overall magnification (Zeiss S100 Microscope).

2.2.11 Protein sample preparation

Cells were seeded into 6-well plates at a density of 3 x 10^5/ml for 24 h prior to treatments. Following experimental treatments the cells were collected and transferred into a 15 ml tube and centrifuged at 1,500 rpm at 4 ^oC for 5 minutes. The supernatant was then discarded and the cell pellet was resuspended in 1ml of 1 x PBS, transferred into a 1.5 ml tube and centrifuged at 5,000 x g at 4 ^oC for 5 minutes. The PBS was removed and the cells were lysed in whole cell lysis buffer (1 M HEPES pH7.5,

350 mM NaCl, 1 mM $MgCl_2$, 0.5 mM Ethylenediaminetetraacetic acid (EDTA), 0.1 mM Ethyleneglycoltetraacetic acid (EGTA) and 1% Nonidet-P40) containing protease inhibitors and reducing agents (0.5 mM dithiothreitol (DTT), 0.1% phenylmethylsulfonyl fluoride (PMSF), 1% aprotinin, 1 mM sodium orthovanadate (Na_3VO_4) and 5 mM sodium fluoride (NaF)). The cell pellet was lysed by resuspending it in 50 µl of whole cell lysis buffer, the cells were then allowed to swell on ice for 30 minutes and centrifuged at 20,000 x g at 4 ^{o}C for 20 min to remove the genomic DNA and cell debris. The supernatant, which contain the cytosolic proteins, was then removed and transferred to a new 1.5 ml tube. The protein concentration was ascertained using the BCA assay (BCA assay kit; Fisher Scientific) and bovine serum albumin (BSA) as the standard. The cytosolic proteins were separated by their size to charge ratio using sodium dodecyl sulphate polyacrylamide gel electrophoresis (SDS-PAGE).

2.2.12 SDS-PAGE

Protein samples were resuspended in 5 x Laemmli's SDS-PAGE sample buffer (62.5 mM Tris-HCL pH 6.8, 2% SDS, 5% β-mercaptoethanol, 1 mM PMSF and 0.05% bromophenol blue) until a concentration of 1X Laemmli's SDS-PAGE sample buffer was reached. The proteins were then denatured for 5 min at 95 ^{o}C. 30 µg of protein was loaded onto the gel and resolved using a 8-15% SDS-PAGE gel (see Table 2.2 for components). The percentage of the gel depended on the size of the protein of interest. A broad range (7-175 kDa) prestained colourplus protein ladder (NEB) was run alongside the protein samples. Gels were electrophoresed at 80 V for 30 min after which the voltage was increased to 110 V and run for another 1.5–2 h. The gels were electrophoresed in running buffer (25 mM Tris base pH 8.3, 2 M glycine and 3 mM SDS).

***Table 2.2*. Components of SDS-PAGE running gels and SDS-PAGE stacking gel**

Component	**8% running gel (ml)**	**12% running gel (ml)**	**15% running gel (ml)**	**Stacking gel (ml)**
H_2O	1.9	1.7	1.2	1.36
30% Acrylamide	1.8	2	2.5	0.34
1.5 M Tris pH 8.8	1.3	1.3	1.3	-
1.5 M Tris pH 6.8	-	-	-	0.26
SDS	0.05	0.05	0.02	0.02
Ammonium Persulfate (APS)	0.05	0.05	0.05	0.02
Tetramethylethylenediamine (TEMED)	0.002	0.002	0.002	0.002
Total volume	**5**	**5**	**5**	**2**

2.2.13 Western Blotting

The proteins in the SDS-PAGE gels were electrophoretically transferred onto nitrocellulose membrane (Whatman; Fisher Scientific) for 90 min at 110 V in transfer buffer (25 mM Tris base pH 8.3, 2 M glycine and 20% methanol). Membranes were then blocked for 1 h in blocking buffer (5% non-fat dried milk in 1 x PBS containing 0.05% Tween 20 (1 x PBS-T) or 1% BSA in 1 x PBS-T). The membrane was then incubated with primary antibodies according to the conditions detailed in Table 2.3. After the primary antibody incubation the antibody was removed and any unbound or nonspecifically bound antibody was detached from the membrane by 3 x 15 min washes in 1 x PBS-T. This was followed by a 1-1.5 h incubation with the appropriate horseradish peroxidise (HRP)-conjugated IgG antibody diluted in 5% non-fat dried milk in 1 x PBS-T according to the conditions outlined in Table 2.3. After the secondary antibody incubation the unbound antibody was removed by 3 x 15 minute washes in 1 x PBS-T. The membrane was then incubated with 1ml Western Chemiluminescent HRP

substrate (Pierce) for 5 minutes and the protein bands were visualised using X-Ray film (AGFA blue film; Medray).

Table 2.3 **Antibodies**

1^o antibody (2^o antibody)	**1^o antibody dilution and incubation conditions**	**Source of Antibodies**
Actin (anti-Rabbit)	1:5000 Overnight @ 4^oC	Sigma; A2066
Bad (anti-Mouse)	1:1000 Overnight @ 4^oC	BD Biosciences; #610392
Bcl-2 (anti-Mouse)	1:1000 Overnight @ 4^oC	Santa Cruz; sc-509
Bcl-X_L (anti-Mouse)	1:1000 Overnight @ 4^oC	Santa Cruz; sc-8392
Bik (anti-Rabbit)	1:1000 Overnight @ 4^oC	Cell Signalling; #4592
Bim (anti-Rabbit)	1:1000 Overnight @ 4^oC	Enzo Life Sciences; ADI-AAP-330
c/EBPα (anti-Mouse)	1:1000 Overnight @ 4^oC	Santa Cruz; sc-61
cFlip (anti-Mouse)	1:1000 Overnight @ 4^oC	Enzo Life Sciences, Alexis; ALX-428-C050
cIAP1 (anti-goat)	1:1000 in 5% BSA Overnight @ 4^oC	Cell Signalling; #4952
cIAP2	1:1000 in 5% BSA Overnight @ 4^oC	Cell Signalling
Cleaved caspase 3 (anti-Rabbit)	1:1000 Overnight @ 4^oC	Cell Signalling; #9644
Mcl-1 (anti-Rabbit)	1:1000 Overnight @ 4^oC	Cell Signalling; #45725
NEDD8 (anti-Rabbit)	1:1000 Overnight @ 4^oC	Abcam; Ab81264
NOXA (anti-Mouse)	1:1000 Overnight @ 4^oC	Calbiochem; #114AC307

p21 (anti-Rabbit)	1:1000 Overnight @ 4^{o}C	Abcam
p53 (anti-Mouse)	1:5000 Overnight @ 4^{o}C	Santa Cruz; sc-126
PARP (anti-Rabbit)	1:1000 Overnight @ 4^{o}C	Cell Signalling; #9542
Phospho IkB (anti-Mouse)	1:1000 Overnight @ 4^{o}C	Cell Signalling; #9246
Puma (anti-Rabbit)	1:1000 Overnight @ 4^{o}C	Cell Signalling; #4976
Total IKB (anti-Rabbit)	1:1000 Overnight @ 4^{o}C	Cell Signalling; #4812
XIAP (anti-Mouse)	1:1000 Overnight @ 4^{o}C	Enzo Life Sciences
2^{o} antibody	**2^{o} antibody dilution and incubation conditions**	**Source of Antibodies**
Mouse (Anti-Rabbit IgG)	1:5000 2h @ Room Temperature (R/T)	Cell Signalling; #5127S
Goat (Anti-Rabbit)	1:5000 2h @ R/T	Jackson ImmunoResearch; # 111-035-003
Anti-Rabbit IgG	1:5000 2h @ R/T	Sigma Aldrich; #A0545

2.2.14 Transformation

Plasmid DNA was transformed into DH5α competent *E. coli* cells to amplify and purify plasmid DNA. 50 ng/ml of the plasmid DNA was added to 50 µl of DH5α competent *E. coli* cells. The plasmid DNA was mixed gently with the *E-coli* cells and left on ice for 20 minutes. The cells were then heat shocked at 42 ^{o}C for 60 seconds followed by incubation on ice for 2 minutes. 450 µl of Luria-Bertani (LB) broth (20% LB broth in dH_20) was then added to the cells and incubated at 37 ^{o}C for 1 h with at shaking at 250rpm. 100µl of the cell suspension was then removed and spread onto LB agar (20% LB Agar in dH_20) containing the appropriate selection antibiotic. The plates were then incubated at 37 ^{o}C overnight. A single colony was inoculated into 5 ml of LB broth containing selective antibiotic and incubated at 37 ^{o}C overnight with shaking at 250

rpm. The culture was centrifuged at 775 x g at 4 ^{o}C for 5 minutes. The supernatant was discarded and the plasmid was purified from the *E-coli* cells as outlined in the QAIfilter plasmid purification kit (Qiagen).

2.2.15 Generation of stable cell lines by lentiviral infection

Lentivirus was made by transfection of expression vectors along with a second generation lentivirus packaging system (pMD2.G, psPAX2 and pRSC-Rev from Addgene) into HEK293T cells using JET PEI transfection reagent (Polyplus Transfection). Medium was collected at 24h and 48h and stored at -80 ^{o}C in 2 ml aliquots.

2.2.16 Lentiviral transduction of OCI-AML2 cells

OCI-AML2 cells were seeded at 3 X 10^5 for 24 h prior to transduction. The medium was removed from the cells and replaced with 2 ml of virus medium containing polybrene (5 µg/ml). Cells were spun in their plate at 1,200 rpm for 90 minutes at room temperature. Following centrifugation the cells were placed in the incubator for 4 h after which the medium was replaced with MEM. The following day cells were selected using puromyocin.

2.2.17 Luciferase Assay

To study the effect MLN4924 has on the activation of NF-κB in OCI-AML2 cells the cells were stably transduced with an NF-κB promoter reporter construct. This construct contains an NF-κB promoter sequence upstream of the firefly luciferase and GFP genes. Treatments that induce NF-κB activation and thus its promoter activity will induce the expression of luciferase and GFP and can be quantified.

OCI-AML2 NF-κB reporter cells were seeded into a 96 well plate suitable for reading a luciferase assay. The cells were seeded for 24 h before being treated. The extent of luciferase expressed in the cells was then analysed using the ONE GLO luciferase assay system (Promega) according to manufacturer's guidelines. The luminescence was then read using the Victor x3 plate reader.

2.2.18 Receptor Expression

Cells were removed from culture dishes, harvested by centrifugation and washed twice with 1% BSA in PBS. Cells were incubated with 1:100 dilution of primary antibodies (DR4 and DR5: neutralizing mouse monoclonal antibodies, Alexis, DcR1 and DcR2: neutralizing goat polyclonal antibodies, R&D Systems) in 1% BSA in PBS for 40 min on ice. After two washes in 1% BSA/PBS, cells were resuspended in 1:50 dilution of FITC-labeled secondary antibody and incubated for 40 minutes on ice. Excess secondary antibody was removed by washing first in 1% BSA in PBS and then PBS. Cells were fixed in 1% formaldehyde/PBS before analysis by flow cytometry (FacsCalibur, Beckton Dickinson).

2.2.19 Enzyme linked immunosorbent assay (ELISA)

A TRAIL ELISA was used to determine the amounts of TRAIL present in plasma and tumour samples at different timepoints. Tumour samples were subjected to homogenisation in RIPA lysis buffer before being used in this ELISA. Plasma samples were used directly. The protocol followed was as per manufacturer guidelines (ABCAM (ab46074-TRAIL Human ELISA kit)).

2.2.20 Statistical Analysis

Statistical analysis was carried out in Excel. Significant differences between treatments were determined using an unpaired student t-test (two-tailed) and $p<0.05$ was deemed significant. All error bars represent standard deviatiation.

Chapter 3

The Effect of MLN4924 on TRAIL-induced Apoptosis

3.1 Introduction

The Ubiquitin Proteasome System (UPS) plays a critical role in maintaining protein homeostasis through the targeted destruction of damaged/misfolded proteins and regulatory proteins that control critical cellular function and no longer needed. It is not surprising then that abnormalities within this system are associated with a number of pathologies including haematological malignancies. For this reason the UPS represents an attractive target for therapies. There are currently two proteasome inhibitors approved for clinical use, Bortezomib and Carfilzomib. Bortezomib has been approved for the treatment of both multiple myeloma and mantle cell lymphoma. Bortezomib was the first of these to enter clinical trials thus validating the UPS as a therapeutic target.

The proteasome plays a key role within the cell so it would be expected that inhibition of the proteasome would have an impact on both malignant and normal cells. However studies have shown that leukemic cells have a high level of proteasome activity in comparison to normal cells which makes them more susceptible to proteasome inhibition (Kumatori, Tanaka et al. 1990). Nontheless, not all patients respond and a proportion of responders relapse. Relapse has been associated with dose limiting toxicities such as peripheral neuropathy (Cavaletti and Jakubowiak 2010). Carfilzomib, the second proteasome inhibitor, is an irreversible inhibitor of the proteasome which has been recently approved by the FDA for treatment of multiple myeloma. To date it has demonstrated greater efficacy and fewer side effects than bortezomib (Crawford, Chan et al. 2014).

A new generation of drugs is focused on targeting different aspects of the UPS or UBL (ubiquitin-like) pathways. In addition to ubiquitin a number of UBL proteins exist such as SUMO and neural precursor cell expressed developmentally down-regulated protein 8 (NEDD8) which use a similar enzymatic cascade as ubiquitin.

This project focuses on one such drug, MLN4923. MLN4924 is a small molecule inhibitor of NEDD8 activating enzyme (NAE). NAE controls the activation of a subset of E3 ligases known as cullin-ring ligases (CRLs). NAE catalyses the formation of a NEDD8-MLN4924 inhibitor adduct which resembles adenylated NEDD8 (Soucy, Smith et al. 2009). NAE-NEDD8 thioester cannot be formed thus locking the enzyme in an inactive state, preventing ubiquitination of CRL substrates and their subsequent degradation by the proteasome (Figure 3.1).

The NEDD8 pathway thus has a critical role in mediating the ubiquitination of numerous CRL substrate proteins many of which have been reported to be involved in cell cycle progression and survival including the DNA replication licensing factor Cdt-1, the NF-κB transcription factor inhibitor pIκBα, and the cell cycle regulators cyclin E and p27 (Soucy, Dick et al. 2010).

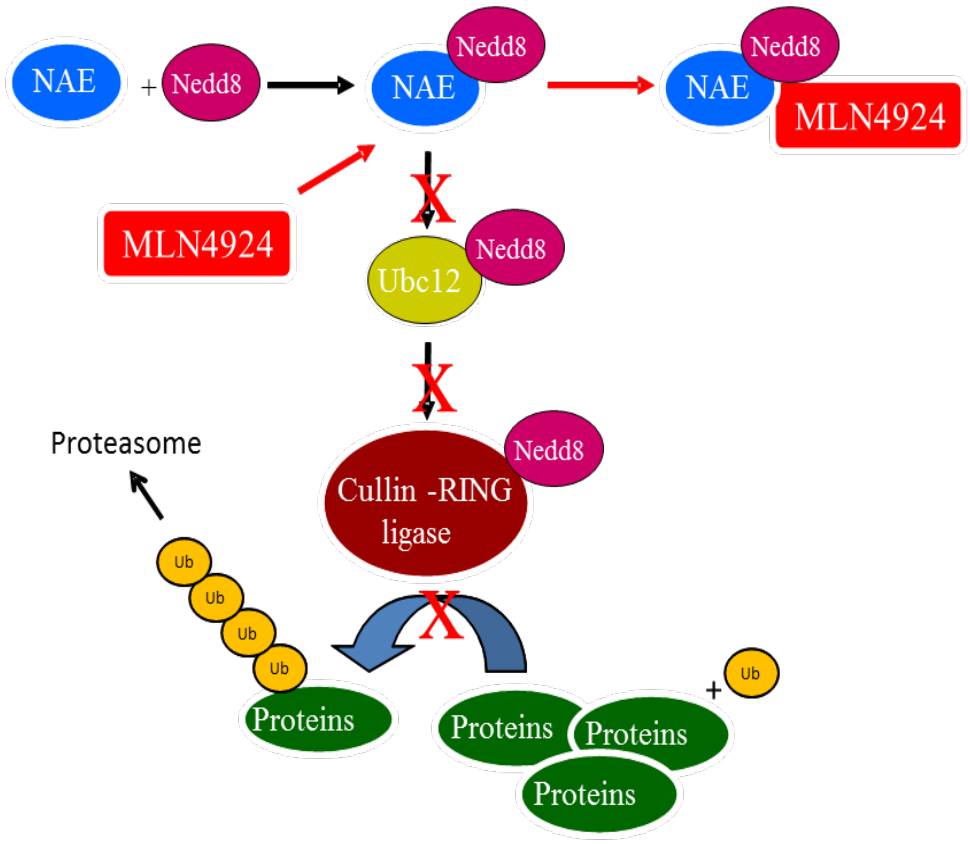

***Figure 3.1* Mechanism of Action of MLN4923.** MLN4924 is an adenosine sulfamate analogue that was identified as a selective, mechanism-based inhibitor of NEDD8-activating enzyme (NAE). MLN4924 competes with ATP and forms a NEDD8-MLN4924 adduct that tightly binds at the active site of NAE. The ubiquitin-like protein NEDD8 is then unable to transfer to its E2 enzyme-Ubc12. Thus ubiquitin turnover of these cullin-dependent proteins within the cell is disrupted. CRL protein substrates accumulate causing dramatic effects on cell cycle progression initiating DNA re-replication, DNA damage and apoptosis.

MLN4924 has completed Phase 1 clinical trials as a single agent in AML, MM, MDS and ALL (Nawrocki, Griffin et al. 2012). MLN4924 appeared to be generally well tolerated and NAE inhibition with MLN4924 resulted in clinical activity in highly refractory/multiply relapsed patients. It is currently in Phase 1 clinical trials in

combination with Azacitidine in AML patients (http://clinicaltrials.gov/show/NCT01814826).

The primary aim of this project is to investigate the effect of MLN4924 in combination with TRAIL (Tumour necrosis factor-related apoptosis-inducing ligand) in a number of haematological malignancies. TRAIL is a type II transmembrane protein which induces apoptosis in a wide variety of transformed cells but is not cytotoxic to normal cells. This has led to the proposal to use recombinant TRAIL as an agent to specifically induce death of tumour cells.

Many malignant cells, including leukemic cells are however resistant to TRAIL. There are many mechanisms of TRAIL resistance which can involve either deficient TRAILR1/TRAIL-R2 expression, enhanced levels of TRAIL decoy receptors, increased expression of inhibitors of TRAIL-mediated DISC formation such as c-FLIP, increased levels of anti-apoptotic proteins such as XIAP or Bcl-2 or other unknown mechanisms (Testa, 2010) (Figure 3.2).

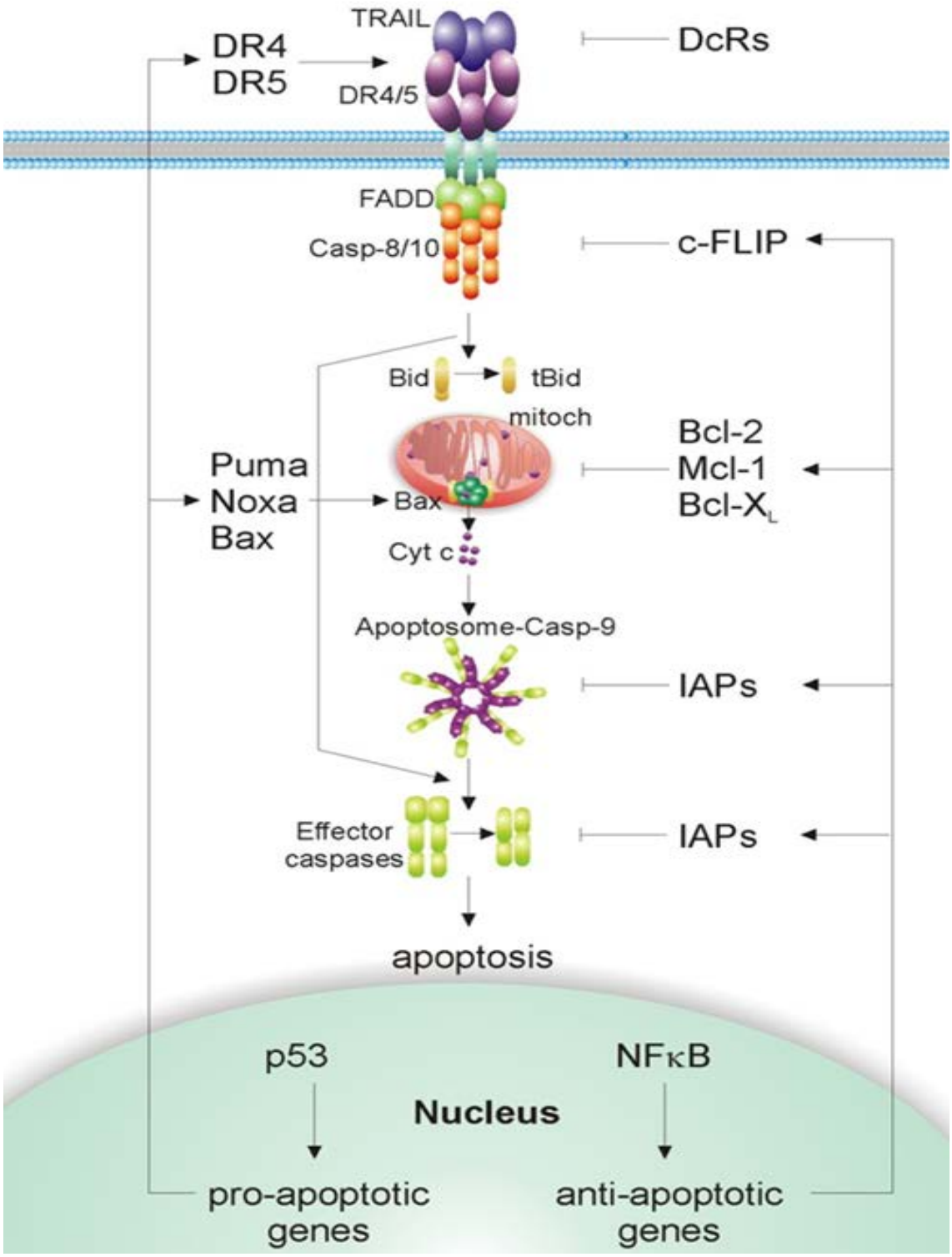

Figure 3.2 **The signalling pathway of TRAIL-induced apoptosis.**

Resistance to TRAIL can occur at different levels of the TRAIL apoptotic pathway (Mahalingam, Szegezdi et al. 2009).

Various types of combination therapies have been shown to enhance TRAIL-mediated apoptosis. Pre-clinical data involving bortezomib in combination with TRAIL receptor agonists was promising and has lead to the initiation of clinical trials in mantle cell lymphoma (MCL), DLBCL, Hodgkins disease and MM (de Wilt, Kroon et al. 2013). As MLN4924 has a much better safety profile than bortezomib we investigated here if inhibition of CRLs with MLN4924 can also sensitise to TRAIL-induced apoptosis. We propose that a combination treatment of MLN4924 and TRAIL in haematological malignancies will induce apoptosis in a synergestic manner. This chapter looks at the effect of this *in vitro*, *in vivo* animal models and *ex vivo* primary human samples. It also examines the mechanism through which such synergism could occur.

3.2 Results

3.2.1 Effects of MLN4924 in combination with TRAIL in haematological malignancies *in vitro*

First we examined the effect of MLN4924 on TRAIL-induced apoptosis *in vitro* using secondary cell lines of acute myeloid leukaemia (AML), diffuse large B cell lymphoma (DLBCL) and multiple myeloma (MM).

3.2.1.1 Acute Myeloid Leukaemia (AML)

AML cell lines (HL60, OCI-AML2, OCI-AML3, MOLM-13 and ML-1) were pre-treated with a dosage of MLN4924 (0.03 μM to 3.0 μM) for 2 h followed by TRAIL treatment for 22 h at a sublethal concentration determined in pilot experiments or with 250 ng/ml for TRAIL-resistant cell lines as detailed in Table 3.1. After treatments cells were harvested and the level of cell death induced was determined by quantifying the cells that lost mitochondrial membrane potential using tetramethylrhodamine ethyl ester (TMRE). TMRE is a cell permeant, positively-charged, red-orange dye that readily accumulates in active mitochondria due to their relative negative charge. During apoptosis the outer mitochondrial membrane is permeabilised leading to the loss of the mitochondrial memebrane potential. Thus, apoptotic cells fail to sequester TMRE in their mitochondria. Results were analysed with flow cytometry and are depicted in Figure 3.3 (A-E).

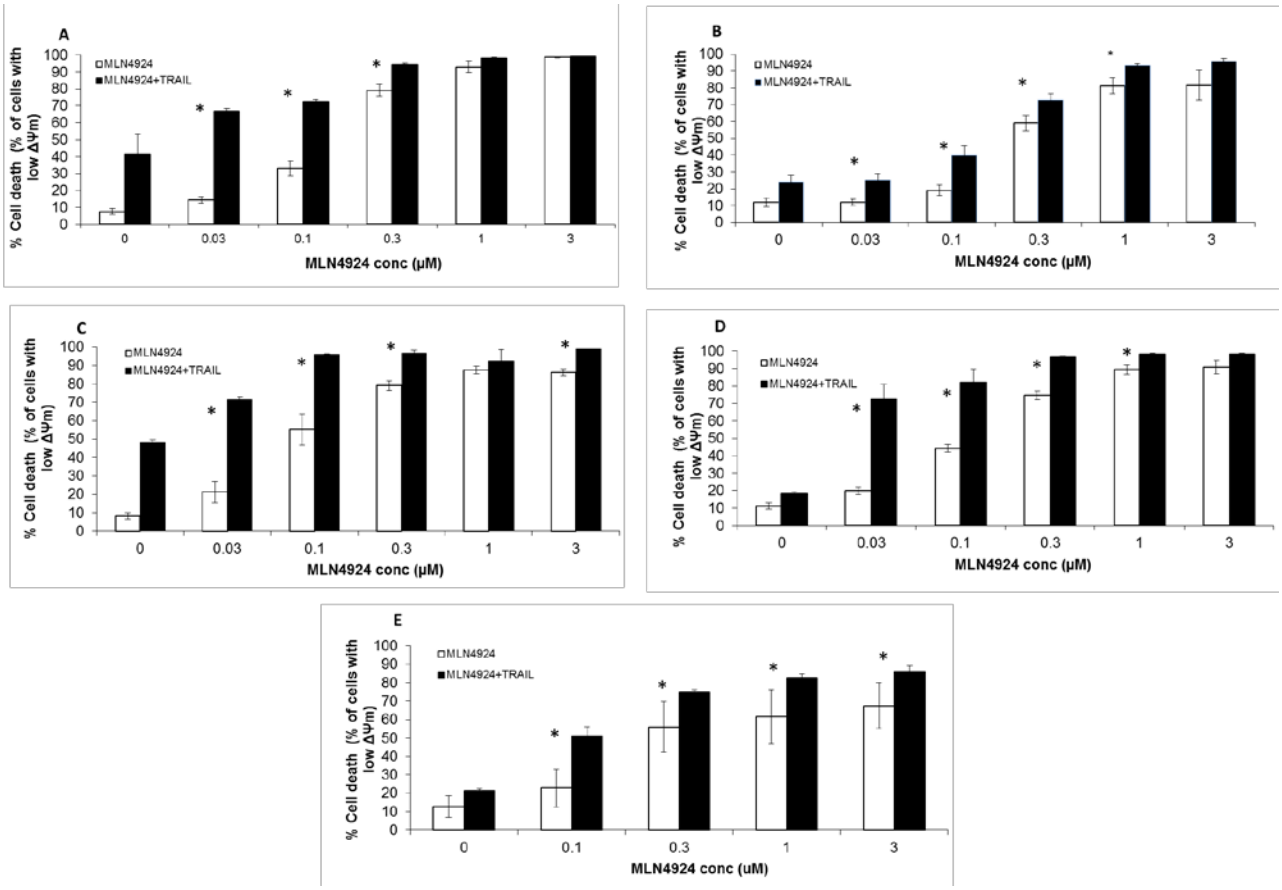

Figure 3.3 **The cytotoxic effect of the combination of MLN4924 and TRAIL in AML cell lines. A)** HL-60, **B)** OCI-AML3, **C)** MOLM-13, **D)** OCI-AML2 and **E)** ML-1 cells were seeded at 300,000/ml for 24 h prior to treatments. Cells were then pre-treated with MLN4924 for 2 h followed by TRAIL for 22 h. TRAIL doses were 250ng/ml for OCI-AML2, OCI-AML3; 25ng/ml for MOLM-13 and HL-60 and 7.5ng/ml for ML-1. Loss of mitochondrial transmembrane potential (ΔΨm) was analysed using TMRE stain. Cells were harvested and treated with 100 nM TMRE for 30 min in the dark. Fluorescence of the cells was measured at 582 nm by flow cytometry. The graphs show the percentage of cells with low ΔΨm. The white bars show the percentage of cell death induced by MLN4924 alone. The black bar at 0 μM of MLN4924 is reflective of the percentage of cell death induced by TRAIL alone and the remaining black bars show the percentage of cell death induced by the combination of MLN4924 and TRAIL. Results shown are indicative of three independent experiments +/- standard deviation. Significant differences were determined using an unpaired student t-test (*$p<0.05$).

In all of the AML cell lines tested MLN4924 could induce cell death as a single agent. With the higher doses of MLN4924 used in these experiments all cell lines reached 70-100% cell death (Figure 3.3).

From these AML cell lines OCI-AML2 and OCI-AML3 are resistant to TRAIL while HL-60, Molm-13 and ML-1 are sensitive to TRAIL-induced apoptosis. The combination of MLN4924 and TRAIL appeared to have a greater than additive effect in the majority of AML cell lines tested seen predominantly in OCI-AML2 and ML-1 cell lines.

In order to condirm the synergism between MLN4924 and TRAIL we calculated the combination index (CI) using the Chou-Talalay equation with the Compusyn software. The Chou-Talalay equation gives an additive effect a CI value of 1. For synergism which is a greater than an additive effect the CI index is lower than 1, and for antagonism which is a less than additive effect, a CI of greater than 1 (Chou 2010).

Table 3.1 **The effect of the combination of MLN4924 and TRAIL varies between AML cell lines.**

	OCI-AML2				**OCI-AML3**				**Molm-13**				**ML-1**				**HL-60**			
Response to TRAIL	Resistant				Resistant				Sensitive				Sensitive				Sensitive			
Dose of TRAIL (ng/ml)	250				250				25				7.5				25			
Dose of MLN4924	0.03	0.1	0.3	1.0	0.03	0.1	0.3	1.0	0.03	0.1	0.3	1.0	0.03	0.1	0.3	1.0	0.03	0.1	0.3	1.0
CI value – 2h pre-	0.07	0.12	0.12	0.32	0.4	0.52	0.4		0.64	0.73	0.37	0.41		0.15	0.36	0.4	0.22	0.63	0.63	0.8
CI value – 15 h pre-	0.18	0.2	0.3	2.6	-	-	-	-	1.1	0.6	1.1	2.5		0.37	0.41	0.77	-	-	-	-

We then examined whether increasing the pre-incubation with MLN4924 would enhance the synergistic effect seen on three cell lines that showed synergism between MLN4924 and TRAIL (OCI-AML2, MOLM-13 and ML-1). Cells were pre-treated with MLN4924 for 15 h prior to treatment with TRAIL for 22 h. Cells were harvested and cell death examined using TMRE stain and flow cytometry. Compusyn was then used to obtain CI values to quantify the level of synergism. These CI values are listed in the bottom row of Table 3.1. Increasing the pre-treatment time from 2 h to 15 h did not enhance synergism. In fact it served to have the opposite effect as can be seen from the observed increase in CI values (Table 3.3).

Following on from this we decided to examine the effect of MLN4924 and the combination of MLN4924 and TRAIL on long-term survival and clonogenic potential of AML cells. In order to do this, OCI-AML2 cells were treated with 0.03 µM of MLN4924 alone and in combination with TRAIL (250 ng/ml) for 22 h before being added to methylcellulose for ten days at which stage the number of colonies was counted. The number of colonies formed after MLN4924 treatment versus MLN4924 and TRAIL treatment is shown in Figure 3.3. The combination of MLN4924 and TRAIL disrupted the ability of OCI-AML2 cells to form colonies compared to either MLN4924 or TRAIL alone. The number of colonies formed after MLN4924 and TRAIL treatment was 50% less than those formed after treatment with TRAIL alone and approximately 40% less than those formed following MLN4924 treatment alone (Figure 3.4). Of note, the concentration of MLN4924 was chosen based on the lowest CI value, not on the single agent efficacy. Accordingly, the reduction in colonies induced by this low dose of MLN4924 does not reflect its maximum efficacy.

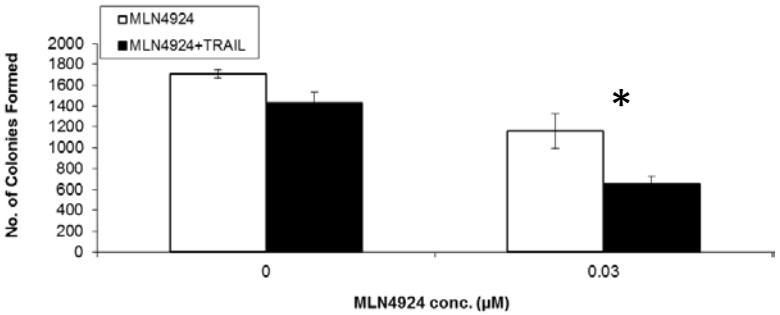

Figure 3.4 **The combination of MLN4924 and TRAIL reduced colony formation greater than MLN4924 or TRAIL alone.** OCI-AML2 cells were treated with MLN4924 and TRAIL for 2+22 h after which they were reseeded in methylcellulose and allowed to develop into colonies for ten days. At this point the number of colonies formed was counted. The white bars reflect colony formation following treatment by MLN4924 alone. The black bar at 0 µM MLN4924 is reflective of the number of colonies formed after treatment by TRAIL alone. The black bar at 0.03 µM MLN4924 shows the number of colonies formed following the combination treatment of MLN4924 and TRAIL. Results shown are the average of three independent experiments +/- standard deviation. Significant differences were determined using an unpaired student t-test (*$p<0.05$).

3.2.1.2 Multiple Myeloma (MM)

The second haematological malignancy examined was multiple myeloma. MMIS, MMIR and KMS18 cell lines were pre-treated with MLN4924 for 2 h followed by TRAIL treatment for 22 h. The percentage of apoptotic cells was then determined using TMRE with flow cytometry (Figure 3.5).

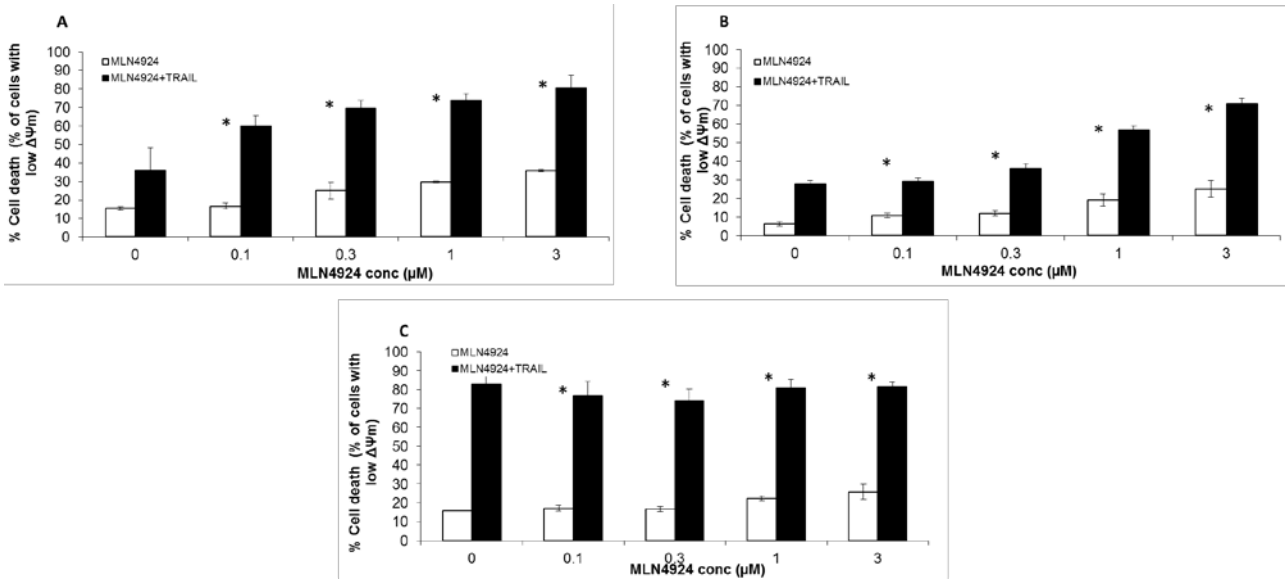

Figure 3.5 **The cytotoxic effect of the combination of MLN4924 and TRAIL in MM cell lines.** MM cell lines **A)** KMS18, **B)** MMIS and **C)** MMIR were seeded at 300,000 cells/ml for 24h prior to treatments. Cells were then pre-treated with MLN4924 for 2 h followed by a TRAIL for 22 h. TRAIL doses were 25ng/ml for KMS18 and MMIR and 250ng/ml for MMIS. Loss of mitochondrial transmembrane potential (ΔΨm) was analysed using TMRE staining with flow cytometry. Cells with low TMRE fluorescence were expressed as a percentage of the total cells. The white bars reflect the percentage cell death induced by MLN4924 alone. The black bar at 0 μM MLN4924 is reflective of the percentage cell death induced by TRAIL alone and the remaining black bars are the percentage cell death induced by a combination of MLN4924 and TRAIL. Results shown are indicative of three independent experiments +/- standard deviation. Significant differences were determined using a paired student t-test (*$p<0.05$).

MLN4924 alone can induce apoptosis in all MM cell lines tested but to a much lesser extent than in AML cell lines. The maximum level of apoptosis reached with MLN4924 was 40% in the KMS18 cell line. Of the three cell lines MMIR and KMS18 were sensitive to TRAIL-induced apoptosis whilst MMIS was resistant. The combined effect of MLN4924 and TRAIL was the highest in the KMS18 cell line followed by MM1S. MMIR failed to show a combination effect likely due to their extremely high TRAIL sensitivity.

As the graph shows, even the low dose (25 ng/ml) TRAIL induced nearly 80% cell death in this cell line. Combination index values were obtained for these experiments also and confirmed the above findings (Table 3.2).

Table 3.2 **The effect of the combination of MLN4924 and TRAIL varies between MM cell lines.**

	KMS18				**MMIR**				**MMIS**			
Response to TRAIL	Sensitive				Sensitive				Resistant			
Dose of TRAIL (ng/ml)	25				25				250			
Dose of MLN4924 (μM)	0.1	0.3	1.0	3.0	0.1	0.3	1.0	3.0	0.1	0.3	1.0	3.0
CI value	0.16	0.4	0.4	0.5	1.1	1.3	1.1	1.5	0.8	0.8	0.4	0.45

3.2.1.3 Diffuse Large B Cell Lymphoma (DLBCL)

In addition to AML and MM, DLBCL was also studied for the effect of MLN4924 and TRAIL. DLBCL cell lines tested included those from the germinal centre (GC) group and the activated B cell (ABC) group. SU-DHL-6, OCI-LY7 and OCI-LY1 are GC DLBCL while RIVA and OCI-LY10 are ABC-DLBCL. Cell lines were pre-treated with MLN4924 for 2 h followed by TRAIL for 22 h. The percentage of viable cells was measured using MTT viability assay. The MTT (3-[4,5-dimethylthiazol-2-yl]-2,5 diphenyl tetrazolium bromide) assay is a colorimetric assay based on the conversion of MTT into formazan crystals by mitochondrial enzymes of living cells (van Meerloo, Kaspers et al. 2011).

SU-DHL-6 and RIVA cells were resistant to MLN4924, while the other cell lines showed varying sensitivity to MLN4923. Of the five cell lines, OCI-LY1 and OCI-LY7 were sensitive to TRAIL and the other three were resistant. SU-DHL-6 and OCI-LY7 cells showed an additive or a low level of synergistic response to the combined treatment, while the other three cell lines the combination treatment reflected the effect of MLN4924 only (Figure 3.6, Table 3.3).

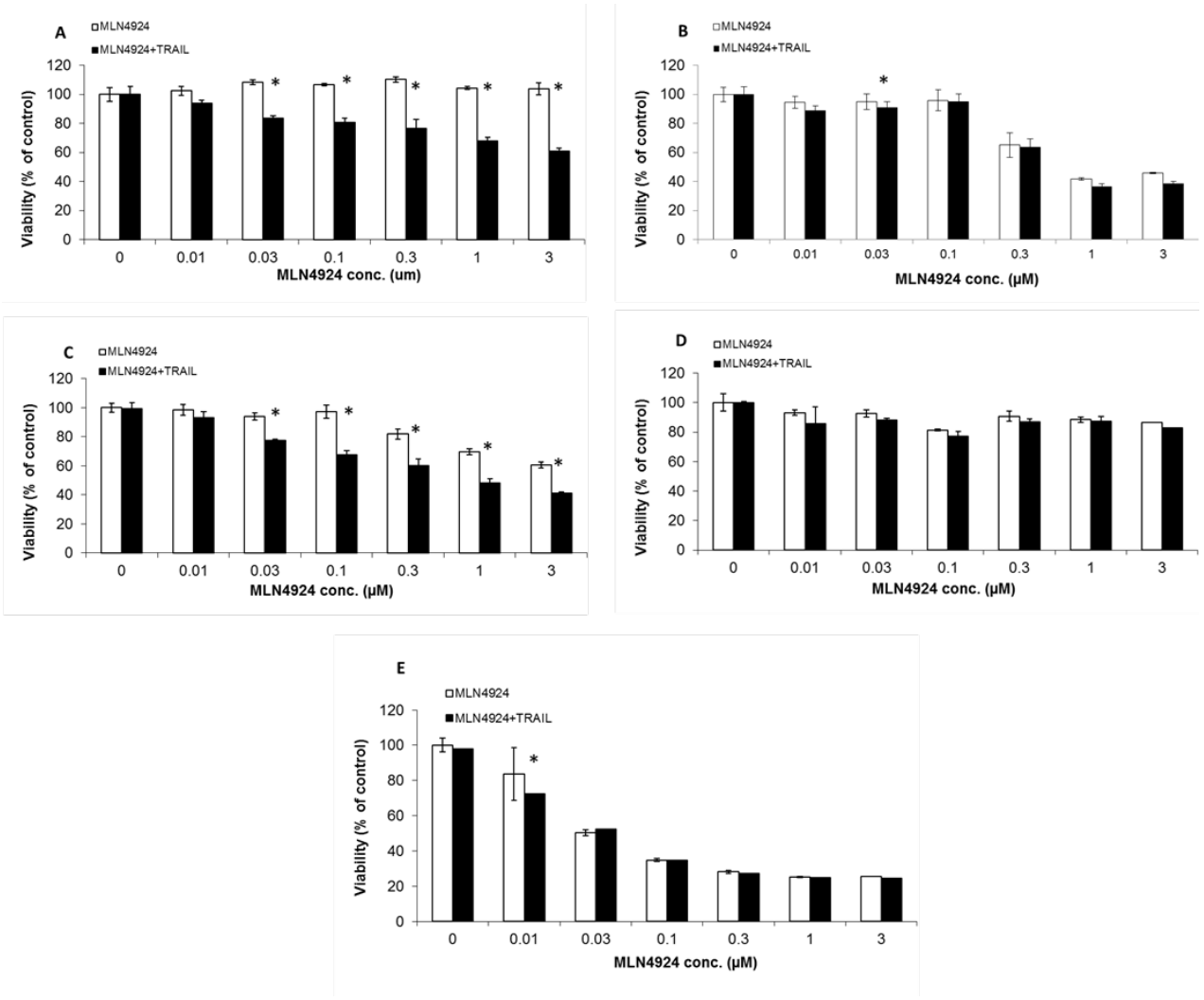

Figure 3.6 **The cytotoxic effect of the combination of MLN4924 and TRAIL in DLBCL cell lines.** DLBCL cell lines including **A)** SU-DHL-6, **B)** OCI-LY1, **C)** OCI-LY7, **D)** RIVA and **E)** OCI-LY10 were pre-treated with MLN4924 for 2 h followed by a TRAIL treatment for 22 h. TRAIL doses were 250ng/ml for SU-DHL-6, OCI-LY10 and RIVA; 10ngml for OCI-LY1 and 5ng/ml for OCI-LY7. MTT was used to examine apoptosis. The white bars reflect the % viable cells following treatment by MLN4924 alone. The black bar at 0 μM MLN4924 is reflective of the % cell death induced by TRAIL alone and the remaining black bars are the % cell death induced by a combination of MLN4924 and TRAIL. Results shown are indicative of three independent experiments +/- standard deviation. Significant differences were determined using an unpaired student t-test (*$p<0.05$).

Table 3.3 **The effect of the combination of MLN4924 and TRAIL varies between DLBCL cell lines.**

	OCI-LY1				**OCI-LY7**				**SU-DHL-6**				**OCI-LY10**				**RIVA**			
Response to TRAIL	Resistant				Resistant				Sensitive				Sensitive				Sensitive			
Dose of TRAIL (ng/ml)	250				250				25				7.5				25			
Dose of MLN4924	0.03	0.1	0.3	1.0	0.03	0.1	0.3	1.0	0.03	0.1	0.3	1.0	0.03	0.1	0.3	1.0	0.03	0.1	0.3	1.0
CI value – 2h pre-	1.6	2.3	2.3	1.1	0.78	0.7	0.78	0.9	0.7	0.65	0.6	0.2	2.6	1.6	1.6	1.6	3.7	2.4	3.6	3.6

3.2.2 Effects of MLN4924 in combination with TRAIL in haematological malignancies *in vivo*

Given that clear synergistic effect was seen *in vitro* with the combination of MLN4924 and TRAIL in AML cells (CI > 0.07) it was decided to further examine this *in vivo*. In collaboration with Millennium Pharmaceuticals two studies were carried out on OCI-M2 xenograft-carrying severe combined immunodeficiency (SCID) mice. The first study examined the effect of the combination of MLN4924 and TRAIL on OCI-M2 xenograft growth using two doses of MLN4923. The second study examined the pharmacokinetics/pharmacodynamics of MLN4924 and TRAIL in both the tumour and the plasma.

3.2.2.1 Efficacy of MLN4924 and TRAIL in AML xenografts

In collaboration with Millennium Pharmaceuticals OCI-M2 xenograft bearing SCID mice were treated with a dose of MLN4924 or TRAIL or a combination of MLN4924 and TRAIL as per Table 3.3. MLN4924 was given subcutaneously on day 1 and 4 of the week. TRAIL was then given intraperitoneally daily for the first five days of the week. Three cycles of the treatment were carried out.

On days 0, 4, 8, 11, 15, 18 and 21, measurements were taken which included the weight of the animal as an indicator of the well-being of the mouse and the volume of the tumour. Figure 3.7 shows the average weight and the average percentage change in body weight of the mice from each group tracked over 21 days for MLN4924 at the dose of 45 mg/kg (A, B) and 90 mg/kg (C, D). There was no change in animal weight during the study that would indicate that any of the treatments had any major toxicity effects (Figure 3.7).

Table 3.5 *The dosing schedule for OCI M2 xenograft carrying SCID mice*

GROUP	A	B	C	D	E	F	G	H
NUMBER OF ANIMALS	5	5	10	10	10	10	10	10
TREATMENT	MLN4924 Vehicle	TRAIL Vehicle	MLN4924 Vehicle + TRAIL Vehicle	MLN4924 45mg/kg	MLN4924 90mg/kg	TRAIL 5mg/kg	MLN4924 45mg/kg + TRAIL 5mg/kg	MLN4924 90mg/kg + TRAIL 5mg/kg

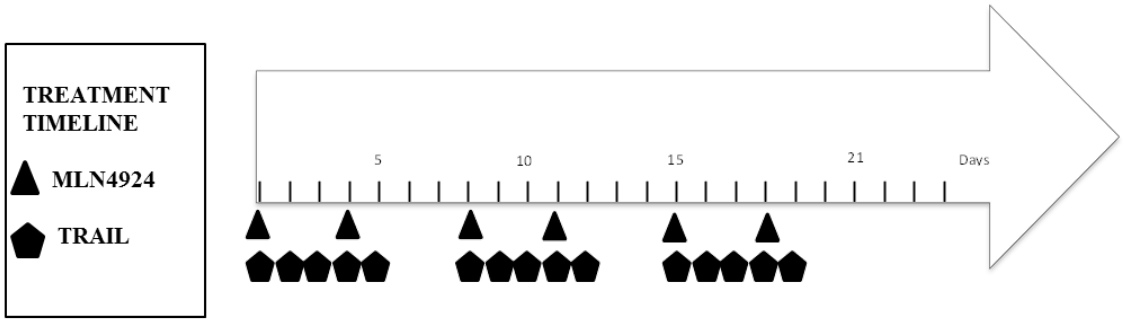

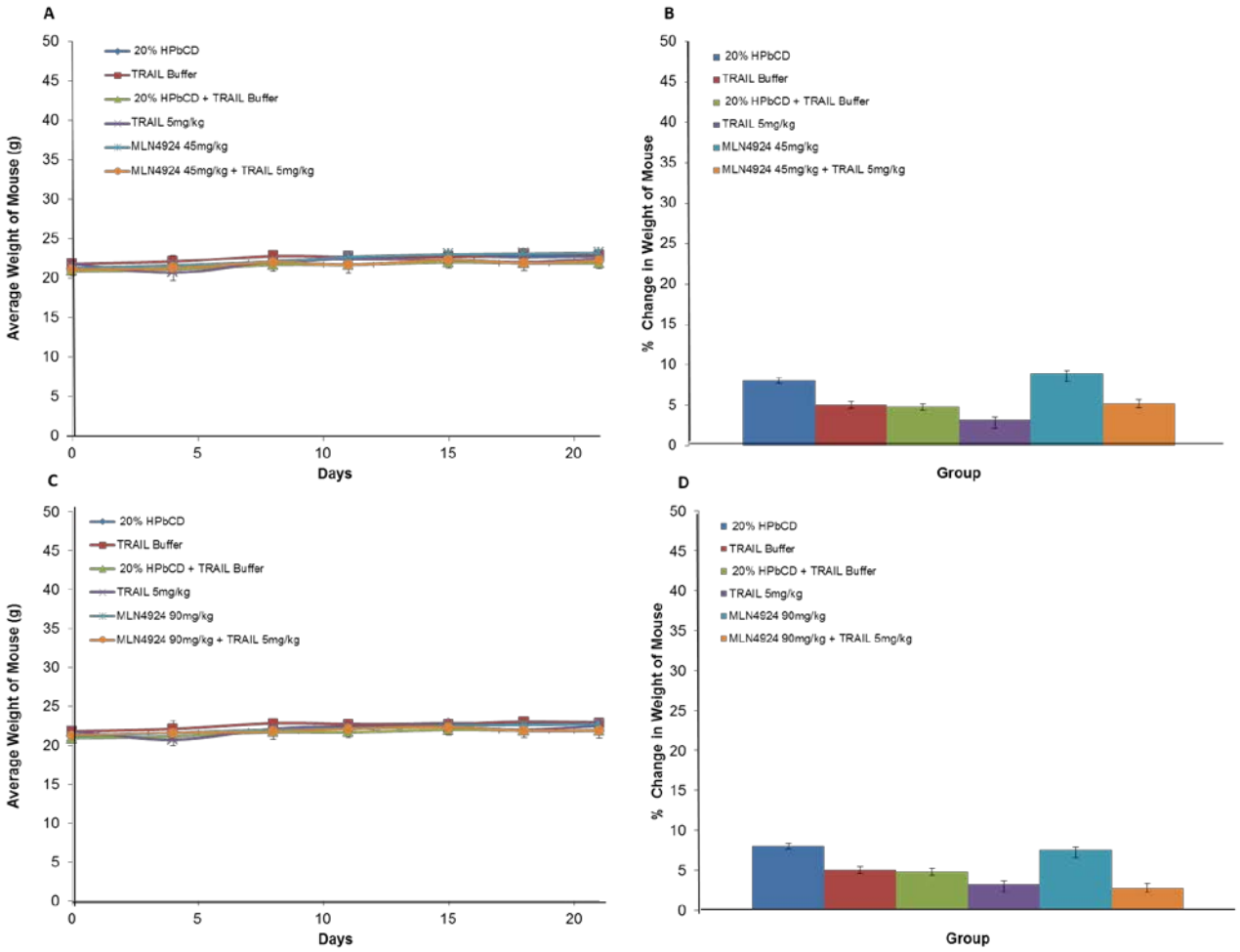

Figure 3.7 **The change in weight of the mice during the study indicates the treatments have no major toxicity effects.** MLN4924, TRAIL and a combination of MLN4924 and TRAIL has no impact on the weight of the mice during the course of the study. A) Mice were treated with MLN4924 (45 mg/kg), TRAIL (5mg/kg) and a combination of MLN4924 and TRAIL as per Table 3.3. The graph shows the weight of the mouse tracked over the course of the study - 21 days. B) This graph shows the % change in the weight of the mouse from Day 0 to Day 21. C) Mice were treated with MLN4924 (90 mg/kg), TRAIL (5 mg/kg) and a combination of MLN4924 and TRAIL as per Table 3.3. This graph shows the weight of the mouse tracked over the course of the study - 21 days. D) This graph shows the % change in the weight of the mouse from Day 0 to Day 21. Data shown is representative of the average from each individual group.

In addition, the volume of the tumour was monitored throughout the study. Figure 3.8 shows the average volume of the tumour and the percentage change in the tumour volume of the mice from each group for MLN4924 treated with 45 mg/kg and TRAIL (A, B) and 90 mg/kg plus/minus TRAIL (C, D). MLN4924 as a single agent could greatly reduce the growth of the tumour. This is evident with both doses of MLN4924 tested –

45mg/kg and 90mg/kg. The combination of MLN4924 at 45 mg/kg with TRAIL resulted in reducing the growth of the tumour even further (Figure 3.8A and B). However the combination of MLN4924 at 90 mg/kg and TRAIL not only impacted on the growth of the tumour but also reduced the size of the tumour (Figure 3.8 C and D).

The initial size of the tumour prior to treatments was approximately 150 $mm^{3.}$ Tumours grew up to approximately 650 mm^3 with TRAIL alone and vehicle controls. Treatments with MLN4924 alone and a combination of MLN4924 (45 mg/kg) and TRAIL disrupted the growth of the tumour causing it not to grow beyond 200 $mm^{3.}$ A dose of MLN4924 (90 mg/kg) and TRAIL (5 mg/kg) also had the ability to inhibit the growth of the tumour and in addition reduced the size of the tumour to less than 100 $mm^{3.}$

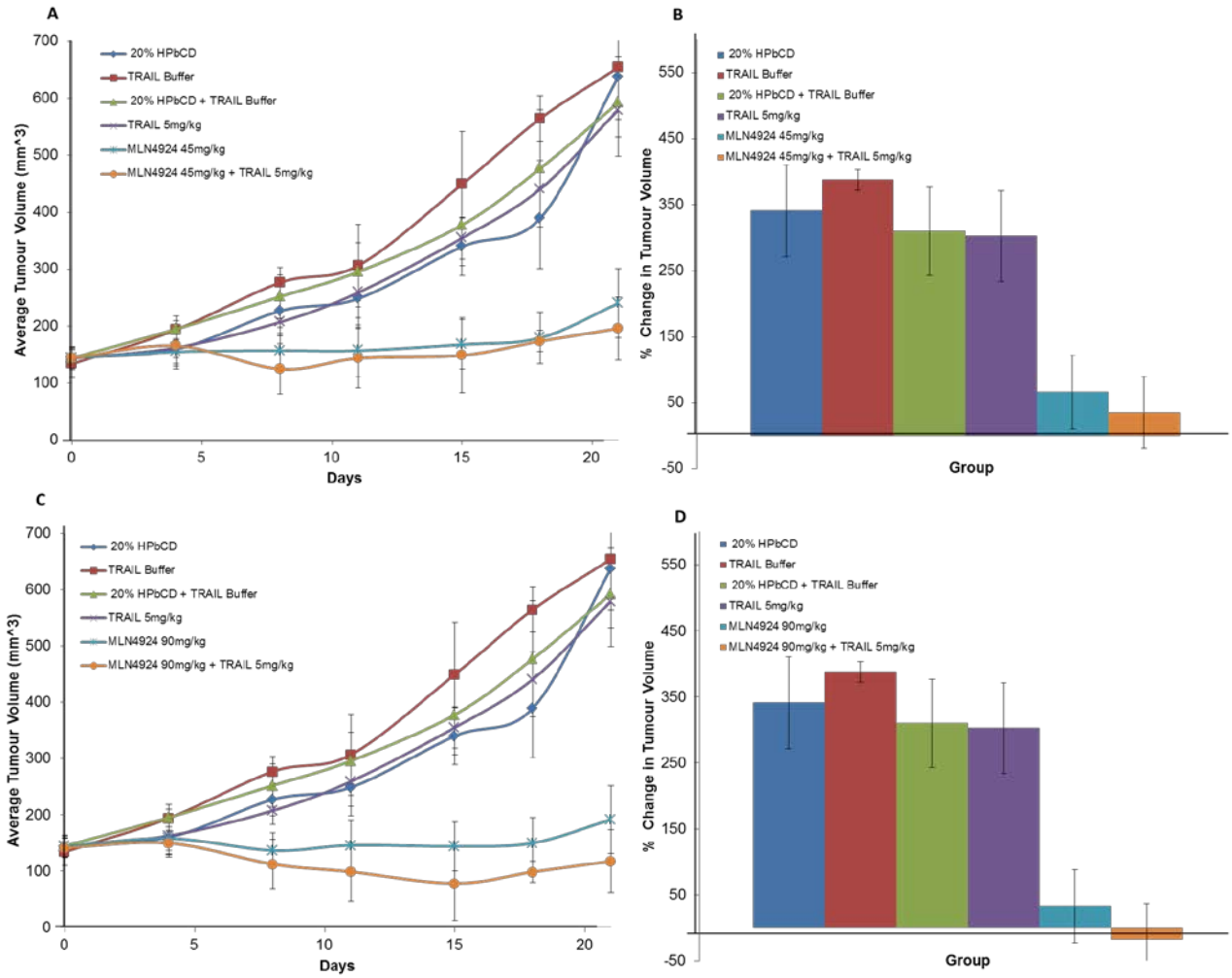

Figure 3.8 **A combination of MLN4924 and TRAIL not only impacts on the growth of the tumour but leads to a reduction in the size of the tumour in an AML xenograft model. A)** OCI M2 xenograft carrying mice were administered with MLN4924 (45 mg/kg), TRAIL (5 mg/kg) and a combination of MLN4924 and TRAIL as per Table 3.4 and the volume of the tumour of each mouse tracked over the course of the study - 21 days. This graph shows the average volume of tumours from each treatment group over 21 days. **B)** The graph is representative of the % average change in the tumour volume of the mouse from Day 0 to Day 21.
C) Mice were treated with MLN4924 (90 mg/kg), TRAIL (5 mg/kg) and a combination of MLN4924 and TRAIL as per Table 3.4 and tumour volume was tracked over the course of the study - 21 days. This graph shows the average volume of tumours from each treatment group over 21 days. **D)** This graph shows the % average change in tumour volume of the mouse from Day 0 to Day 21. Data shown is representative of the average from each individual treatment group.

3.2.2.2 Pharmacokinetic/Pharmacodynamic (PK/PD) study in AML xenografts.

Whilst the results from the initial *in vivo* study (Figure 3.8) were promising it was questionable if the optimal dosing schedule was in place. We also noticed that the effect of MLN4924 plateaued between day 15-18 and then tumour volume started to slightly increase. In order to investigate this we again collaborated with Millennium Pharmaceuticals to carry out a pharmacokinetic/pharmacodynamics study. OCI M2 xenograft-carrying SCID mice were used for this study with a dosing schedule as per Table 3.6. Mice were treated with a dose of MLN4924 at 45 mg/kg or 90 mg/kg alone and in combination with TRAIL at 5 mg/kg. Samples were taken at 1 h, 4 h, 8 h, 24 h and 48 h timepoints. Samples at each of these timepoints included tumour tissue and plasma to determine MLN4924 and TRAIL concentrations (Figure 3.9). In addition tumour tissue samples were taken at each timepoint for Western blot analysis (Figure 3.10).

Table 3.6 *Treatment schedule for OCI M2 xenograft carrying SCID mice*

Group	Number of Animals	Treatment	Schedule (h)
A	3	vehicle (20% cyclodextrin) s.c.	24
B	3	45	4
C	3	45	8
D	3	45	24
E	3	45	48
F	3	90 mg/kg MLN4924 (s.c.)	4
G	3	90 mg/kg MLN4924 (s.c.)	8
H	3	90 mg/kg MLN4924 (s.c.)	24
L	3	90 mg/kg MLN4924 (s.c.)	48
M	3	TRAIL 5 mg/kg IP	4
N	3	TRAIL 5 mg/kg IP	8
O	3	TRAIL 5 mg/kg IP	24
P	3	TRAIL 5 mg/kg IP	48
Q	3	45 mg/kg MLN4924 SC + TRAIL 5 mg/kg IP	4
R	3	45 mg/kg MLN4924 SC + TRAIL 5 mg/kg IP	8
S	3	45 mg/kg MLN4924 SC + TRAIL 5 mg/kg IP	24
T	3	45 mg/kg MLN4924 SC + TRAIL 5 mg/kg IP	48
U	3	90 mg/kg MLN4924 SC + TRAIL 5 mg/kg IP	4
V	3	90 mg/kg MLN4924 SC + TRAIL 5 mg/kg IP	8
W	3	90 mg/kg MLN4924 SC + TRAIL 5 mg/kg IP	24
X	3	90 mg/kg MLN4924 SC + TRAIL 5 mg/kg IP	48

NAE inhibition by MLN4924 was determined by detecting NEDDylated cullins via western blotting on samples taken from the tumour at 4h, 8h, 24h and 48h (Figure 3.9). NEDD8 is an 8 kDa protein. When NEDD8 is attached to cullins it can be detected on Western blot at 80 kDA. MLN4924 results in NEDD8 becoming detached from the cullins, inhibiting their E3 ligase activity and is no longer detectable at 80 kDa. Figure 3.9 shows cullin-bound NEDD8 signal at 80 kDa. A dose of 45 mg/kg of MLN4924 achieved a near complete inhibition of NAE for up to 8 h after treatment. By 24 h NEDD8 is again detectable attached to the cullins (Figure 3.9A). The higher 90 mg/kg MLN4924 dose had the same level but longer lasting effect where reattachment of NEDD8 to the cullins was detectable again between 24 h and 48 h (Figure 3.9(B)). This indicates that the effect of MLN4924 diminishes between 24 h and 48 h post administration and therefore a more optimal dosing strategy for an *in vivo* study would involve treating with MLN4924 every 24 h instead of every 3-4 days.

To further investigate the pharmacokinetics of MLN4924 the concentrations of MLN4924 in both the plasma and tumour at 1 h, 4 h, 8 h, 24 h and 48 h were determined. Levels of MLN4924 in the plasma were depleted by at least 1000-fold by 6 h (Figure 3.9A). By 24 h MLN4924 concentration in the plasma returned to baseline, below detectable level in line with the cullin NEDDylating pattern detected in the tumour tissue. This observation applies to both doses of MLN4924 used – 45 mg/kg and 90 mg/kg. The concentration of MLN4924 in the tumour is retained longer than in the plasma. It dropped by approximately 100-fold after 24 h and was almost depleted by 48 h (Figure 3.9B). The presence of TRAIL had no effect on the pharmacokinetics of MLN4923. Treatments with MLN4924 were given on days 1 and 4 of each week throughout the initial *in vivo* study. The results seen from the pharmacokinetic study (Figure 3.9) suggest that these treatments would need to be given more frequently in a future study in order to see greater reduction in tumour size.

Levels of TRAIL in both the tumour and plasma were measured by enzyme-linked immunosorbent assay (ELISA). In order to measure the level of TRAIL in the tumour, the samples were homogenised and lysed in RIPA buffer. We found that despite earlier reports about the very short in vivo half-life time of TRAIL (a few minutes in mice), TRAIL remained in the plasma for up to 4 h but by this time levels have dropped significantly. In the tumour however TRAIL was detectable up to 24 h post-administration (Figure 3.9 (D)).

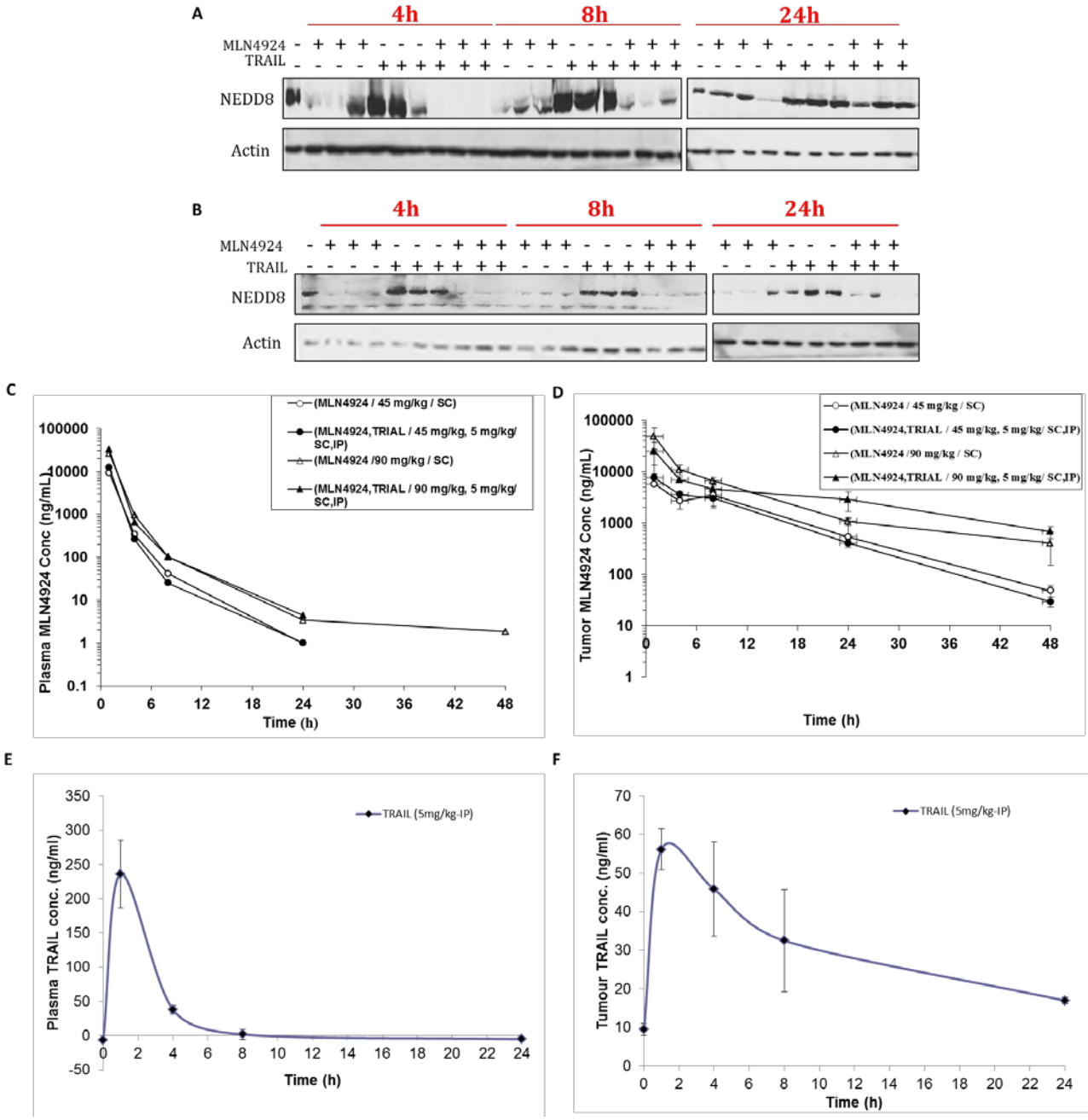

Figure 3.9 **Pharmacokinetic/pharmacodynamic analysis in AML xenograft models**. OCI M2 xenograft carrying mice were administered with MLN4924 at a dose of 45 mg/kg or 90 mg/kg alone and in combination with TRAIL at a dose of 5 mg/kg. Tumour tissue samples were taken at different timepoints up to 24 h. These samples were then lysed and analysed for cullin-NEDD8 levels by western blot and densiotometry. **(A)** Treatment groups analysed include MLN4924 (45 mg/kg), TRAIL (5 mg/kg) and a combination of MLN4924 and TRAIL at these doses. **(B)** Treatment groups analysed include MLN4924 (90 mg/kg), TRAIL (5 mg/kg) and a combination of MLN4924 and TRAIL at these doses. Actin was used as a loading control. The levels of MLN4924 in the plasma **(C)** and in the tumour **(D)** were determined at different timepoints up to 48 h. The levels of TRAIL in the plasma **(E)** and in the tumour **(F)** were also assessed at different timepoints up to 24 h. This data is representative of the average of three mice in each group.

In addition, the effect of MLN4924 and TRAIL inducing tumour cell death was looked at. Levels of cleaved caspase-3 and PARP were used as an indicator of tumour cell apoptosis examined with Western blotting on samples taken from the tumour at 4 h, 8 h, 24 h and 48 h (Figure 3.10). Pro-caspase-3 processing and caspase-3-mediated PARP cleavage were then quantified using densitometry (Figure 3.10).

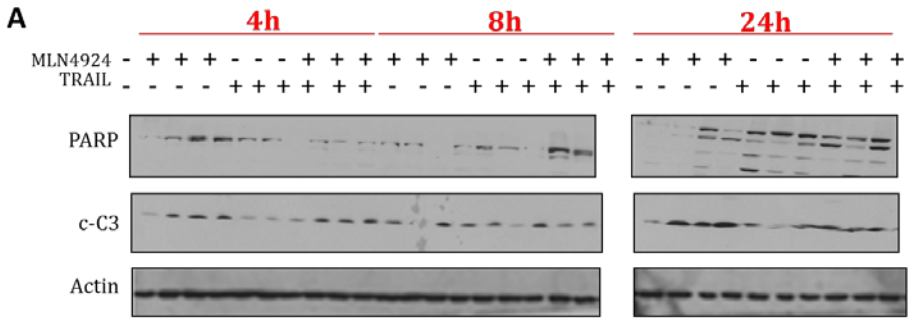
A
4h
8h
24h
MLN4924
TRAIL
PARP
c-C3
Actin

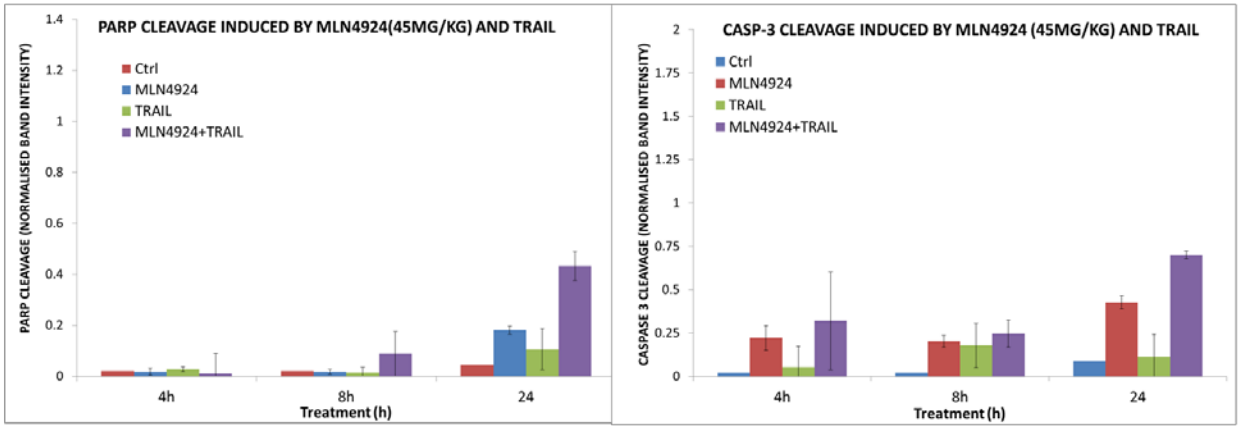
PARP CLEAVAGE INDUCED BY MLN4924(45MG/KG) AND TRAIL
PARP CLEAVAGE (NORMALISED BAND INTENSITY)
Ctrl
MLN4924
TRAIL
MLN4924+TRAIL
Treatment (h)
CASP-3 CLEAVAGE INDUCED BY MLN4924 (45MG/KG) AND TRAIL
CASPASE 3 CLEAVAGE (NORMALISED BAND INTENSITY)

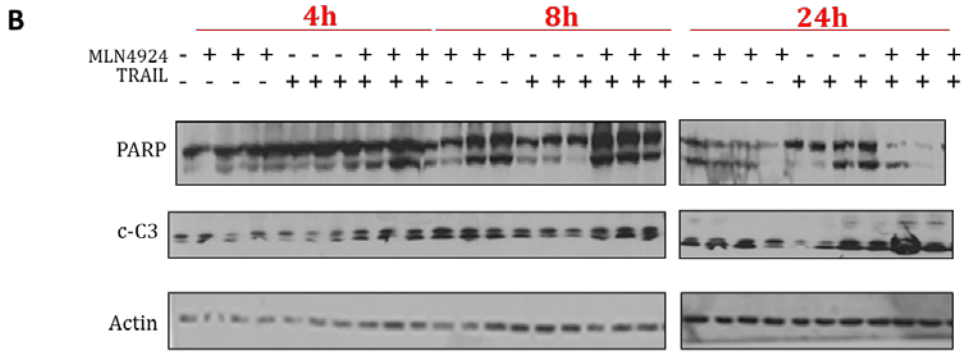
B
4h
8h
24h
MLN4924
TRAIL
PARP
c-C3
Actin

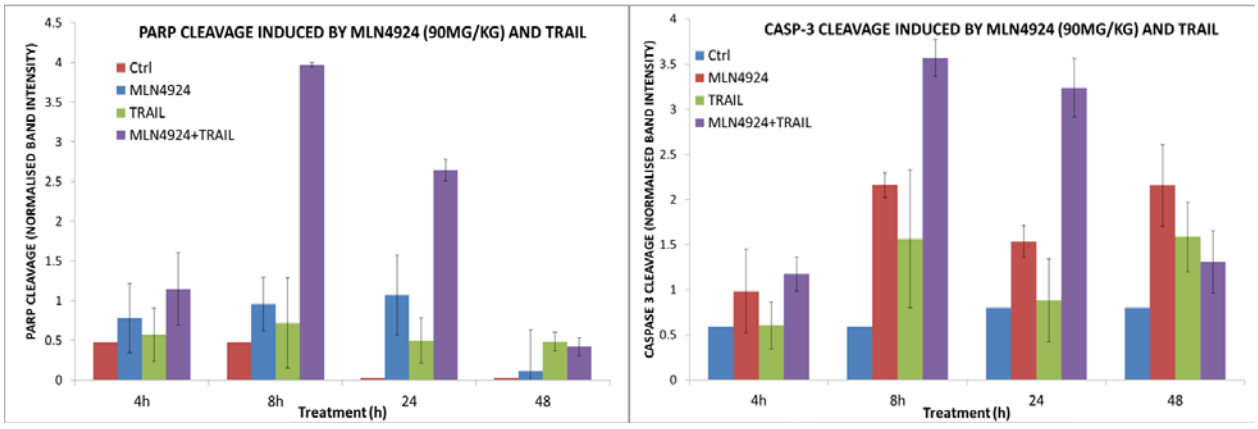
PARP CLEAVAGE INDUCED BY MLN4924 (90MG/KG) AND TRAIL
PARP CLEAVAGE (NORMALISED BAND INTENSITY)
Ctrl
MLN4924
TRAIL
MLN4924+TRAIL
Treatment (h)
CASP-3 CLEAVAGE INDUCED BY MLN4924 (90MG/KG) AND TRAIL
CASPASE 3 CLEAVAGE (NORMALISED BAND INTENSITY)

Figure 3.10 **Levels of caspase-3 and PARP processing indicate a synergestic effect between MLN4924 and TRAIL at both doses of MLN4924 tested.** Tumour tissue samples were taken at different timepoints up to 48 h. These samples were then lysed and analysed for cleaved caspase-3 and PARP by western blot and densiotometry. **(A)** Treatment groups analysed include MLN4924 (45 mg/kg), TRAIL (5 mg/kg) and a combination of MLN4924 and TRAIL at these doses. **(B)** Treatment groups analysed include MLN4924 (90 mg/kg), TRAIL (5 mg/kg) and a combination of MLN4924 and TRAIL at these doses. Actin was used as a loading control.

3.2.3 Mechanism by which MLN4924 sensitises AML to TRAIL-induced apoptosis

3.2.3.1 TRAIL Apoptotic machinery is not involved in MLN4924 sensitisation to TRAIL-induced apoptosis

The interaction of TRAIL with its two death receptors DR4 and DR5 is the initial step in TRAIL-induced apoptosis. The binding of TRAIL leads to trimerization of the death receptors and activation of a receptor-mediated death pathway. The activated death receptors can recruit FADD which in turn leads to the recruitment of caspase-8 and formation of the death-inducing signalling complex (DISC). DISC formation leads to activation of the caspase protease cascade, resulting in cell death (Walczak et al, 2007).

In order to determine the mechanism by which OCI-AML2 cells can be sensitised by MLN4924 to TRAIL we initially looked at different members of the TRAIL apoptotic pathway. OCI-AML2 cells are resistant to TRAIL treatment. TRAIL can incur resistance at different stages and we examined if MLN4924 could have an impact at one of these stages.

Resistance can occur at the level of the death receptors so we began by looking at the effect of MLN4924 on DR4, DR5, DCR1 and DCR2. For these experiments OCI-AML2 cells were treated with MLN4924 for 6 h after which we looked at the cell surface expression of DcR1, DcR2, DR4 and DR5. This revealed that OCI-AML2 cells contain higher levels of DR5 than the other death receptors but MLN4924 had no impact on DcR expression or increased DR4/DR5 expression (Figure 3.11A).

We proceeded by using Western blotting to monitor changes in apoptosis-regulatory proteins following treatment with 0.1 µM of MLN4924 over a 12 h timecourse. These proteins included the caspase-8 inhibitor, c-FLIP (Figure 3.11(B)), the pro- and anti-apoptotic members of the Bcl-2 family: Bcl-2, Bcl-X_L, Mcl-1, Bim, Puma, Noxa, Bik and Bad (Figure 3.11C), the inhibitor of apoptosis protein family proteins: cIAP1, cIAP2 and XIAP (Figure 3.11D). Detection of Cullin-NEDD8 by Western blotting was used in these experiments to monitor that MLN4924 is functional (Figure 3.11 D).

Of these proteins, we could detect a slight reduction of cFLIP-long by MLN4924 (Figure 3.11B) however the levels of cFlip-short remained uchanged making it an unlikely target of MLN4923. Of the IAP family, we could not detect any decrease in levels of the

IAPs. BV6, an IAP inhibitor was used in these experiments as a positive control for IAP degradation (Figure 3.11C). The most notable change we found amongst the apoptosis-regulatory proteins examined was in the Bcl-2 family members. Expression levels of Noxa, Mcl-1 and Bim increased after 6 h of MLN4924 treatment (Figure 3.11D).

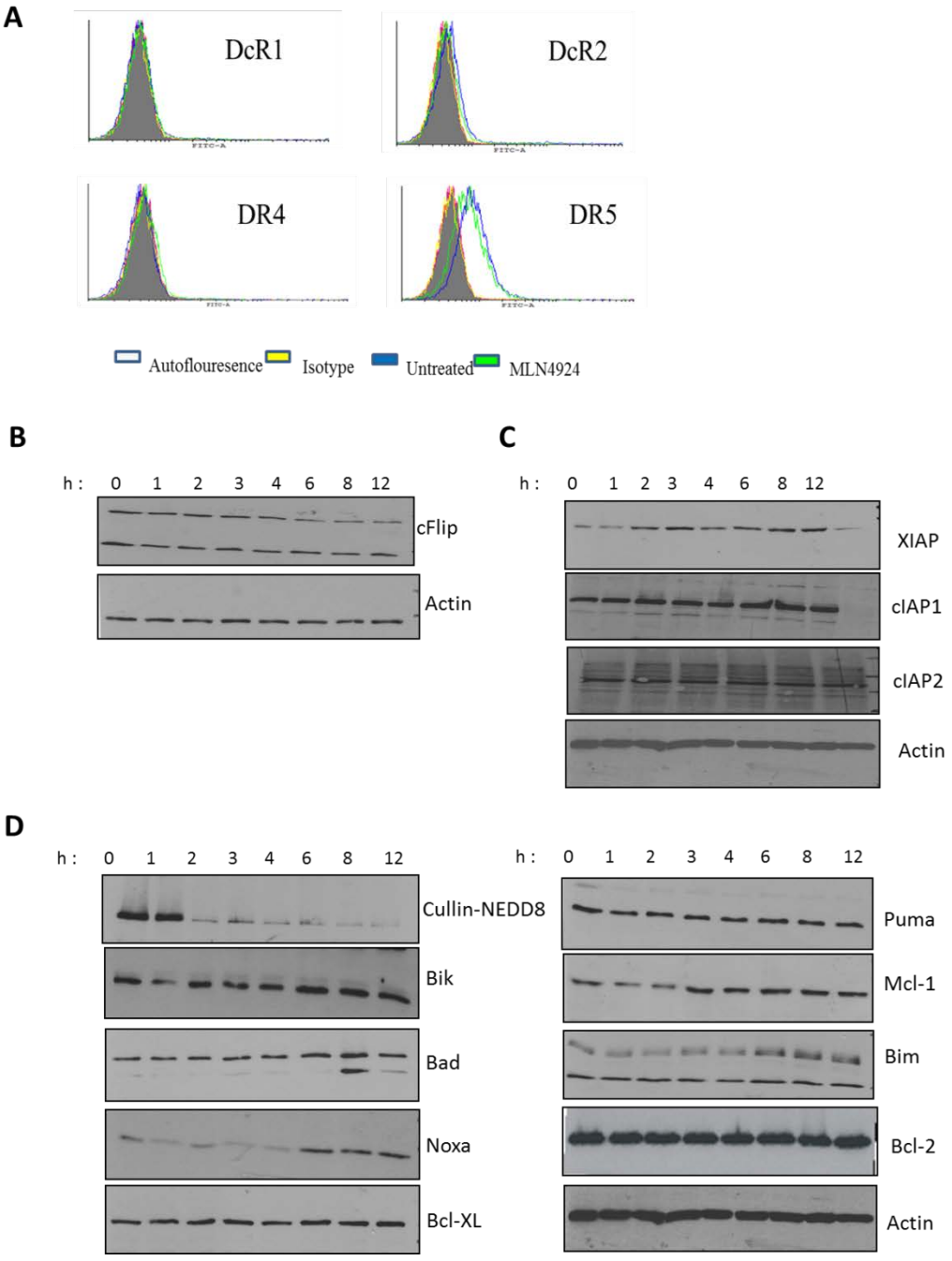

Figure 3.11 **OCI-AML2 cells are not sensitised to TRAIL and MLN4924 via alteration of DISC components.** **A)** OCI-AML2 cells were treated with 0.1 µM MLN4924 for 6 h before being harvested, incubated with cell surface receptor antibody and analysed for cell surface expression of DR4, DR5, DcR1 and DcR2 using flow cytometry. OCI-AML2 cells were treated with 0.1 µM MLN4924 and harvested at different timepoints over 12 h. Cells were lysed and proteins detected with western blotting.Membranes were probed overnight for detection of **B**) cFlip, **C)** IAPs and **D)** Bcl-2 family members. The data are representative of three experiments.

From examining the TRAIL apoptotic machinery it was evident that the greatest change was in Bcl-2 family members. We looked at this further in tumour samples from OCI-M2 xenografts (Figure 3.12 (A)). These samples had been treated with 180 mg/kg of MLN4924 for a timecourse up to 48 h. Samples were then lysed and analysed by Western blot for the proteins of interest, namely Noxa, Bim and Mcl-1. Noxa and Mcl-1 were upregulated inresponse to MLN4924 treatment as was also evident in the *in vitro* experiments. Bim was also upregulated *in vitro,* but we failed to detect an induction of Bim *in vivo*.

We further analysed Noxa and Mcl-1 levels in the samples from the pharmacokinetic/ pharmacodynamics study (Section 3.2.2.2). Samples were treated with MLN4924, TRAIL and a combination of MLN4924 and TRAIL for 4 h, 8 h and 48 h. Doses of MLN4924 included 45 mg/kg (Figure 3.12B) and 90 mg/kg (Figure 3.12C). This data corroborated that MLN4924 treatment increased the expression of both Noxa and Mcl-1.

Noxa is a pro-apoptotic BH3 protein whilst Mcl-1 is an anti-apoptotic/pro-survival protein. Downregulation of Mcl-1 is associated with the apoptotic process. Mcl-1 has the ability to bind Bcl-2 family members, in particular Noxa. Noxa has been shown to be involved in modulating the expression of Mcl-1. It has been shown to trigger the degradation of Mcl-1 (Dousset et al, 2011). We focused on learning more about the role Noxa may play in sensitising TRAIL-resistant OCI-AML2 cells to MLN4923.

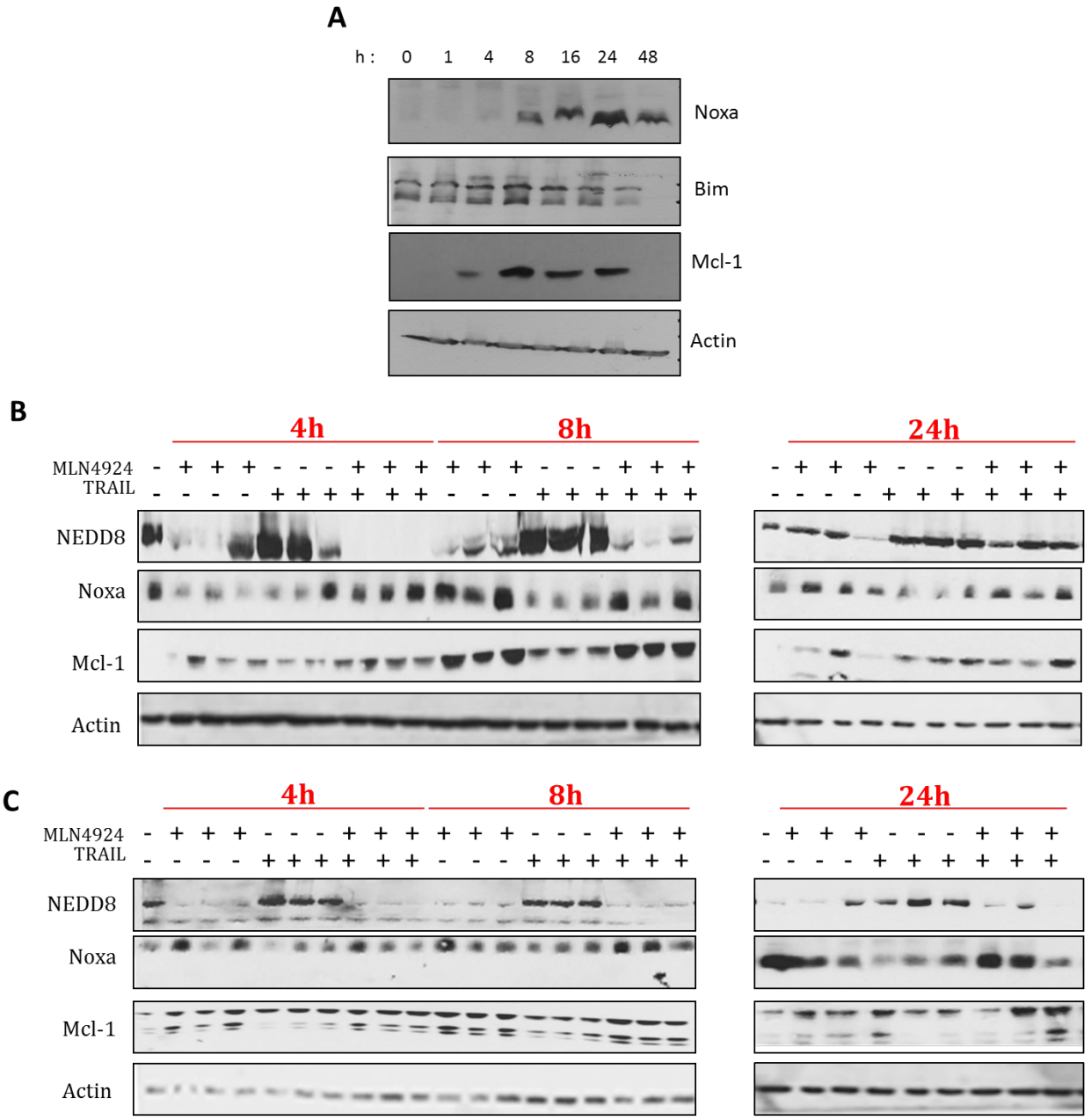

Figure 3.12 **Tumour samples from OCI M2 xenograft carrying mice treated with MLN4924 show increased expression of the Bcl-2 family members Noxa and Mcl-1. A)** OCI M2 xenograft carrying mice were treated with 180 mg/kg of MLN4924 for the times indicated. Samples were harvested and lysed for analysis of Bim, Noxa and Mcl-1 via western blot. Actin served as a loading control. **B**) OCI M2 xenograft carrying SCID mice were treated with MLN4924 45 mg/kg alone or in combination with TRAIL at 5 mg/kg for the indicated timepoints. Samples were lysed and analysed by western blot for NEDD8, Noxa and Mcl-1. Actin served as a loading control. **C)** OCI M2 xenograft carrying SCID mice were treated with MLN4924 90 mg/kg alone or in combination with TRAIL at 5 mg/kg for the indicated timepoints. Samples were lysed and analysed by western blot for NEDD8, Noxa and Mcl-1. Actin served as a loading control.

In order to learn more about Noxa in this scenario we investigated whether upregulation of Noxa was as a direct result of its degradation being inhibited by inhibiting the cullin-ring ligases by MLN4924 or was a result of a transcription factor level being modified by MLN4923. For these experiments OCI-AML2 cells were treated with 0.1 μM MLN4924 with or without the protein translation inhibitor cyclohexamide (CHX, 5 μg/ml) for a timecourse up to 12 h. Samples were then lysed and underwent Western blot analysis for Noxa (Figure 3.13(A)). MLN4924 causes an increase in the expression levels of Noxa but in the presence of CHX Noxa is undetectable. This is an indication that Noxa is transcriptionally upregulated and its increase is not a direct result of its degradation being inhibited.

To then investigate the importance of Noxa in MLN4924 sensitising to TRAIL-induced apoptosis we incorporated an shRNA-xpressing plasmid against Noxa into OCI-AML2 cells. This shRNA against Noxa is in the lentiviral plK0 vector so as a control measure an empty plk0 vector was used. OCI-AML2 cells were transduced with both of these lentiviral vectors and cells expressing the plasmids were selected using puromycin. Transduced cells were then treated with 0.1 μM MLN4924 for 12 h to determine whether the shRNA was able to knock down basal expression as well as MLN4924-mediated induction of Noxa (Figure 3.13B). It was evident on the Western blots that the shRNA could substantially reduce basal Noxa expression and reduce upregulation of Noxa following MLN4924 treatment.

We proceeded to look at the effect of silencing Noxa on the effect of MLN4924 (Figure 3.13 (C) and MLN4924 combined with TRAIL (Figure 3.13D). Downregulation of Noxa partially protected the cells from apoptosis induced by MLN4924 alone. On the other hand downregulation of Noxa had absolutely no effect on apoptosis induced by the combination of MLN4924 and TRAIL.

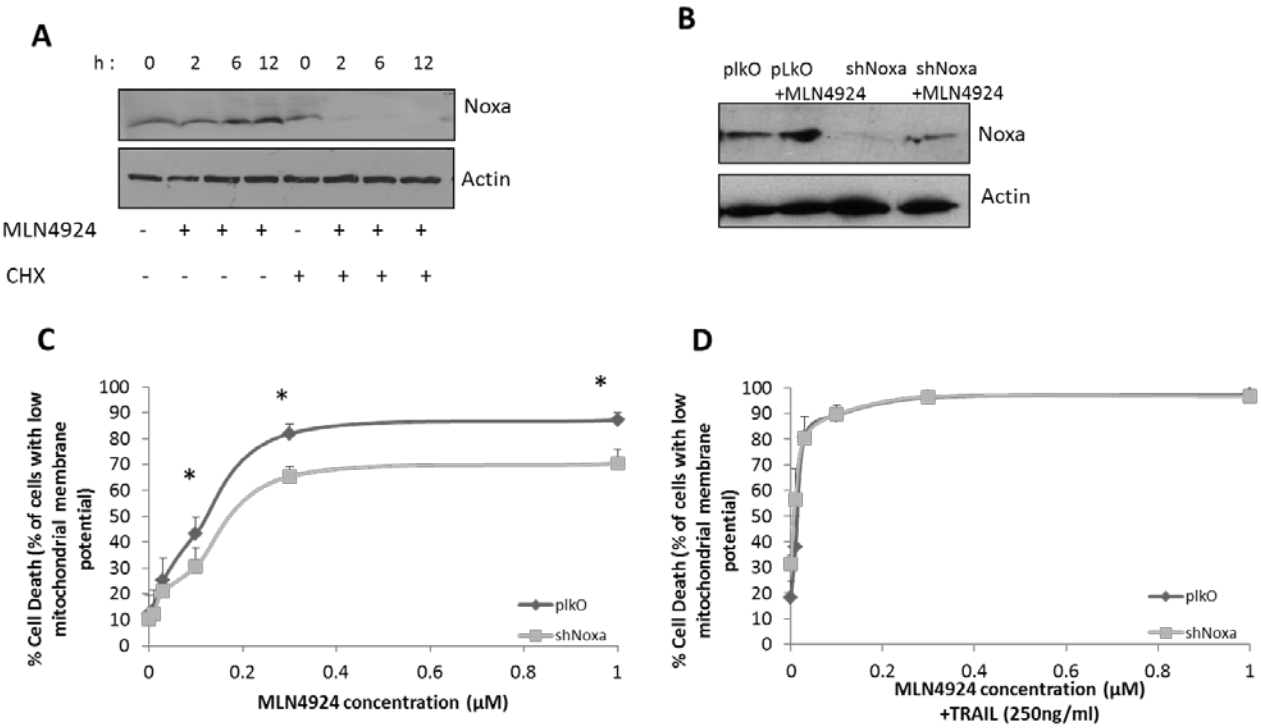

Figure 3.13 **Noxa is transcriptionally upregulated but does not play a role in MLN4924 mediated sensitisation to TRAIL. A)** OCI-AML2 cells were treated with 0.1 μM MLN4924 alone and in combination with 5 μg/ml CHX for the times indicated. Samples were then harvested and lysed and analysed via western blotting for Noxa. Actin served as a loading control. **B)** OCI-AML2 cells transduced with either empty plk0 vector or plk0-shNoxa were treated with 0.1 μM MLN4924 for 12 h. Samples were harvested, lysed and western blotting used to detect Noxa. **C)** Transduced OCI-AML2 as in B) were treated with a dose range of MLN4924 for 24 h. Cells were harvested and cell death analysed with TMRE staining and flow cytometry. This graph shows percentage cell death following MLN4924 treatment of OCI-AML2 cells with and without Noxa. **D)** Transduced OCI-AML2 cells were pre-treated with MLN4924 for 2h prior to treatment with 250 ng/ml TRAIL for 22 h. Cell death was then analysed via TMRE staining and flow cytometry. This graph shows percentage cell death following MLN4924 and TRAIL treatment of OCI-AML2 cells with and without Noxa. This data is representative of 3 independent repeats +/- standard deviation. Significant differences were determined using an unpaired student t-test (*$p<0.05$).

3.3.2 Role of AML-associated transcription factors

MLN4924 allows for the accumulation of certain transcription factors that could drive the expression of pro-apoptotic genes. To test whether a transcription factor driven de novo gene expression was necessary for sensitisation to TRAIL, cells were treated with cyclohexamide (CHX), a combination of CHX and MLN4924 and a combination of CHX, MLN4924 and TRAIL. Cell death was then examined by looking at loss of mitochondrial membrane potential with TMRE staining and flow cytometry (Figure 3.14(A), (B)).

CHX is an inhibitor of protein translation and resulted in sensitising the cells to TRAIL, possibly by downregulation of cFlip expression or other anti-apoptotic proteins. CHX when combined with TRAIL induced potent cell death unfortunately not leaving us room to analyse if the MLN4924 and TRAIL combination induced cell death through transcription machinery.

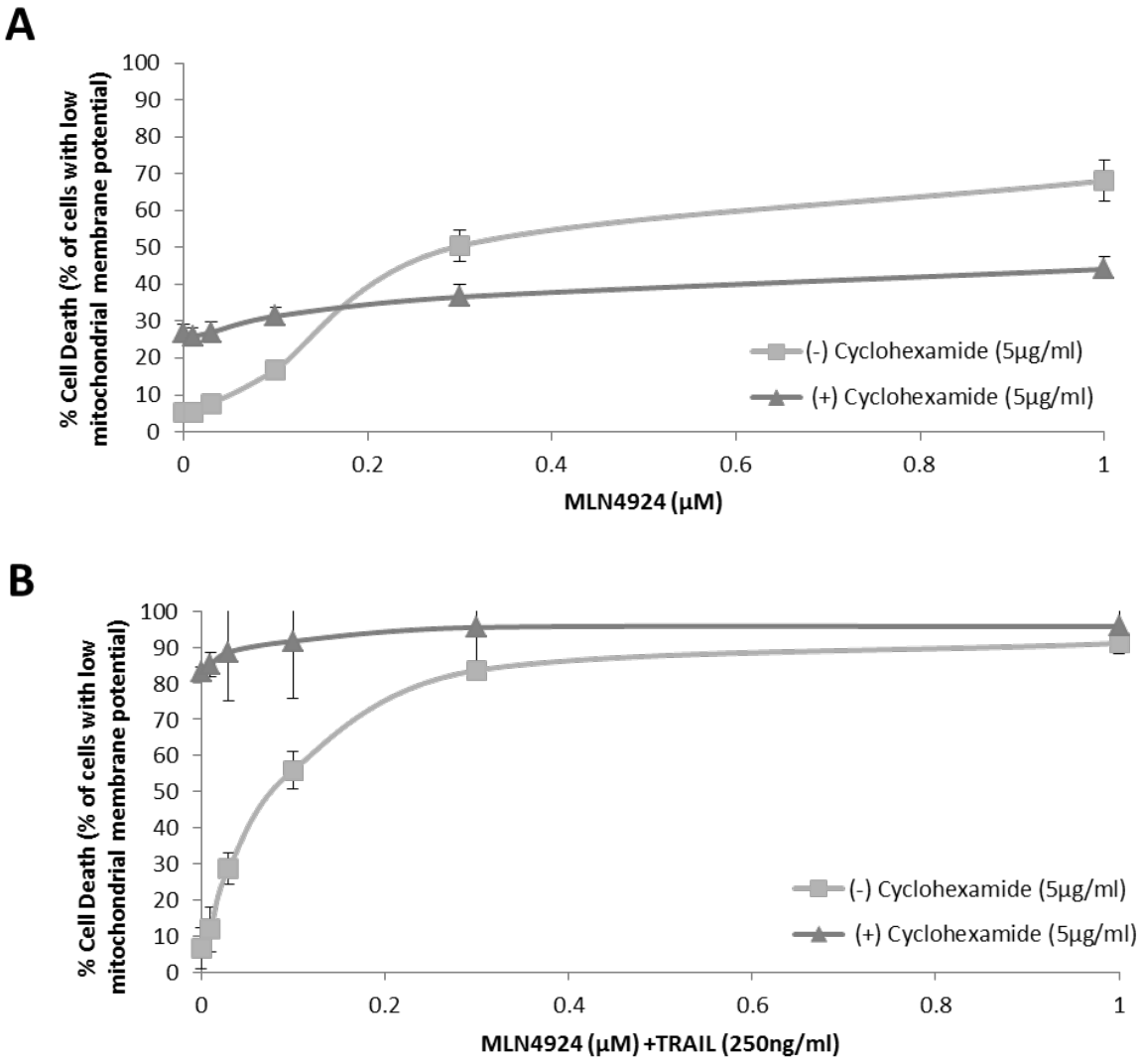

Figure 3.14 **The effect of inhibiting protein synthesis on MLN4924 and/or TRAIL-induced apoptosis is inconclusive**. **A)** OCI-AML2 cells were pre-treated with 5 µg/ml of cyclohexamide for 2 h before being treated with doses of MLN4924 for 22 h. Loss of mitochondrial membrane potential was analysed with TMRE staining and flow cytometry. The graph shows percentage cell death following treatment with MLN4924 vs MLN4924 and CHX**. B)** OCI-AML2 cells were pre-treated with 5 µg/ml of cyclohexamide before being treated with doses of MLN4924 for 2 h. This was followed by a TRAIL treatment of 250 ng/ml for 20 h. Cell death was analysed via TMRE staining and flow cytometry. The graph shows percentage cell death following treatment with MLN4924 and TRAIL vs MLN4924, TRAIL and CHX. This data is representative of three independent experiments +/- standard deviation.

As an alternative approach to identifying the mechanism through which MLN4924 sensitises to TRAIL we have identified transcription factors from the literature associated with AML and/or known to be targeted by MLN4923. Transcription factors commonly associated with AML include NF-E2 (Nrf2), nuclear factor kappa-light-chain-enhancer of activated B cells (NF-κB), p53, activating transcription factor 4 (ATF4) and CCAAT/enhancer-binding protein alpha (c/EBPα). Many of these have also been identified as substrates of cullin-ring ligases.

Nrf2 for example is expressed at high levels in AML and is implicated in protecting cancer cells from apoptosis. Its expression has been reported to be driven by NF-κB (MacEwan et al, 2012). Both Nrf2 and NF-κB have been reported several times in the literature as known substrates of cullin-ring ligases following MLN4924 treatment (Smith et al, 2012), (Danilov et al, 2014). So we began our investigation into the role of transcription factors which may influence sensitisation of OCI-AML2 cells to TRAIL-induced apoptosis with NF-kB. Under normal conditions, NF-κB transcription factors are maintained in an inactive state by binding to IκB proteins. On stimulation of the IKK complex, IκBα is phosphorylated resulting in its polyubiquitination and degradation leading to transcription of NF-κB target genes. Polyubiquitination of IκBα is reportedly regulated by CRL1 (Smith et al, 2010).

For these experiments OCI-AML2 cells were treated with 0.1 μM MLN4924 over a 12 h timecourse. Samples were harvested, lysed and analysed for total IκB and phospho IκB via western blot. Both levels of total and phospho IκB increase upon MLN4924 treatment (Figure 3.14(A)).

NF-κB activity was also looked at by using OCI-AML2 cells lentivirally transduced with an NF-κB luciferase reporter plasmid. These cells were treated with MLN4924, TNF and a combination of TNF and MLN4924 for 2 h, 4 h, 6 h and 18 h. TNF is a known inducer of NF-κB and acted here as a positive control to validate the system (Figure 3.15(B). TNF caused an increase in NF-κB activity and this increase could be inhibited by MLN4923. TRAIL, however did not have the ability to induce NF-κB activity in OCI-AML2 cells (Figure 3.15B) indicating that MLN4924-mediated inhibition of TRAIL-mediated NF-kB activation is not a likely mechanism of sensitisation. Of note, MLN4924 could reduce bases NF-kB activity when the cells were treated with MLN4924 for at least 18 h.

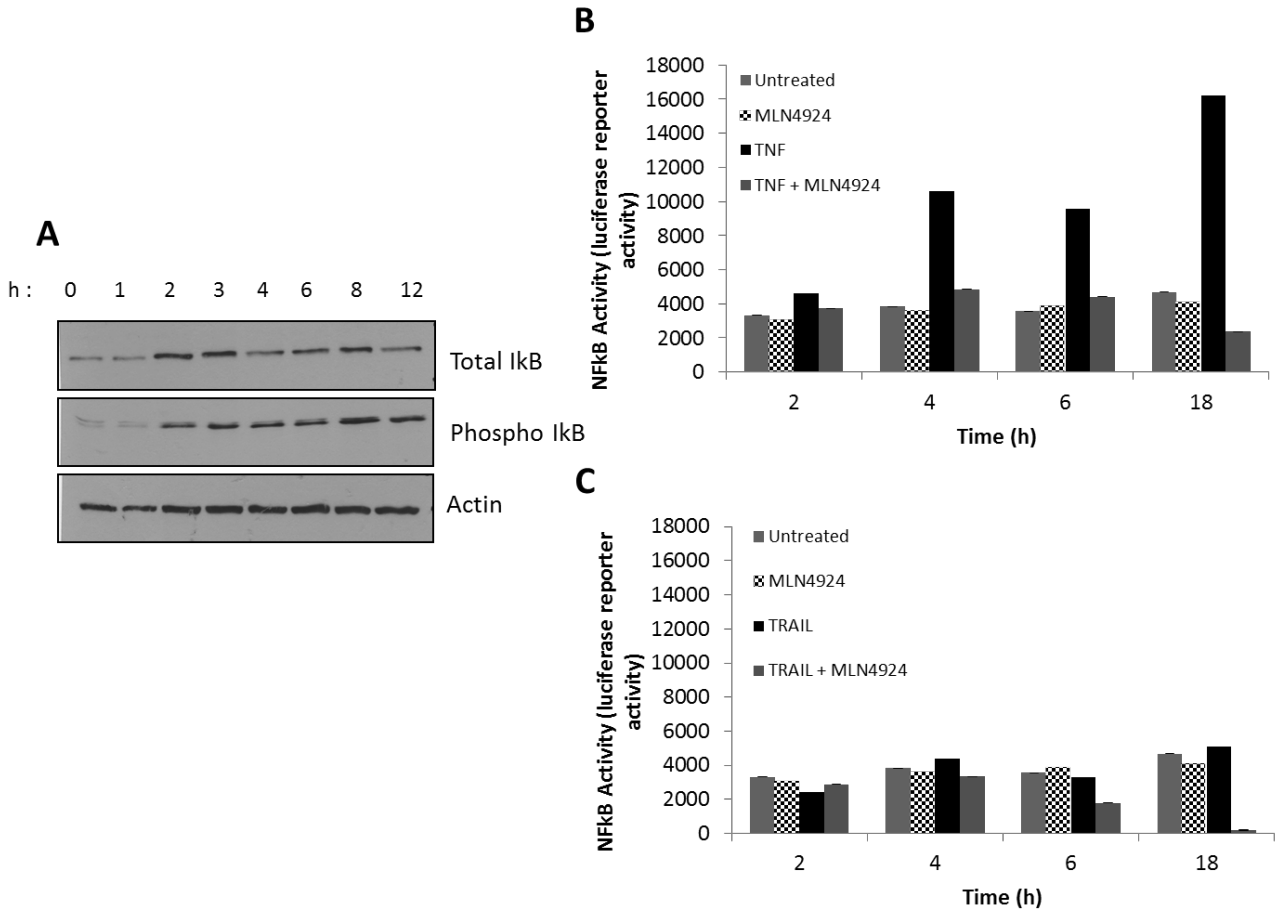

Figure 3.15 **MLN4924 reduces NF-κB activity. A)** OCI-AML2 cells were treated with 0.1 μM MLN4924 for the times indicated. Cells were harvested, lysed and analysed by western blot for total and phospho IκB expression levels**. B)** OCI-AML2 cells lentivirally transduced with an NF-κB reporter plasmid were treated with MLN4924 (0.1 μM), TNF (180 ng/ml) and a combination of TNF and MLN4924 for the times indicated. **C)** OCI-AML2 cells lentivirally transduced with an NF-κB reporter plasmid were treated with MLN4924 (0.1 μM), TRAIL (250 ng/ml) and a combination of TRAIL and MLN4924 for the times indicated. Activation of NF-κB was measured by luciferase activation. Results shown are indicative of three independent repeats +/- standard deviation.

From here we went on to look at the possible role of p53 in sensitising cells to TRAIL-induced apoptosis through MLN4923. p53 is a tumour suppressor protein which limits proliferation in response to cellular stress. MLN4924 has previously been shown to activate p53 in melanoma cells (Lightcap et al, 2012). A loss of p53 has also been associated with promotion of AML (Lowe et al, 2010).

Here we assessed the effects of MLN4924 on p53 and its downstream target p21. OCI-AML2 cells which express wild type p53 were treated with 0.1 μM MLN4924 and harvested at 2 h, 4 h, 6 h, 8 h and 12 h. Samples were then lysed and analysed for p53,

p21 and actin via western blotting (Figure 3.16(A)). p53 expression levels increase with MLN4924 treatment but not to the same extent that the levels of p21, its downstream target increase.

We further examined the relevance of p53 in our study by treating OCI-AML2 cells with a dose range of Nutlin3 from 0 to 10 μM for 12 h. Nutlin3 is an activator of p53. Its mechanism of action involves disrupting the interaction between the E3 ligase for p53 - Mdm2 and p53 itself. This results in an accumulation of p53 in the cells. Samples treated with Nutlin3 were analysed by western blotting for p53, p21 and actin (Figure 3.16(A)). We also observed that Nutlin3 increases levels of p53 and p21 (Figure 3.16(B)). The question arose then if Nutlin3 could sensitise OCI-AML2 cells to TRAIL-induced apoptosis in a manner similar to MLN4923. For these experiments cells were pretreated for 2 h with Nutlin3 at the doses indicated in Figure 3.16 (C). TRAIL was then added for 22 h. Cells were harvested and analysed for exposure of phosphatidyl serine with Annexin V staining and flow cytometry.

Nutlin3 has the ability to increase levels of p53 and p21 and sensitise OCI-AML2 cells to TRAIL-induced apoptosis in a manner similar to MLN4923. This is a positive indicator, though not conclusive that in this model p53 may play a role partial or otherwise in sensitising cells to TRAIL with MLN4923.

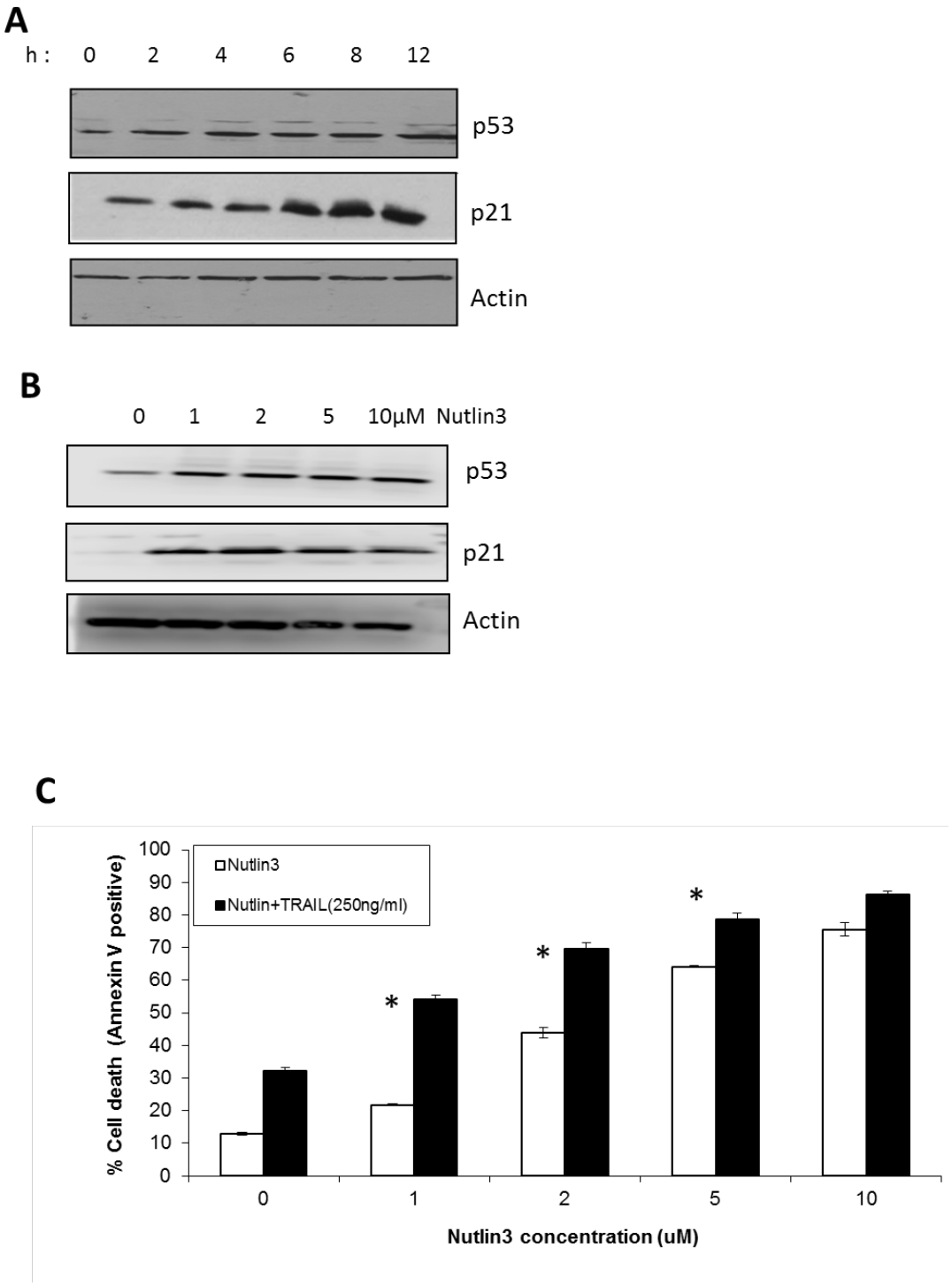

Figure 3.16 **MLN4924 increases levels of p53 and p21 and activation of p53 is sufficient for TRAIL sensitisation. A**) OCI-AML2 cells were treated with 0.1µM MLN4924 for the times indicated. Samples were harvested, lysed and analysed for p53 and p21 with western blotting. **B)** Cells were treated with the doses of Nutlin3 indicated and analysed with western blotting for p53 and p21. Actin served as a loading control. **C)** OCI-AML2 cells were pre-treated with Nutlin3 for 2h prior to treatment with 250ng/ml of TRAIL for 22h. Cell death was then monitored with Annexin V staining and flow cytometry. Significant differences were determined using an unpaired student t-test (*$p<0.05$).

To prove whether or not p53 was a critical factor in the mechanism through which MLN4924 can sensitise to TRAIL we attempted to inhibit p53 activity. There are a limited number of inhibitors available for this purpose. Pifithrin alpha (pftα) inhibits the transcriptional activity of p53 whereas another inhibitor available pifithrin mu (pftμ) inhibits p53-mediated apoptosis by preventing p53 binding to Bcl-Xl and Bcl-2 at the mitochondria. To test these inhibitors OCI-AML2 cells were pre-treated with pftα or pftμ for 2 h prior to treating with Nutlin3, an activator of p53 for 10 h. Samples were then harvested and examined for p53, p21 and actin with western blotting (Figure 3.17(A)). Whilst Nutlin3 can activate p53, neither pftα nor pftμ could inhibit p53 or p21 levels. Perhaps the effect of these p53 inhibitors is not always detectable by western blot so we went on and examined the effect of pftα and pftμ on MLN4924 and TRAIL induced apoptosis.

For these experiments cells were again pre-treated for 2 h with pftα (Figure 3.17 (B)) or pftμ (Figure 3.17 (C)) before treating cells with MLN4924 for 2 h followed by TRAIL treatment for 20 h. Inhibiting p53 with either of these inhibitors has no impact on apoptosis induced by MLN4924 or on apoptosis induced by a combination of MLN4924 and TRAIL. Given that we are unable to prove that these inhibitors are functional in OCI-AML2 cells these experiments are inconclusive.

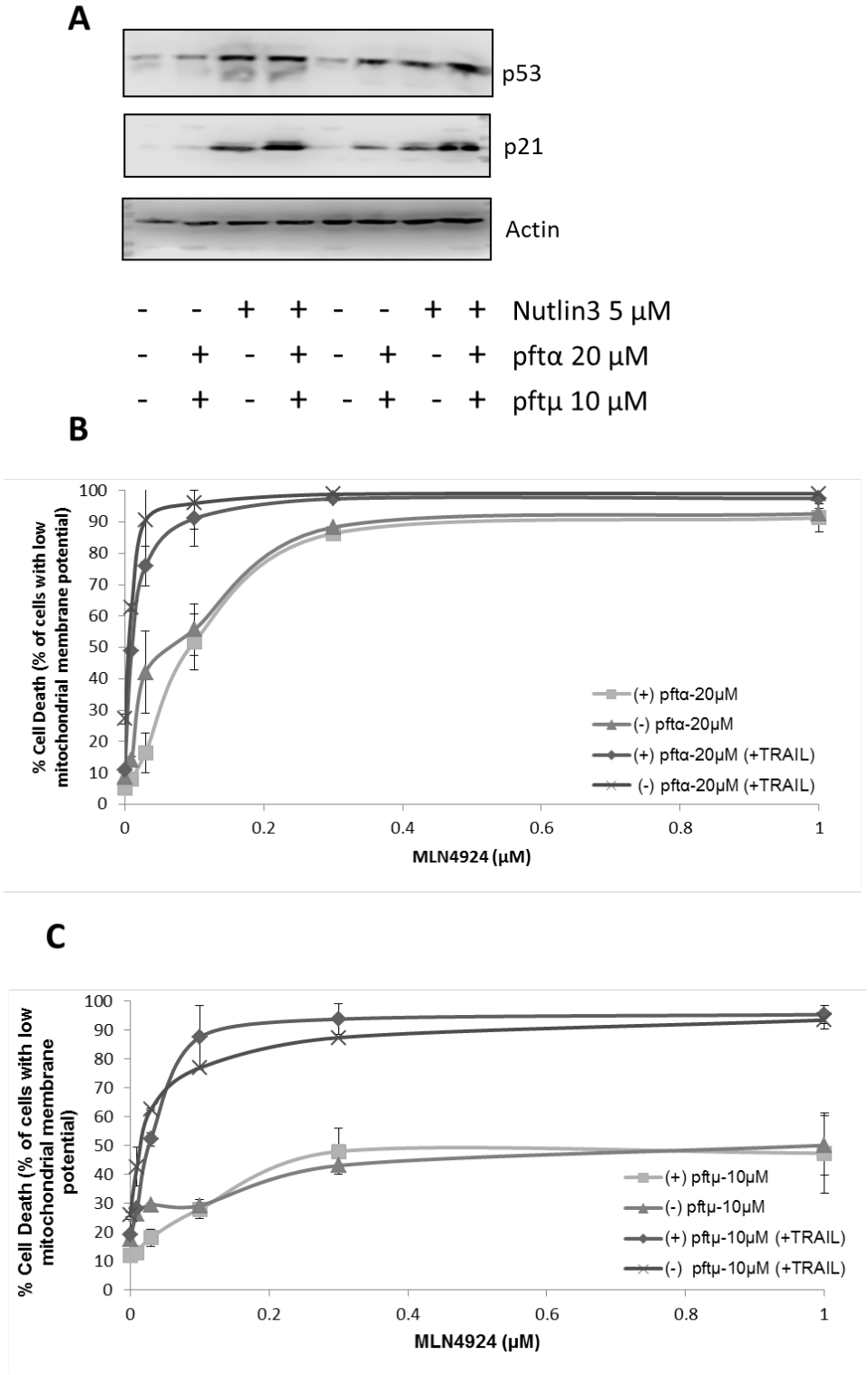

Figure 3.17 **p53 could not be inhibited in OCI-AML2 cells with currently available inhibitors A)** OCI-AML2 cells were pre-treated with pifithrin α or pifithrin µ for 2h prior to Nutlin3 treatment for 10h. Samples were harvested and analysed with western blotting for p53 and p21. Actin served as a loading control. **B)** Cells were pre-treated with pifithrin α for 2 h followed by MLN4924 +/- TRAIL treatment. Loss of mitochondrial membrane potential was analysed with flow cytometry. **C)** Cells were pre-treated with pifithrin µ followed by MLN4924 +/- TRAIL treatment. Cells were harvested and analysed for cell death via TMRE staining and flow cytometry. This data is representative of 3 independent repeats +/- standard deviation.

From here we moved on to examine the role c/EBPα may play in the synergism seen between MLN4924 and TRAIL. Tribbles homolog 2 (TRIB2), an oncogene that has been reported to induce AML can lead to the inactivation of c/EBPα. c/EBPα is a critical transcription factor that is frequently dysregulated in AML (Pear et al, 2006). Two isoforms of c/EBPα exist, namely p42 and p30. p42 is the transcriptionally active full length isoform. p30 is a dominant-negative isoform which can inhibit the transcriptional activity of p42. The cullin-ring ligases have been reported to help stabilise TRIB2. We propose that through inhibiting cullin-ring ligase activity, TRIB2 will no longer have the ability to inactivate c/EBPα which can lead to AML. A connection between MLN4924 and c/EBPα has not yet been reported in the literature. We assessed the effects of MLN4924 on c/EBPα in OCI-AML2 cells. In addition we examined the effects of 2-cyano-3,12-dioxo-oleana-1,9(11)-dien-28-oic acid (CDDO) in a similar manner. CDDO is a known inducer of c/EBPα.

These experiments involved treating OCI-AML2 cells with MLN4924 over a 12 h timecourse. After cells were harvested and lysed they were subjected to analysis for c/EBPα via western blotting (Figure 3.18(A)). c/EBPα levels increase at the 6 h timepoint with MLN4924 treatment. Additionally OCI-AML2 cells were treated with CDDO over a 12 h timecourse and analysed for c/EBPα expression with western blotting. As expected there is an increase in c/EBPα levels with this treatment (Figure 3.18(B)).

We then examined if CDDO had the ability to sensitise OCI-AML2 cells to TRAIL-induced apoptosis. Cells were pre-treated for 2 h with CDDO at the doses indicated in Figure 3.18(C). TRAIL was then added for 22 h before the cells were stained with TMRE and analysed by flow cytometry. CDDO, as with MLN4924 has the ability to sensitise these cells to TRAIL-induced apoptosis.

As with the experiments carried out with Nutlin3 these results suggest an involvement of c/EBPα in the mechanism through which MLN4924 sensitises to TRAIL but are not conclusive.

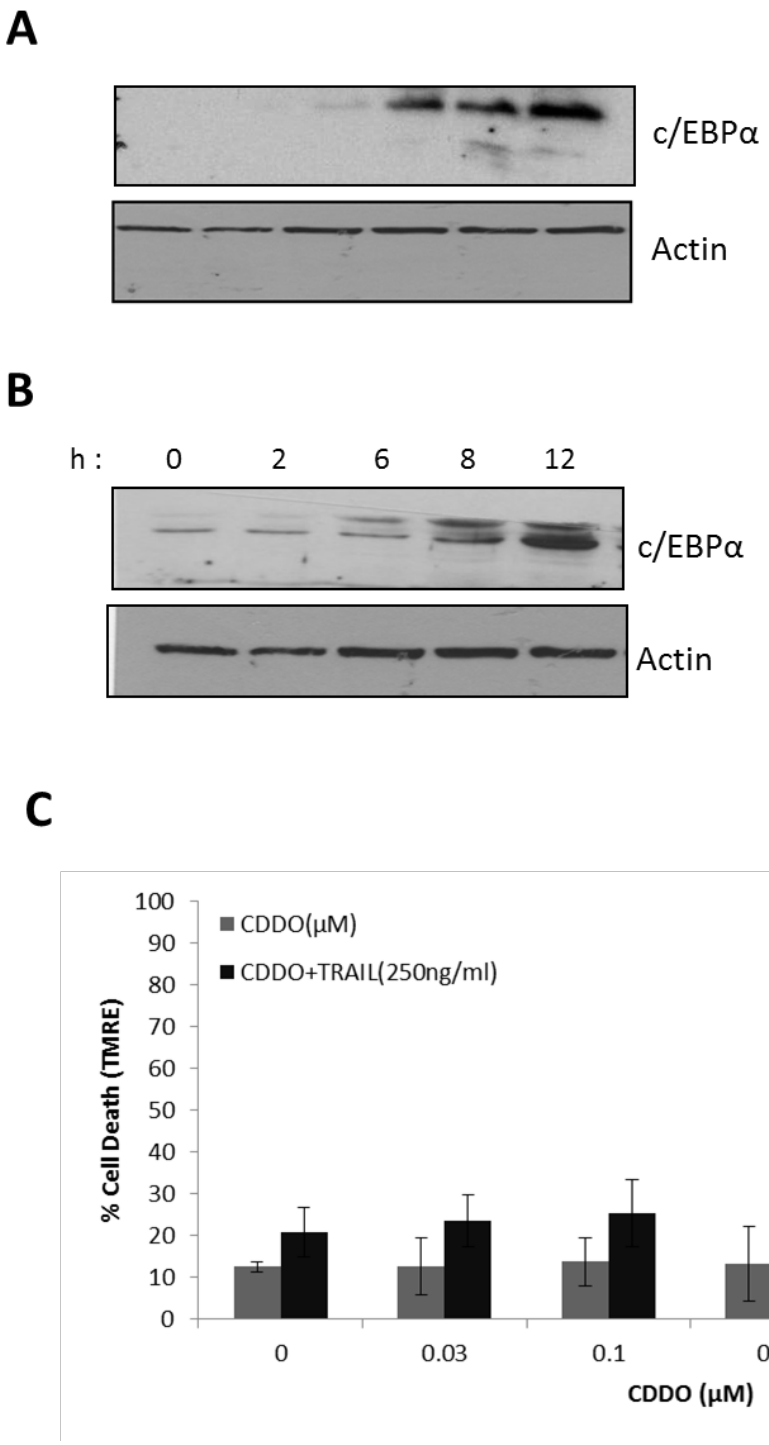

Figure 3.18 **MLN4924 increases expression of c/EBPα in OCI-AML2 cells**

A) OCI-AML2 cells were treated with 0.1 μM MLN4924 for the times indicated. Samples were harvested, lysed and c/EBPα detected with western blotting. **B)** Cells were treated with the doses of CDDO indicated and analysed via western blot for c/EBPα. Actin served as a loading control. **C)** OCI-AML2 cells were pre-treated with CDDO for 2 h prior to treatment with 250 ng/ml of TRAIL for 22 h. Cell death was then monitored with TMRE staining and flow cytometry. Significant differences were determined using an unpaired student t-test (*$p<0.05$).

To confirm the importance of c/EBPα in MLN4924 sensitising to TRAIL-induced apoptosis we incorporated a shRNA plasmid against c/EBPα into OCI AML2 cells. This shRNA against c/EBPα is in the lentiviral plK0 vector so as a control an empty plk0 vector was used. OCI-AML2 cells were transduced with both of these lentiviral vectors and cells expressing the plasmid of interest were selected using puromycin. OCI-AML2 cells transduced with plk0-empty and OCI-AML2 cells transduced with plk0-sh c/EBPα were treated with 0.1 μM MLN4924 for 12 h to determine if c/EBPα was still being expressed (Figure 3.19(A)). It was evident from the image that this shc/EBPα construct could reduce basal levels of c/EBPα and reduce the level of c/EBPα induced by MLN4923.

We thus proceeded to look at the effect of silencing c/EBPα in OCI-AML2 cells when treating with a dose of MLN4924 (Figure 3.19 (B)) and MLN4924 combined with TRAIL (Figure 3.19(C)). The absence of c/EBPα protects the cells from apoptosis induced by MLN4924 by approximately 10% suggesting that c/EBPα plays a minor role in inducing cell death by MLN4924 as a single agent in these cell lines. On the other hand the absence of c/EBPα protects OCI-AML2 cells by approximately 30% from apoptosis induced by the combination treatment of MLN4924 and TRAIL. This implicates c/EBPα in having a key role in the mechanism by which MLN4924 synergises with TRAIL.

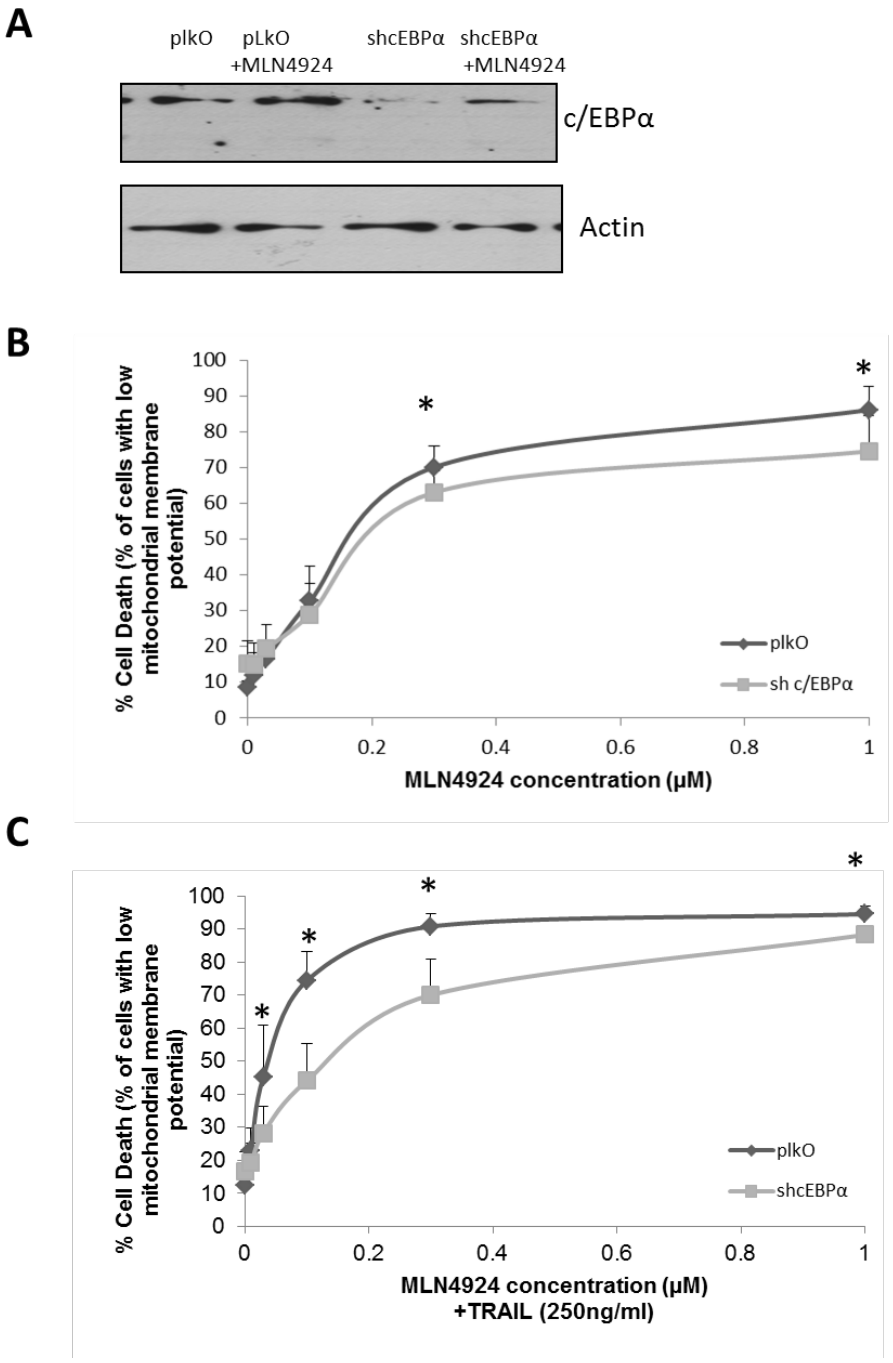

Figure 3.19 **c/EBPα plays a pivotal role in the mechanism through which MLN4924 sensitises to TRAIL-induced apoptosis.**

A) OCI-AML2 cells transduced with either empty plk0 vector or plk0-shc/EBPα were treated with 0.1 μM MLN4924 for 12h. Samples were harvested, lysed and c/EBPα probed for on a western blot**. B)** Transduced OCI-AML2 as in A) were treated with a dose range of MLN4924 as indicated for 24 h. Cells were harvested and cell death analysed with TMRE staining and flow cytometry. **C)** Transduced OCI-AML2 cells were pre-treated with MLN4924 for 2 h prior to treatment with 250 ng/ml TRAIL for 22 h. Cell death was then analysed with TMRE staining and flow cytometry. Significant differences were determined using an unpaired student t-test (*p<0.05).

It has been reported in the literature that there is a link between c/EBPα and p53. To investigate this we examined if c/EBPα can regulate p53 or if perhaps p53 can regulate c/EBPα. Therefore OCI-AML2 cells, OCI-AML2 cells transduced with plk0 and OCI-AML2 cell transduced with shc/EBPα were treated with MLN4924 for 12 h. Samples were harvested and analysed for c/EBPα, p53, p21 and actin (Figure 3.20(A)). In the absence of c/EBPα, p53 and p21 also disappear suggesting that c/EBPα regulates p53. To confirm whether or not this was the case cells were treated with CDDO (1 μM) over a 12 h timecourse (Figure 3.20 (B)) and cells were also treated with Nutlin3 for 12 h with a range of doses from 0-10 μM (Figure 3.20 (C)). All samples were lysed and probed for c/EBPα, p53, p21 and actin on western blot. As previously observed CDDO can increase levels of c/EBPα and in addition it can also increase levels of p53 and p21. This further confirms that c/EBPα can regulate p53 and p21 in this system.

However, Nutlin3 which is an activator of p53 and its downstream target p21 also has the ability to increase the expression of c/EBPα. This data as a whole indicates that a feedback loop exists between c/EBPα and p53.

Nutlin3 can activate p53 and increase expression levels of c/EBPα and in turn senstitise to TRAIL-induced apoptosis. So in OCI-AML2 cells transduced with shc/EBPα where there are no c/EBPα or p53 levels detectable by western blot it would be expected that Nutlin3 would no longer be able to sensitise cells to TRAIL-induced apoptosis. To test this OCI-AML2 cells transduced with an empty plk0 plasmid or a shRNA plasmid against c/EBPα were treated with Nutlin3 for 2 h prior to TRAIL treatment for 22 h. Cell death was then analysed using TMRE stain and flow cytometry (Figure 3.20 (D)). Nutlin3 alone can induce cell death in cells where c/EBPα is silenced and no p53 is detectable. This is possibly due to the fact that Nutlin3 treatment can also upregulate levels of Tap73 and E2F1 which in turn can induce apoptosis. c/EBPα can repress levels of E2F1 so in the absence of c/EBPα Nutlin3 can induce apoptosis in this manner (Findley et al, 2009), (Keeshan et al, 2014).

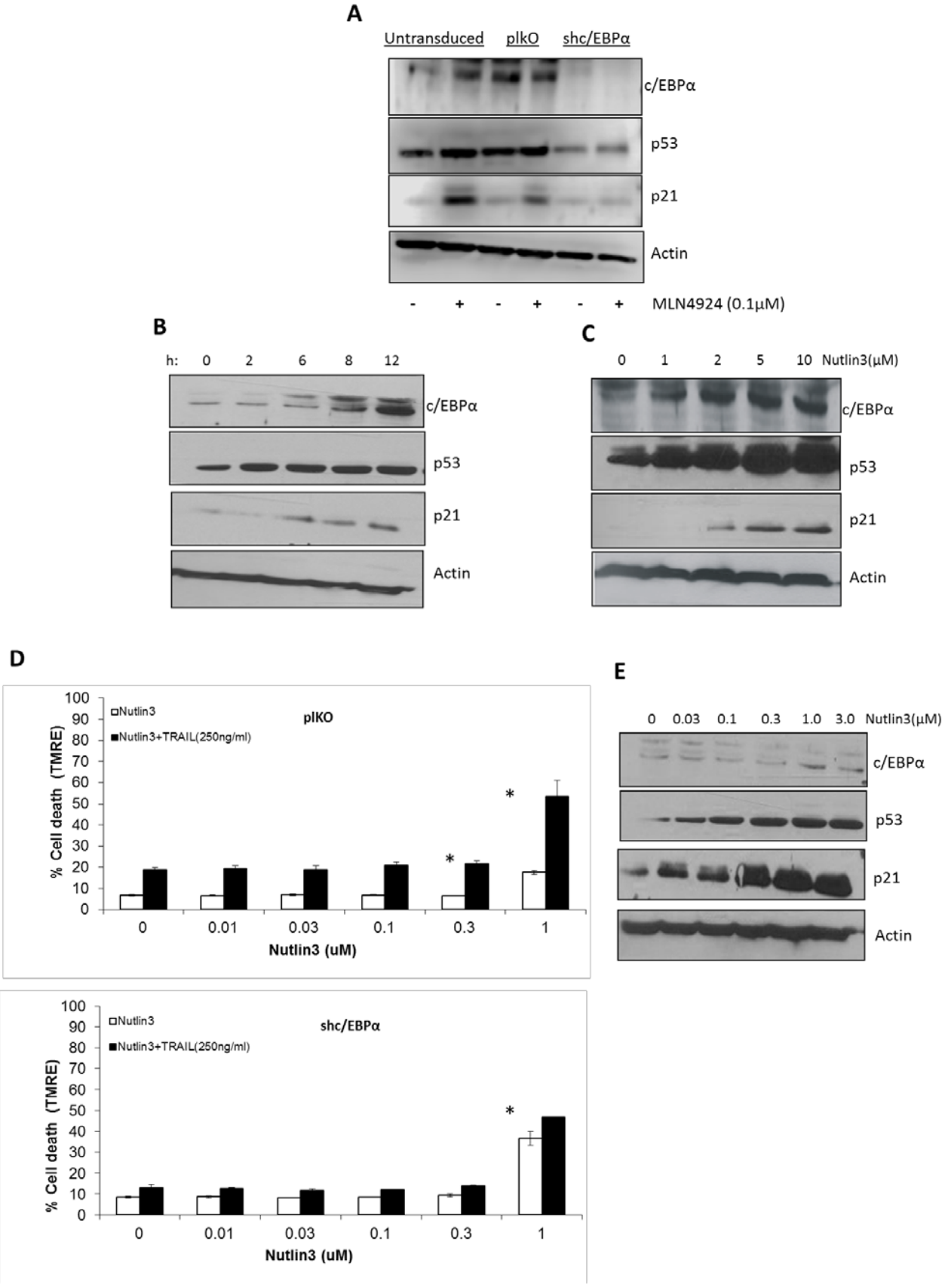
A
Untransduced
plkO
shc/EBPα
c/EBPα
p53
p21
Actin
- + - + - + MLN4924 (0.1μM)
B
h: 0 2 6 8 12
c/EBPα
p53
p21
Actin
C
0 1 2 5 10 Nutlin3(μM)
c/EBPα
p53
p21
Actin
D
pIKO
Nutlin3
Nutlin3+TRAIL(250ng/ml)
% Cell death (TMRE)
Nutlin3 (uM)
0 0.01 0.03 0.1 0.3 1
shc/EBPα
Nutlin3
Nutlin3+TRAIL(250ng/ml)
% Cell death (TMRE)
Nutlin3 (uM)
0 0.01 0.03 0.1 0.3 1
E
0 0.03 0.1 0.3 1.0 3.0 Nutlin3(μM)
c/EBPα
p53
p21
Actin

***Figure 3.20* c/EBPα and p53 regulate each other in a feedback loop fashion.**

A) OCI-AML2 cells untransduced, transduced with empty plk0 vector or transduced with plk0-shc/EBPα were treated with 0.1 μM MLN4924 for 12 h after which samples were harvested and lysed before being subjected to analysis via western blot for c/EBPα, p53 and p21. **B**) OCI-AML2 cells were treated with 1 μM CDDO for the times indicated. Samples were lysed and analysed by western blot for c/EBPα, p53 and p21. **C**) OCI-AML2 cells were treated with the indicated doses of Nutlin3 for 12 h. Samples were lysed and analysed by western blot for c/EBPα, p53 and p21. OCI-AML2 cells transduced with empty plk0 vector and those transduced with plk0-shc/EBPα were pre-treated with Nutlin3 for 2 h prior to TRAIL treatment at 250 ng/ml for 22 h. Cell death was then analysed with TMRE staining for loss of mitochondrial membrane potential and flow cytometry. **E)** OCI-AML2 cells were treated with the indicated doses of Nutlin3 for 12 h. Samples were lysed and analysed by western blot for c/EBPα, p53 and p21. Actin served as a loading control. Significant differences were determined using an unpaired student t-test (*$p<0.05$).

3.2.4 Effects of MLN4924 in combination with TRAIL in primary AML samples

Bone marrow aspirates and peripheral blood samples were obtained from patients diagnosed with AML. Ficoll was used to separate blood into its individual components. The sample was layered on top of the ficoll and centrifuged for a short time. Differential migration during centrifugation results in the formation of layers containing different cell types. The lymphocytes can be found between the plasma and the ficoll solution allowing them to be removed.

These cells were then used to assess the effects of MLN4924 and/or TRAIL on cell viability and on the percentage of CD34+ and CD38- cells. 7-aminoactinomycin D (7-AAD) is a fluorescent intercalator that undergoes a spectral shift upon association with DNA. It is generally excluded from live cells. It was used in these experiments to examine apoptotic cells with flow cytometry. CD34+/38- cells are indicative of leukaemic initiating cells (LICs) and leukaemic stem cells (LSCs). LICs survive chemotherapy and are probably the cause of relapse (Wang et al, 2013).

For these experiments primary AML cells were seeded on HS-5 cells. HS-5 cells are a human stromal cell line. They were seeded at 50,000 cells/ml for 48 h prior to addition of the primary AML cells at 300,000/ml. Cells derived from the bone marrow (Figure 3.21(A-B)) and from the plasma (Figure 3.21(C-F)) were pre-treated with MLN4924 for 2 h prior to TRAIL treatment at 2 h and 24 h. The total treatment time was 48 h. MLN4924 was added in the range 0 - 1.0 μM whilst the dose of TRAIL remained consistent at 250 ng/ml. The white bars in Fig 3.10 represent the % of viable cells or in the lower graph the % of CD34+/38- cells following MLN4924 treatment. The black bars represent the % of viable cells or in the case of the lower graph the % of CD34+/38- cells following the combination treatment of MLN4924 and TRAIL.

In addition samples were also taken of primary AML cells seeded on HS-5s and treated with the same range of MLN4924 for the purpose of western blot analysis of cullin-NEDD8, c/EBPα, p53 and actin. As explained previously lack of cullin-Nedd8 is a good marker that MLN4924 is functional in these cells. We also looked at protein levels of c/EBPα and p53 as data from our *in vitro* studies showed that c/EBPα in particular plays a role in the synergism observed between MLN4924 and TRAIL.

The cytogenetic data associated with these samples is predominantly unknown at the time of thesis submission. It is known that patient 2 has a normal karyotype and is

positive for a Flt3 mutation. Patient 5 has a complex karyotype and was resistant to all treatment.

MLN4924 as a single agent can cause a loss in cell viability in bone marrow samples (Figure 3.21 (A) and (B)). Additionally for both bone marrow samples there is a very slight synergism observed with 7-AAD measurements following the combination treatment of MLN4924 and TRAIL. Synergism is defined as a greater than additive effect. The % of CD34+/38- cells increases with increasing doses of MLN4924, alone and combined with TRAIL. This increase is due to a drop in the population of leukemic blasts causing a rise in concentration of the remaining leukemic stem cell and leukaemic initiating cell population which are CD34+/38- and resistant to these treatments.

Western blot analysis for patient 1 and patient 2 shows that NEDD8 becomes detached from the cullins with 0.3µM and 0.1µM MLN4924, respectively. Levels of c/EBPα increase upon MLN4924 treatment for patient 1 but no c/EBPα is detected in samples from patient 2 even though there is a slight synergestic effect observed for both of these bone marrow samples. Western blot analysis also shows a decrease in p53 levels in bone marrow samples (Figure 3.21 (A) and (B)).

Figure 3.21 (C), (D), (E) and (F) are peripheral blood samples from patients diagnosed with AML. As with the bone marrow samples tested, MLN4924 as a single agent can cause a loss in cell viability in all peripheral blood samples tested but to a much lesser extent for patient 5. A very slight syngeristic effect can be observed in viability levels of patient sample 3 (Figure 3.21 (C)).

For all peripheral blood samples MLN4924 +/- Trail causes an increase in the CD34+/38- population due to its potent effect on leukemic blasts. Again patient 5 shows this to a much lesser extent than the other peripheral blood samples.

MLN4924 is deemed functional as levels of cullin-Nedd8 decrease as levels of MLN4924 increase. Levels of p53 and c/EBPα either increase, decrease or stay the same. There appears to be no correlation with p53 and the results obtained.

In patient sample 3 where a small level of synergism is observed levels of c/EBPα increase. Other samples where we see synergism include patient 1 and 2. Patient 1 also shows an increase in c/EBPα levels but patient 2 has no detectable levels of c/EBPα. Perhaps the levels of c/EBPα are increasing and go undetected by this system or perhaps this sample is an outlier. To truly determine the relationship between

c/EBPα and the synergistic effect observed with MLN4924 and TRAIL a larger sample number would be required.

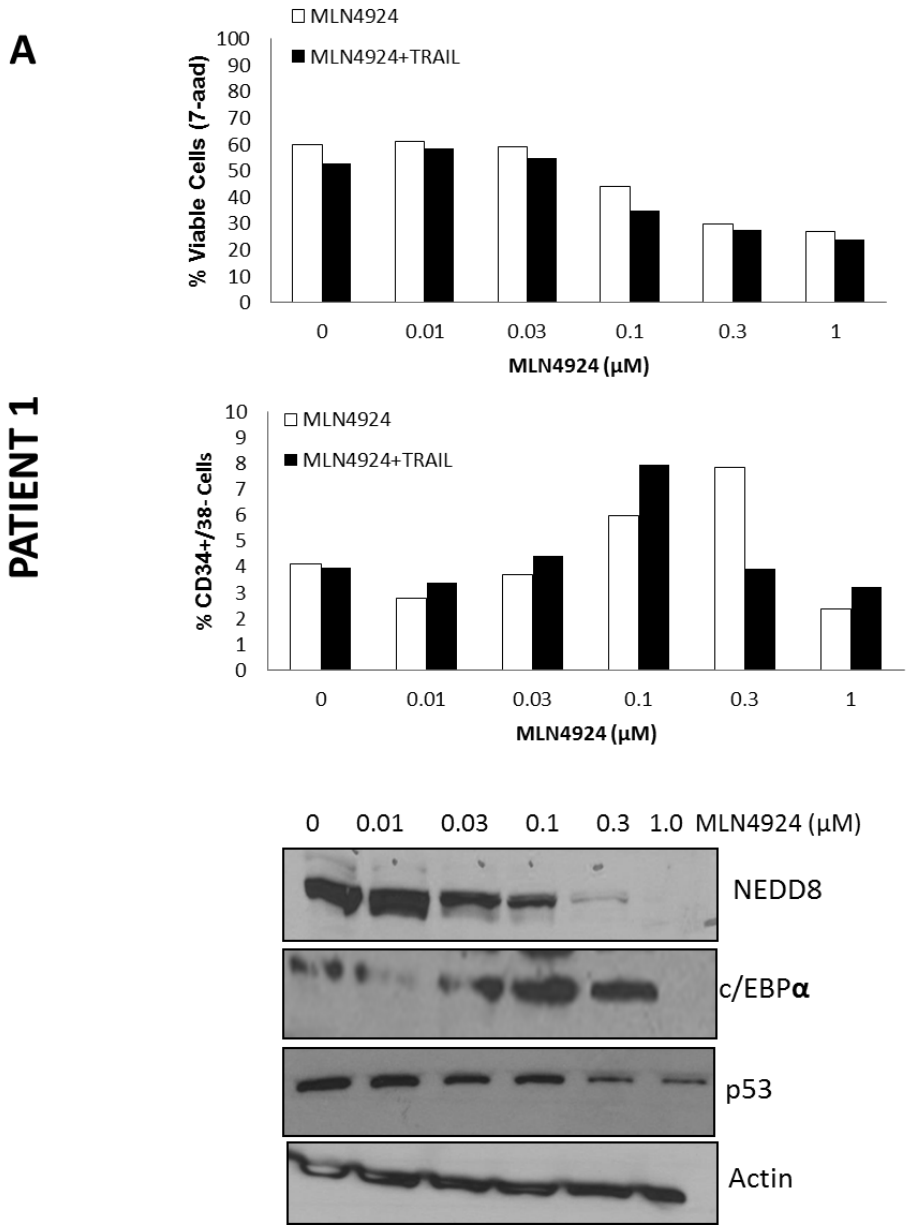

B

PATIENT 2

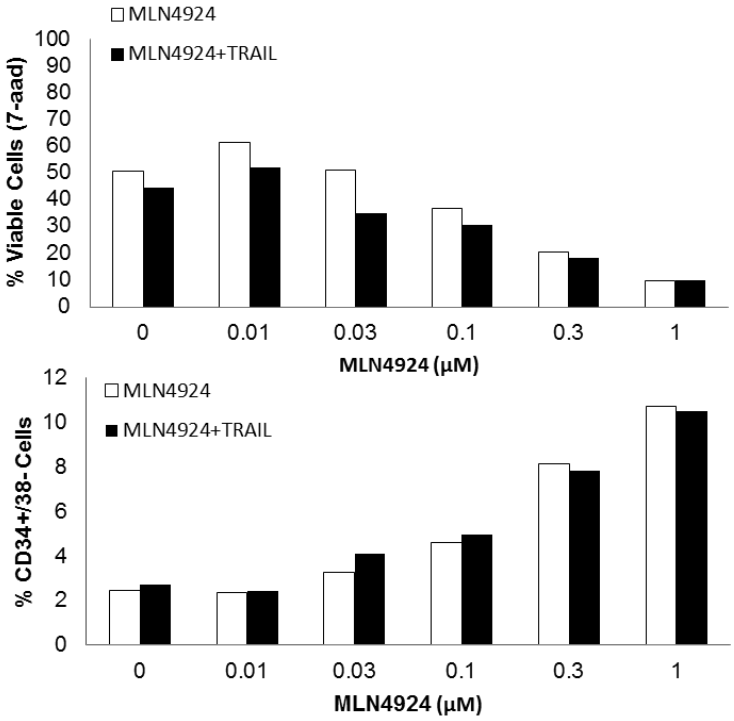
MLN4924
MLN4924+TRAIL
% Viable Cells (7-aad)
100
90
80
70
60
50
40
30
20
10
0
0
0.01
0.03
0.1
0.3
1
MLN4924 (μM)
MLN4924
MLN4924+TRAIL
% CD34+/38- Cells
12
10
8
6
4
2
0
0
0.01
0.03
0.1
0.3
1
MLN4924 (μM)

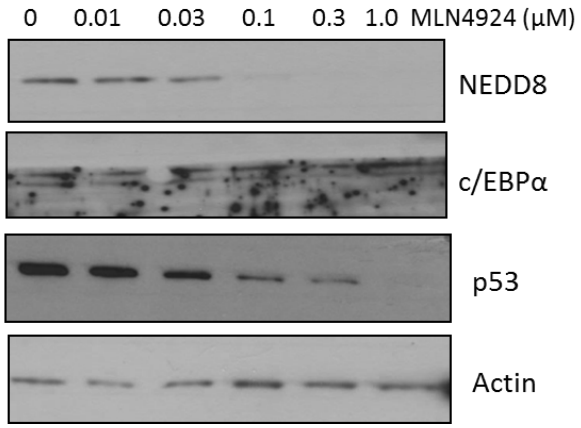
0 0.01 0.03 0.1 0.3 1.0 MLN4924 (μM)
NEDD8
c/EBPα
p53
Actin

C

PATIENT 3

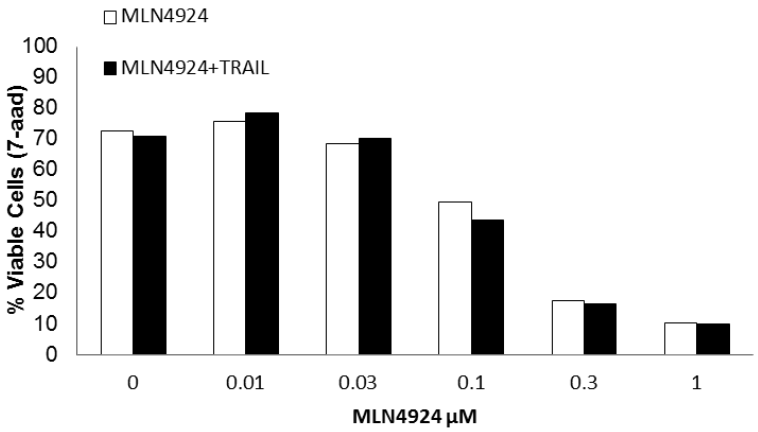
MLN4924
MLN4924+TRAIL
% Viable Cells (7-aad)
100
90
80
70
60
50
40
30
20
10
0
0
0.01
0.03
0.1
0.3
1
MLN4924 µM

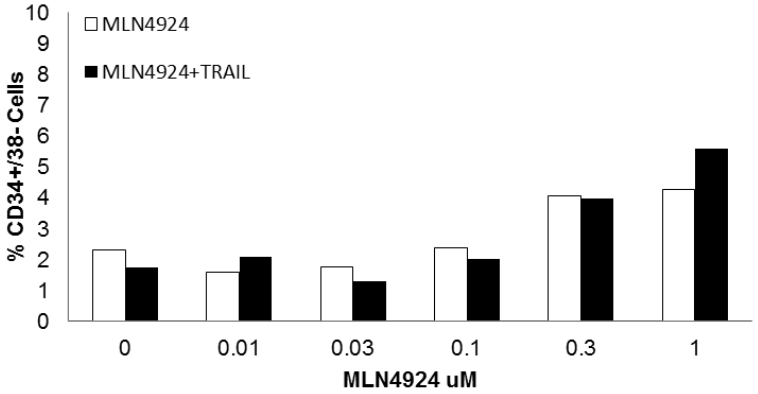
MLN4924
MLN4924+TRAIL
% CD34+/38- Cells
10
9
8
7
6
5
4
3
2
1
0
0
0.01
0.03
0.1
0.3
1
MLN4924 uM

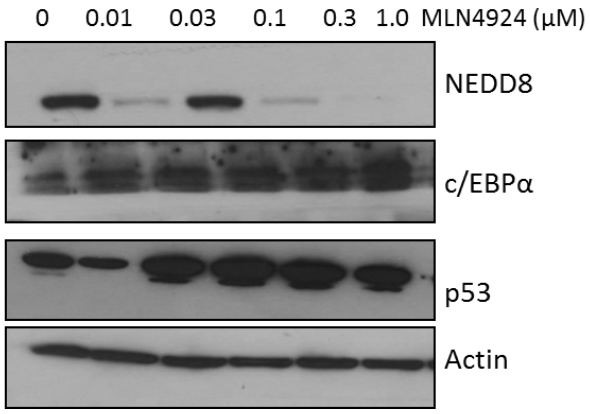
0 0.01 0.03 0.1 0.3 1.0 MLN4924 (µM)
NEDD8
c/EBPα
p53
Actin

D

PATIENT 4

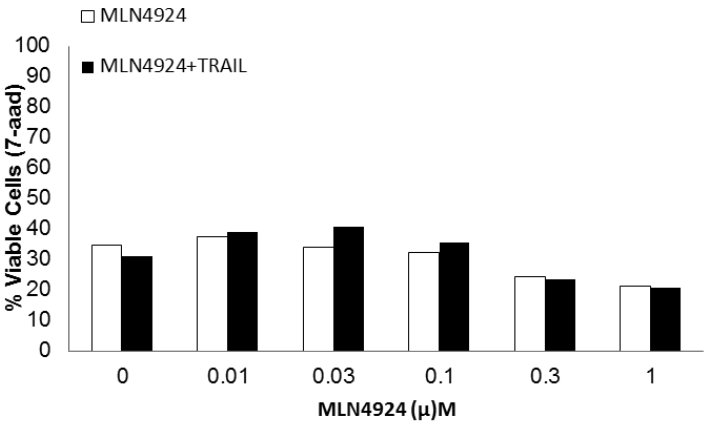
MLN4924
MLN4924+TRAIL
% Viable Cells (7-aad)
100
90
80
70
60
50
40
30
20
10
0
0
0.01
0.03
0.1
0.3
1
MLN4924 (μ)M

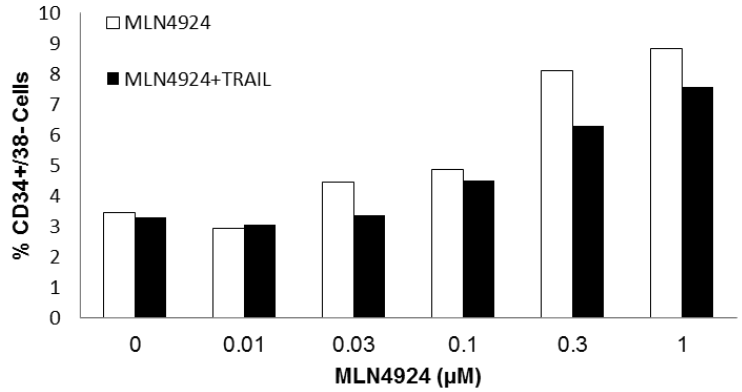
MLN4924
MLN4924+TRAIL
% CD34+/38- Cells
10
9
8
7
6
5
4
3
2
1
0
0
0.01
0.03
0.1
0.3
1
MLN4924 (μM)

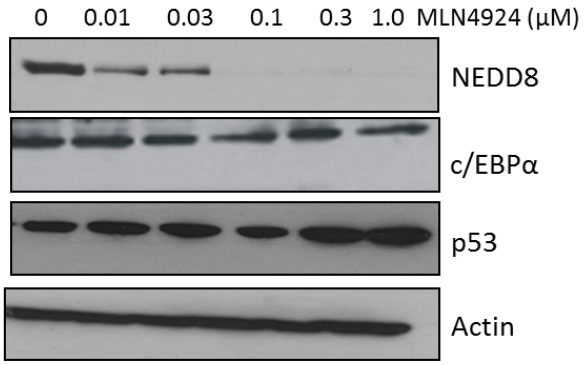
0 0.01 0.03 0.1 0.3 1.0 MLN4924 (μM)
NEDD8
c/EBPα
p53
Actin

E

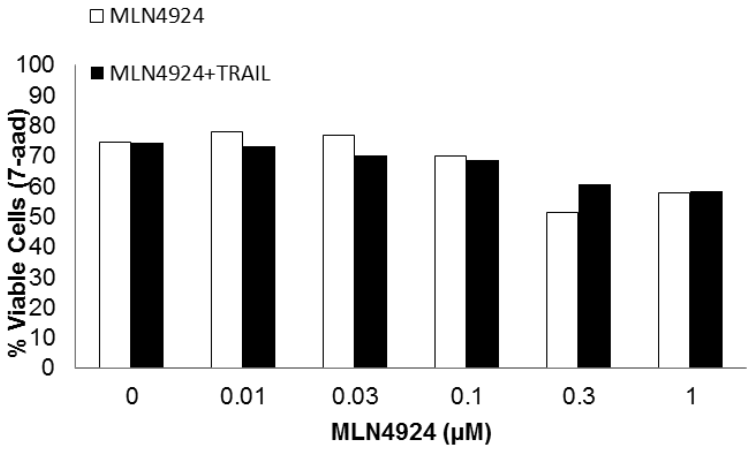
MLN4924
MLN4924+TRAIL
% Viable Cells (7-aad)
100
90
80
70
60
50
40
30
20
10
0
0
0.01
0.03
0.1
0.3
1
MLN4924 (μM)

PATIENT 5

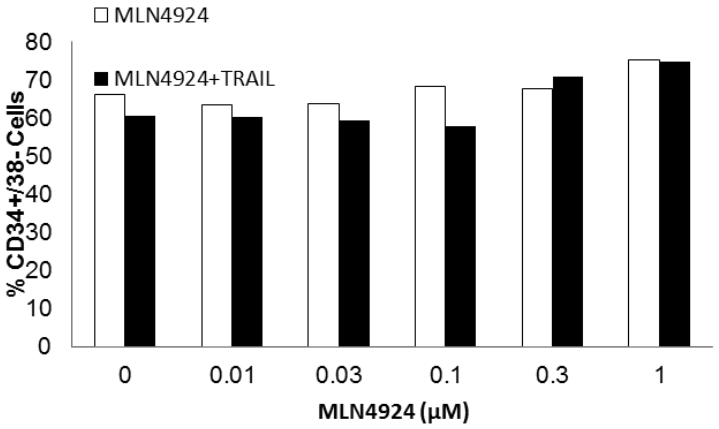
MLN4924
MLN4924+TRAIL
% CD34+/38- Cells
80
70
60
50
40
30
20
10
0
0
0.01
0.03
0.1
0.3
1
MLN4924 (μM)

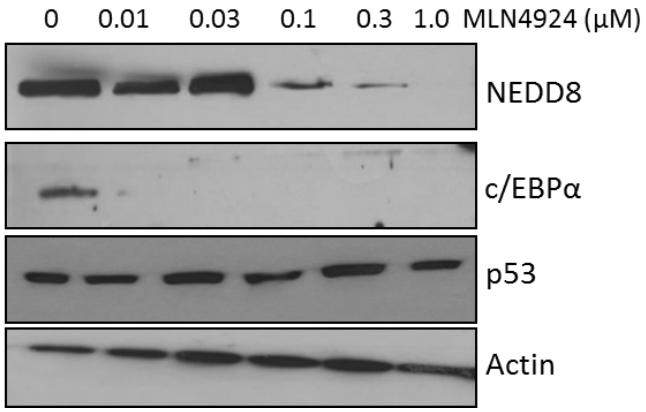
0
0.01
0.03
0.1
0.3
1.0
MLN4924 (μM)
NEDD8
c/EBPα
p53
Actin

F

PATIENT 6

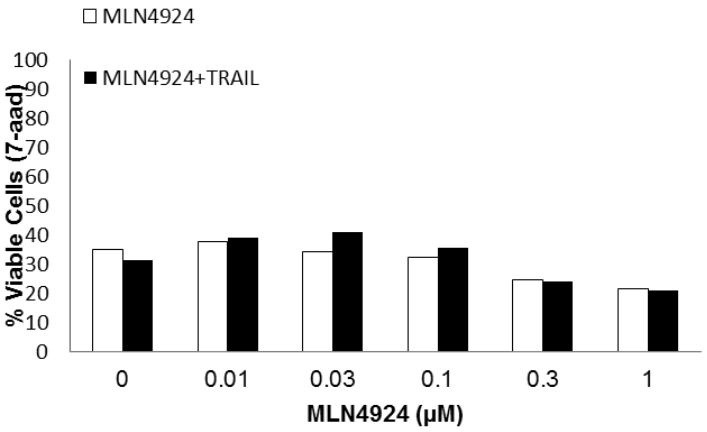
MLN4924
MLN4924+TRAIL
% Viable Cells (7-aad)
100
90
80
70
60
50
40
30
20
10
0
0
0.01
0.03
0.1
0.3
1
MLN4924 (μM)

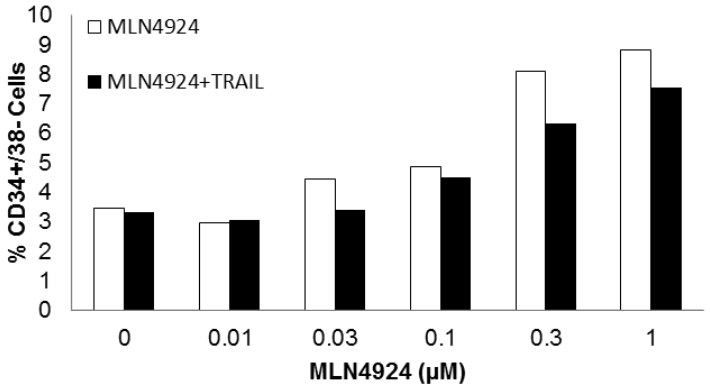
MLN4924
MLN4924+TRAIL
% CD34+/38- Cells
10
9
8
7
6
5
4
3
2
1
0
0
0.01
0.03
0.1
0.3
1
MLN4924 (μM)

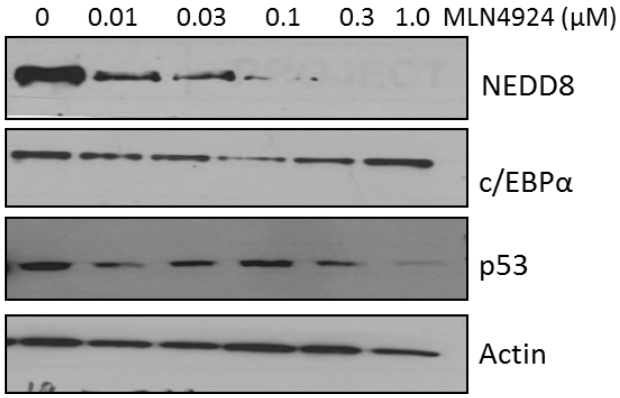
0 0.01 0.03 0.1 0.3 1.0 MLN4924 (μM)
NEDD8
c/EBPα
p53
Actin

Figure 3.21 **Primary AML samples show varied synergism in response to MLN4924 +/- TRAIL. Primary AML samples show varied expression of c/EBPα and p53 upon MLN4924 treatment.**

A-B represents bone marrow samples whilst **C-F** represents peripheral blood samples.

The effect of MLN4924 and TRAIL on patient samples was assessed by seeding primary AML cells at a concentration of 300,000/ml on HS-5 cells. HS-5 cells were seeded at 50,000/ml. Cells were pre-treated with MLN4924 at the doses indicated followed by a TRAIL treatment of 250 ng/ml at 2 h and again at 24 h. After 48 h cells were harvested, and viability was assessed by 7-AAD and flow cytometry (top graph).

The lower graph shows the effect of MLN4924 and TRAIL on leukemic cells. This was analysed by incubating samples with CD34+ and CD38- antibodies for 40 minutes before being measured by flow cytometry.

To examine the effects of MLN4924 on the expression levels of NEDD8, c/EBPα and p53 in primary AML cells, cells were seeded on HS-5 cells at concentrations described above. Cells were then treated with a range of MLN4924 for 12 h after which cells were harvested, lysed and proteins detected with western blotting. Actin served as a loading control.

All primary samples received for these experiments were approved by ethical committee.

3.3 Discussion

In this chapter we have demonstrated that MLN4924, as a single agent can induce apoptosis in a number of haematological malignant cell lines. These included AML, MM and DLBCL cell lines. In addition we have shown that MLN4924 can also when combined with TRAIL synergistically induce apoptosis in a number of these cell lines. Table 3.7 shows the number of cell lines found to have a synergistic effect.

Table 3.7 **Summary of response of haematological malignant cells to MLN4924 and TRAIL**

Cell Line	MM	AML	DLBCL
Response to TRAIL	1 resistant 2 sensitive	2 resistant 3 sensitive	2 resistant 3 sensitive
Synergism	2/3	4/5	1/5

Synergism was not observed with all cell lines tested. MLN4924 alone could induce apoptosis in almost all of the cell lines tested. Two DLBCL cell lines were entirely resistant to MLN4924 treatment. A recent publication has shown that mutations can exist in the NEDD8 activating enzyme in leukemic cells. These mutations increase the enzymes affinity for ATP whilst decreasing its affinity for MLN4924 (Schimmer et al, 2014; Smith et al, 2012). Given that MLN4924 is an inhibitor of this NEDD8 activating enzyme it is possible that this resistance occurs as a result of these mutations.

Our data from these *in vitro* studies was most promising for AML cell lines, OCI-AML2 in particular. For this reason *in vivo* studies were carried out in collaboration with Millenium Pharmaceuticals. The initial animal study was done on AML (OCI M2) xenografts engrafted into SCID mice. The data from this study shows that MLN4924 can reduce the growth of the tumour when compared to vehicle and TRAIL alone. Tumours treated with vehicle or TRAIL alone grew from 150mm^3 to approximately

700mm^3 while those treated with MLN4924 grew to at most 200mm$^{3.}$ This observation is true for both does of MLN4924 used (45mg/kg and 90mg/kg). The combination of MLN4924 and TRAIL also impacts on the growth of the tumour but in addition the size of the tumour was reduced to a size smaller than it was prior to treatments (<150 mm^3). The length of this study was 21 days. The final treatment of MLN4924 and TRAIL was on day 18 and 19, respectively. This could explain why we observe some growth of the tumours which had been treated with MLN4924 +/- TRAIL on day 21.

It was considered that the optimal dosing strategy may not have been in place for this study so for this reason it was followed up with a pharmacokinetic and a pharmacodynamics study on OCI M2 xenografts. Samples from this study were analysed through ELISA for MLN4924 and TRAIL levels and western blot analysis for NEDD8, cleaved caspase 3 and PARP expression levels. The resulting data showed that MLN4924 was depleted by more than 100-fold by 24 h and was barely detectable by 48 h. Similarly western blots for cleaved caspase-3, PARP and NEDD8 showed that MLN4924 was no longer functional between 24 and 48 h. Given that in the initial study MLN4924 was given on day 1 and 4 of each week for a 3 week period it is highly possible that a more frequent dosing of MLN4924 would lead to a much greater effect on AML xenografts. Whilst this data is very promising another *in vivo* study would need to be carried out to know if an alternative dosing schedule would be advantageous.

The response of haematological malignancies to TRAIL-induced apoptosis is varied, as is the case with many other cancers. Many AML cell lines are resistant to apoptosis but in our model MLN4924 could sensitise otherwise resistant cells to TRAIL-induced apoptosis. Key components of the TRAIL apoptotic pathway can lend to TRAIL resistance. These include the death receptors, the IAPs, cFlip and Bcl-2 family members. Modulations of levels of these proteins have all previously been reported to sensitise cancer cells to TRAIL-induced apoptosis.

The death receptors, namely, DR4, DR5, DcR1 and DcR2 are TRAIL receptors that can initiate (DR4 and DR5) or inhibit apoptosis (DcR1 and DcR2). In our study we showed that MLN4924 had no effect on the death receptors in OCI-AML2 cells. These cells do have higher levels of the DR5 receptor so it quite possible that when apoptosis occurs it is through this receptor.

In addition to the TRAIL receptors, cFlip, the IAPs and Bcl-2 family members are also involved in regulation of TRAIL-induced apoptosis. In this study we also determined the effect of MLN4924 on these proteins. The most notable result was increased expression of the pro-apoptotic protein Noxa. It has been reported in the literature that siRNA mediated knockdown of Noxa decreased sensitivity to MLN4924 in chronic lymphocytic leukaemia cells (Danilov et al, 2014). Our findings indicate a similar result in OCI-AML2 cells however we have also shown that shRNA silencing of Noxa had no impact on the synergestic effect observed between MLN4924 and TRAIL.

Our most notable finding in studying the mechanism of synergism between MLN4924 and TRAIL was that MLN4924 can increase expression levels of the transcription factors p53 and c/EBPα.

p53 and its downstream target p21 have both been linked to MLN4924 in the literature. MLN4924 has been shown to have an anti-proliferative effect in a manner dependent on p21 and p53 (Dutta et al, 2010). The expression levels of p53 and its downstream target p21 are both increased upon MLN4924 treatment in our model.

Nutlin3 is an activator of p53 which functions by breaking up the interaction between p53 and its E3 ligase Mdm2. In our model Nutlin3 increases the expression level of p53 and p21. Nutlin3 also sensitises OCI-AML2 cells to TRAIL-induced apoptosis in a manner similar to that seen with MLN4924 and TRAIL. This suggests that p53 has a possible role to play in the mechanism through which MLN4924 can sensitise to TRAIL-induced apoptosis. To make this more conclusive we would need to examine how inhibiting p53 would affect this synergism. Commercially available inhibitors include pifithrin mu and pifithrin alpha. Neither of these could inhibit p53 in our model.

p53 has previously been associated with c/EBPα, a transcription factor commonly associated with AML. c/EBPα plays an important role in myeloid differentiation. Diminished C/EBPα activity is widely known to contribute to the transformation of myeloid progenitors via reduction of their differentiation potential (Tien et al, 2005). c/EBPα was linked with p53 in a study that examined the effect of UVB-induced DNA damage on keratinocytes. DNA damage resulted in induction of both p53 and c/EBPα but in p53 -/- cells or in cells where p53 was mutated there was also no induction in c/EBPα (Smart et al, 2004). Our study revealed that targeting c/EBPα with a short hairpin construct could reverse the synergism observed between MLN4924 and TRAIL (~30%) marking it as a prime player in the mechanism of synergism between the

combination of MLN4924 and TRAIL. We propose that MLN4924 breaks up the interaction between cullins and TRIB2 therefore TRIB2 is no longer able to inactivate c/EBPα, leading to an increase in its transcriptional activity with the end result being sensitisation to TRAIL-induced apoptosis (Figure 3.22).

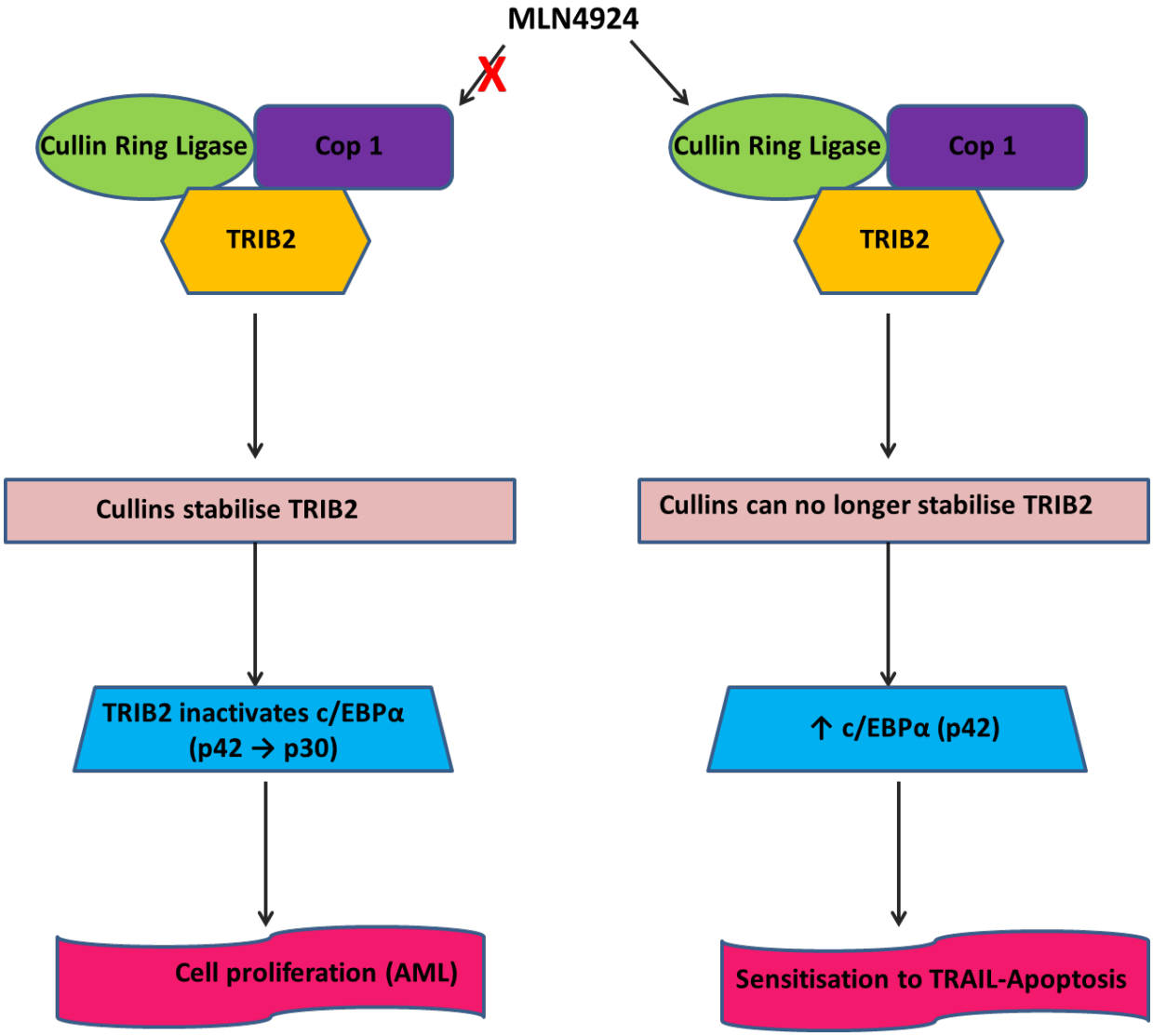

Figure 3.22 **Schematic of proposed mechanism through which MLN4924 sensitises to TRAIL-induced apoptosis in our model.**

Under normal circumstances the cullin proteins stabilise TRIB2 which leads to the inactivation of c/EBPα. This can be caused by the conversion of the full length transcriptionally active p42 isoform to the dominant negative p30 form. This affects the differentiation of myeloid cells leading to proliferation of AML blasts. The addition of MLN4924 disrupts the stabilisation between the cullins and TRIB2. TRIB2 is no longer able to inactivate c/EBPα therefore there is an upregulation of its transcriptionally active isoform, p42 which leads to TRAIL-induced apoptosis.

Silencing of c/EBPα also resulted in lack of induction of p53 or p21 following MLN4924 treatment. CDDO a known inducer of c/EBPα caused an induction in p53 and p21 levels and resulted in sensitising OCI-AML2 cells to TRAIL-induced apoptosis. This data suggests that c/EBPα regulates p53 which is contrary to what has already been published.

As c/EBPα has previously been associated with a feedback loop with E2F1 we were interested in knowing if something similar was occurring here (Keeshan et al, 2014). Nutlin3 which activates p53 causing an increase in its expression levels along with p21 also caused an induction in c/EBPα levels. Thus we suggest that p53 and c/EBPα can regulate each other in a feedback loop fashion.

The potential of MLN4924 and TRAIL was examined in *ex vivo* AML samples. MLN4924 can induce apoptosis to different extents in all primary AML samples tested. In 3 of the 6 samples tested synergism exists between MLN4924 and TRAIL. In two of these samples MLN4924 causes an upregulation in levels of c/EBPα while in the third sample c/EBPα cannot be detected. Levels of p53 either increase or decrease with MLN4924 treatment but there is no correlation between synergism and p53 or between changes in c/EBPα and p53.

Given that c/EBPα mutations occur in approximately 10% of patients diagnosed with AML may explain why we only detect synergism between MLN4924 and TRAIL in a subset of the samples tested. Two main types of mutations have been identified in c/EBPα. The first included mutations in the N-terminal region which causes translation of a 30 kDa protein that lacks transcriptional activity and has a dominant-negative effect over the full-length p42 protein The second includes mutations in the C terminal domain which disrupts binding to DNA (Gale et al, 2010). A minority of cases of AML without CEBPA mutations show silencing of the gene by promoter hypermethylation.

Whilst the potential of the combination of MLN4924 and TRAIL is promising a much larger patient sample set would be essential to determine its *ex vivo* efficacy and thus its potential in a clinical setting.

Chapter 4

Modular assembly of macrocyclic compounds with embedded saccharides & triazoles from readily available building blocks. Identification of inducers of apoptosis and a ligand for G-protein coupled receptor

4.1 Introduction

Adult acute myeloid leukemia *(*AML*)* is a type of *cancer* of the myeloid blood cells that is characterised by the rapid growth and accumulation of these cells in the bone marrow. It is the most common leukemia-affecting adults with its incidence increasing with age. Treatment options for AML have changed little over the past 20 years.

There is a requirement for new therapeutic targets for the treatment of AML and in collaboration with Prof.Murphy's group in NUI Galway we tested a number of compounds that contain macrocyclic rings. This group are part of a research programme aimed to prepare bioactive macrocyclic structures with potential use as biochemical probes or as medicinal agents. The synthesis of macrocyclic compounds within medicinal and biological chemistry is important given there are drugs with macrocyclic rings. Despite this, macrocyclic peptidomimetics are underrepresented in screening collections. An additional feature of macrocyclic compounds is that they have been considered as more like biomolecules than small molecules because they can have functional sub-domains (Driggers, Hale et al. 2008). Macrocycles have also been found to target a variety of protein receptors in peptide and natural product chemistry.

Prof. Murphy's group have been active in the preparation of, amongst other macrocycles, glycophanes and have been exploring their application as scaffolds. They have been used in glycomimetic research and provided interesting inhibitors of lectins. The glycophane scaffold can be considered somewhat analogous to macrocycles found in natural products such as cyclophanes or resin glycosides, the latter having embedded carbohydrates.

The compounds tested were based on a macrocycle with a triazole fused to a chiral saccharide, which was embedded in the macrocycle ring. This was called a glycotriazolophane. This approach led to the generation of a series of macrocyclic peptidomimetics. These products were then screened against AML cell lines and normal non-transformed cells. Their toxicity was analysed and lead to the identification of compounds that displayed toxicity to AML cells. The target of this compound was then further analysed and tested to better understand the molecular mechanism of the drug as well as to identify the therapeutic potential of the compound in AML.

4.2 Results

We obtained a number of compounds containing macrocyclic rings from our collaborators (Prof. Murphy's group) and investigated the biological properties on transformed and non-transformed cells to analyse their toxicity. The compounds with two saccharides & protected derivatives were found to be insoluble at concentrations above 1 µM and the biological effect of these compounds gave inconsistent results so these results will not be described here. Compounds with one saccharide and the acetonide derivatives of these compounds had improved solubility and thus were tested. Normal human fibroblasts and the leukemic cell line OCI-AML2 were treated with a dosage of the compounds.

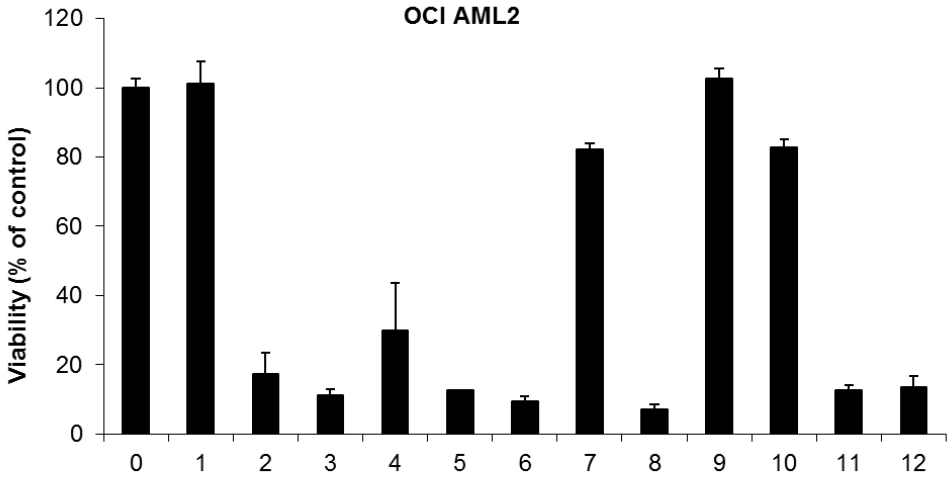

Figure 4.1 **The cytotoxic effects of macrocyclic compounds in leukemic cells**

OCI AML2 cells were treated for 24 h with a range of compounds (1-12) @ 200µM. 0 is representative of an untreated sample. This graph shows percentage viable cells after analysis by MTT.

The viability of the fibroblast cells was not affected on treatment, however, the viability of the OCI-AML2 sharply reduced upon exposure to the compounds. The most potent of these was macrocyclic compound **40** which contains the acetonide group. Figure 3.1 shows the effect of Compound **40** on fibroblasts and OCI-AML2 cells.

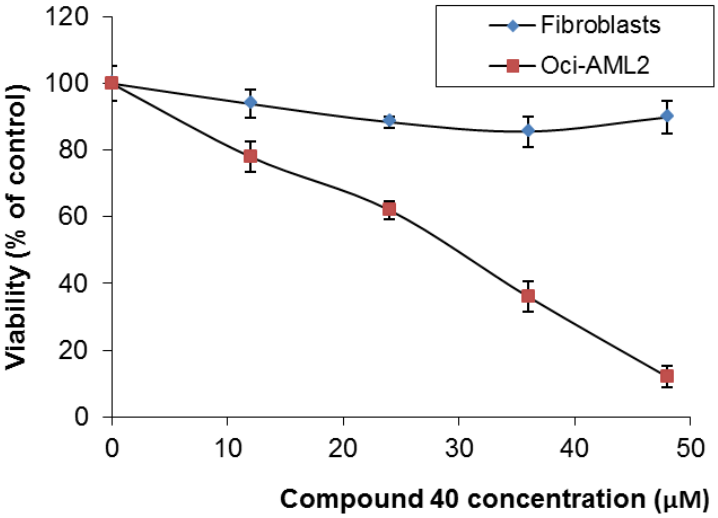

Figure 4.2 **Effect of compound 40 on normal, non-transformed human fibroblasts and OCI AML2 leukaemia cells.**

Cells were seeded in a 96 well plate and treated with the indicated doses of **40** for 24 h after which the viability of the cells (proportion of cells alive) was determined with the viability dye, MTT. The graph shows average viability expressed as percentage of the untreated control sample +/- standard deviation from 3 independent repeats.

In order to further explore the potential cytotoxic effect of compound **40** against leukemic cells, four different leukaemia cell lines were treated with a dosage of compound **40** and the toxicity was determined using MTT cell-viability assay. Compound **40** reduced the viability of all four leukemic cell types by 80-90% compared to the untreated control sample (Figure 4.3).

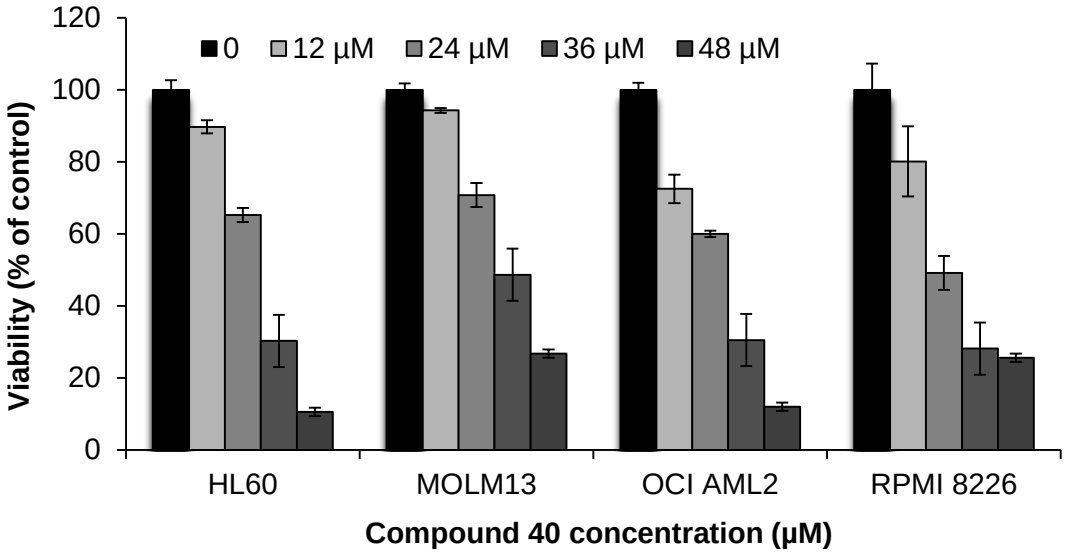

Figure 4.3 The effect of **compound 40 on haematological malignant cells.**

Four different haematological malignant cell lines (HL-60, Molm-13, OCI-AML2, RPMI 8226) were treated with 12, 24, 36 and 48µM of **40** for 24h after which cell viability was measured with MTT assay. The graph shows average percentage viability compared to the untreated control sample +/- standard deviation from 3 independent repeats.

The MTT assay shows that there is a reduction in viability of the cells, however, it cannot differentiate if this is a reduction is due to necrosis, apoptosis or inhibition of cell growth. To identify what mechanism caused the reduced viability, OCI-AML2 cells were treated with compound **40** and the cell morphology, using Hematoxylin and eosin stain was analysed **(Figure 4.4 A and B).** The externalisation of the membrane lipid phosphatidyl serine to the outer leaflet of the plasma membrane was monitored using Annexin V binding assay **(Figure 4.4 (C))**. Phoshatidyl serine exposure is a typical event in cells dying through apoptosis. We found that compound **40** induced a dose dependent increase in the number of cells exposing phosphatidyl serine on their cell surface. This was associated with the morphological characteristics that define apoptosis such as shrunken cell morphology with condensed, darkly stained nuclei as seen in **Figure 4.4 A and B.** This confirmed that the cause of reduced viability was induction of apoptotic cell death (Figure 4.4).

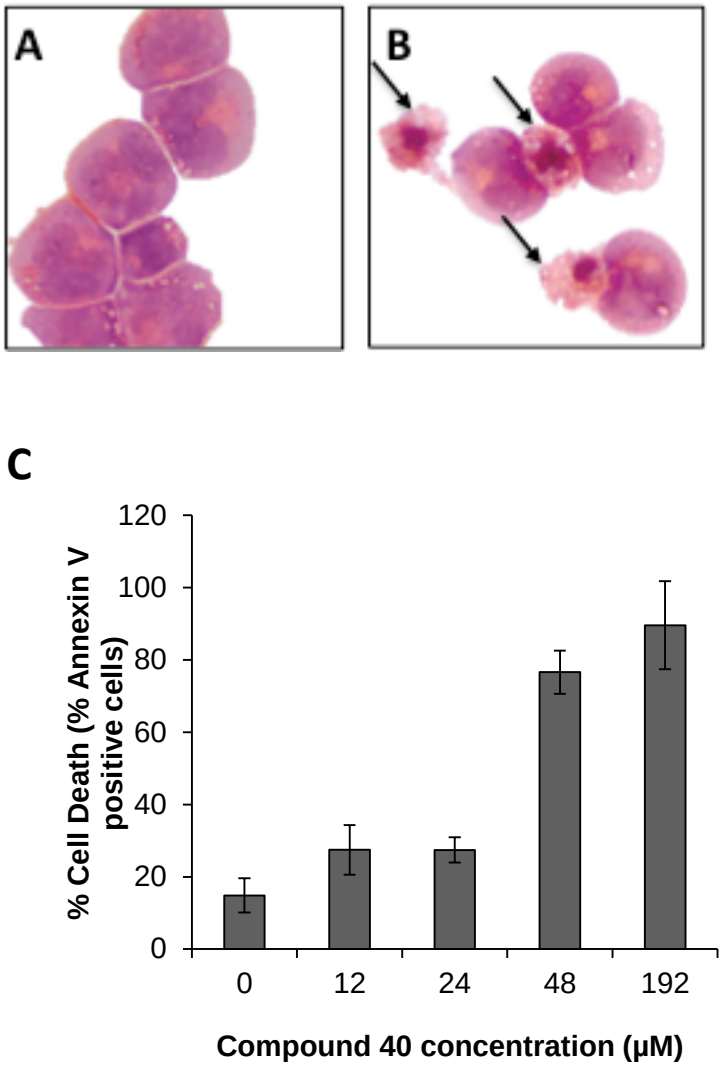

Figure 4.4 **Compound 40 induces apoptotic cell death in OCI-AML2 leukaemia cells. (A), (B)** OCI-AML2 cells were treated with 24 μM of **40** for 15 h after which the cells were collected on a microscope slide and their nucleus was stained purple with haematoxylin and their cytosol was stained pink with eosin. (A) control, untreated cells with homogeneously stained nuclei and a ring of pink-stained cytosol typical of live leukemic cells and (B) cells treated with **40** where some cells show shrunken and condensed (darkly stained) nuclei typical of apoptotic cells. **(C)** OCI AML2 cells were treated with the indicated doses of **40** for 24 h. Induction of apoptotic cell death was measured by detecting exposure of phosphatidyl serine in the outer layer of the plasma membrane of apoptotic cells using Annexin V staining

While these compounds showed interesting effects on the leukemic cell lines, the mechanism by which they could be exerting their effects was unclear. It is possible that compound **40** was acting as a peptide mimetic and thus, the ability of glycotriazolophanes to bind to peptide-binding receptors was considered. A general screening of **40** was thus carried out against 55 such receptors by our collaborators (Prof. Murphy's group). The majority of the receptors were G-protein coupled

receptors and other receptors such as GABA, Ion Channels (Ca^{2+} & Na^{+}) and transporters (dopamine, norepenephrine & serotonin (5-HT)) were also included. At 10 μM Compound **40** inhibited >90% of the serotonin receptors (5-HT1A and 5-HT2A), the neurokinin receptor (NK-2), two ion channels (Ca2+ and Na+) and opiod receptor type μ, binding affinity. Lower binding affinity was observed (80-90%) for two other serotonin receptors (5-HT2B & 5-HT5A), the adrenergic A3 receptor and opiod receptor ð2. Several of the targets of this molecule are serotonin receptors (5-HT1A, 5-HT2A, 5-HT2B and 5-HT5A). The serotonin transporter was found to be an additional target.

Table 4.1 **Inhibition by 40 of the binding of radioligand to proteins**

Protein	**% Inhibition (standard deviation)**
Na^+ channel (site 2)	103 (2)
NK2 (h)	99 (2)
□(MOP) (h)	96 (2)
5-HT2A (h)	93 (2)
Ca^{2+} channel (L, verapamil site)	91 (2)
5-HT1A (h)	90 (2)
5-HT5a (h)	89 (0)
A3 (h)	87 (5)
□2(DOP) (h)	83 (2)
5-HT2B (h)	82 (3)
k (KOP)	78 (7)
5-HT transporter (h)	68 (3)
dopamine transporter (h)	64 (4)
Cl^- channel (GABA-gated)	62 (1)
CCK1 (CCKA) (h)	61 (2)
H1 (h)	60 (3)
D2S (h)	60 (2)
a1 (non-selective)	58 (9)
norepinephrine transporter (h)	56 (1)

Inhibition of serotonin signalling has previously been associated wwith inducing apoptosis in leukemic cells (Serafeim, Holder et al. 2003). A major target for serotonin in leukemic cells is the 5-HT1A receptor (Abdouh, Storring et al. 2001). A broad spectrum of primary leukemic cells has also been shown to express the serotonin transporter and show growth arrest when exposed to serotonin transporter ligand.

In order to examine the potential of targeting serotonin receptors OCI-AML2 cells were treated with a series of serotonin receptor agonists and antagonists for 24h after which cell death was monitored. Compromised mitochondria is a feature of cell death thus on completion of the treatments cells were harvested and tetramethylrhodamine ethyl ester (TMRE) was used to detect active mitochondria. TMRE is a cell permeant, positively-charged, red-orange dye that readily accumulates in active mitochondria due to their relative negative charge. Depolarized or inactive mitochondria have decreased membrane potential and fail to sequester TMRE. Results were analysed with flow cytometry.

We found that 8-hydroxy-dpat (8-OH-DPAT) which is primarily an agonist for the 5-HT1A receptor did not induce apoptosis in OCI-AML2 cells. Cyproheptadine, Ketanserin and Ritanserin are all antagonists of serotonin receptors. Cyproheptadine for 5-HT2A, Ketanserin for 5-HT2A and 5-HT2C, and Ritanserin is an antagonist for the 5-HT2A receptor mainly. Cyproheptadine and Ritanserin can both induce apoptosis whilst OCI-AML2 cells are resistant to Ketanserin **(Figure 4.5).** This could be explained by the fact that all of these drugs have targets in addition to the serotonin receptors.

Imipramine and Citalopram are two drugs which both target the serotonin transporter (SERT). Both of these are capable of inducing apoptosis in OCI AML2 cells **(Figure 4.5)**. Table 4.1 also shows that Compound 40 can inhibit the serotonin transporter by 68%.

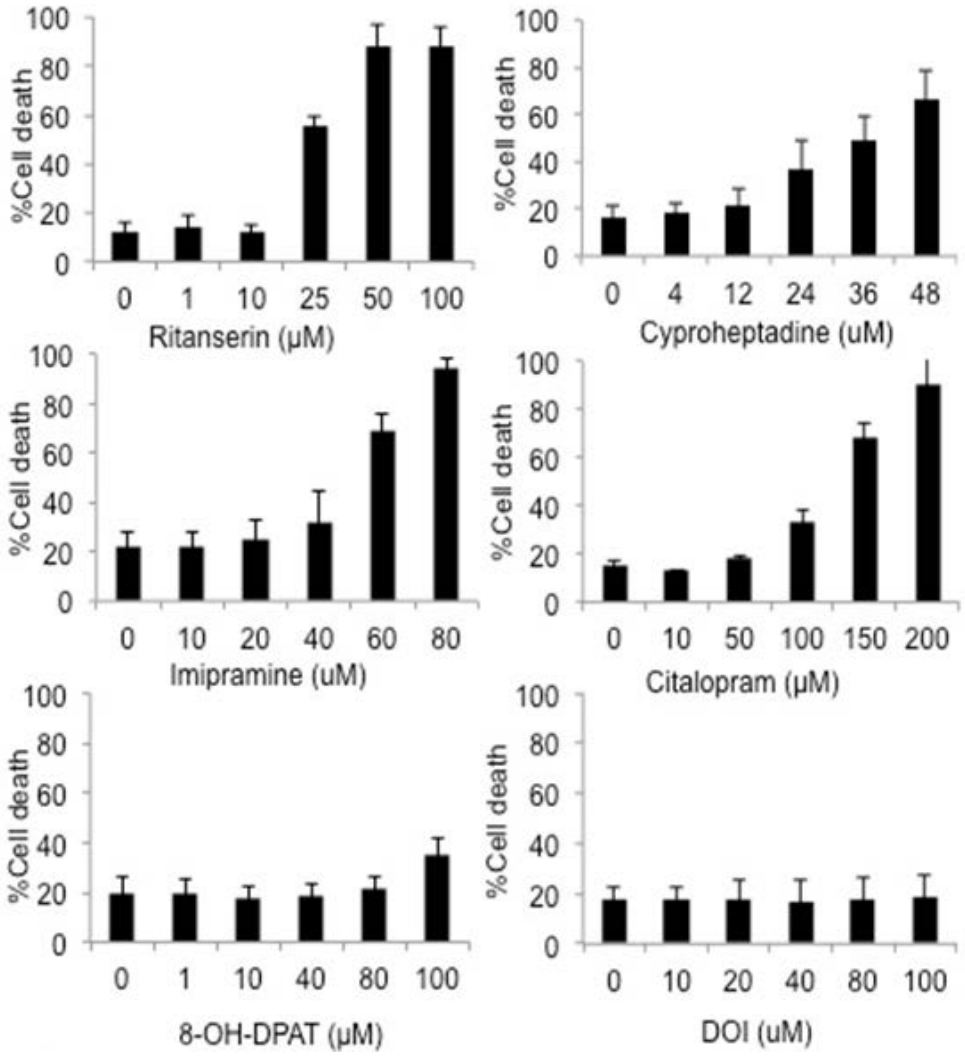

Figure 4.5 **Serotonin receptor agonists/antagonists and their apoptotic effect in OCI-AML2 cells in a dose dependent manner.**

OCI AML2 cells were treated with a number of agonists and antagonists of the serotonin receptors. These include 8-OH-DPAT, Cyproheptadine, Ketanserin, Ritanserin, Imipramine and Citalopram. Cells were seeded at 300,000/ml and treated for 24h. Cells were then harvested and cell death was analysed using TMRE and flow cytometry. These graphs show percentage cell death and are representative of 3 independent repeats +/- standard deviation.

4.3 Discussion

We have established that compound 40 can induce apoptosis in a number of leukemic cells but not in normal cells. This highlights the need for learning more about this drug and the mechanism through which it can induce apoptosis. In an attempt to understand this mechanism a binding study of compound 40 against 55 different receptors was carried out. Such receptors included primarily G-protein coupled receptors. Also included were receptors for gamma-aminobutyric (GABA), ion channels (L-type Ca^{2+} & Na^{+}) and transporters for serotonin, dopamine and norepinephrine. The top five hits from this study included the sodium channel, neurokinin receptor (NK) 2, an opioid receptor (MOP), the serotonin receptor, 5-HT2A and the calcium channel. These were defined as hits, as they inhibited binding of the cognate ligand by greater then 90%.

All of these hits have previously been linked to cancer and some to leukaemia. The neurokinin receptor-2 has been linked to breast cancer proliferation (Munoz et al, 2010). Blocking of the sodium channel has been linked to reducing the invasiveness of both breast and prostate cancer (Djamgoz et al, 2014). Calcium channels have also been linked to cancer cells. Calcium channels are classified into six subtypes based on the channel characteristics and their sensitivity to certain drugs: L, N, P, Q, R, and T types. While L-type Ca^{2+} channels are predominantly found in the brain and in skeletal- and cardiac muscle studies have also shown the existence of L-type Ca^{2+} channels in a variety of hematopoietic cells such as B cells. The L-type Ca^{2+} channels are involved in the growth and proliferation of these white blood cells (Thwaite et al, 2001). Expression of a subtype of L-type calcium channels has also been found in colon cancer cells where its increased expression correlates with increased number of colon cells differentiating into colon cancer cells (Guggino et al, 2000). An agonist for the opioid receptor, methadone has been identified as an inducer of apoptosis in the leukemic cell line HL-60 (Miltner et al, 2008). Whilst all of these hits may have a role to play in the mechanism through which compound 40 can induce apoptosis we focused on the role the serotonin receptors and its transporter had in compound 40 induced cell death due to the multiple hits the serotonin receptors received during the screen.

Serotonin (5-HT) receptors have the ability to impose a broad range of actions due to the wide range of serotonin receptors. There are seven families of 5-HT receptor

subtypes, 5-HT1 - 5-HT7. Each of these families have a number of subtypes, which are all members of the G-protein coupled receptor superfamily with the exception of 5-HT3 (Martin et al, 2001). Serotonin receptors control a number of signal transduction pathways that are known contribute to tumour cell survival and growth, such as Akt, STAT3 and ERK. The 5-HT2A receptor is included in the top five hits in the list of proteins inhibited by compound 40 (Table 4.1). In addition 5-HT1A, 5-HT5A and 5-HT2B rank in the top 10 hits. The serotonin transporter although further down the list can be inhibited by 68% by compound 40. Serotonin has been shown to induce calcium signalling through the 5-HT1A receptor in the AML cell line, K562 (Deschaux et al, 1995). This may explain the presence of calcium channels in the list of proteins inhibited by compound 40. Selective serotonin reuptake inhibitors (SSRIs) have illustrated that they can induce apoptosis in Burkitt Lymphoma cells (Gordon et al, 2003). SSRIs have also recently been highlighted as having a potential role in antimyeloma therapy (Rivero et al, 2013). Thus the serotonin receptors highlight a pathway not previously investigated in the context of AML.

Through treating the AML cell line OCI-AML2 with a series of compounds targeting various serotonin receptors and the serotonin transporter we further highlighted the potential of serotonin as a novel target in AML. Table 4.2 shows compounds used and their serotonin-related targets and a summary of the results.

Table 4.2 **Compounds and their serotonin-related targets**

	Agonist/Antagonist	**Primary Serotonin Targets**	**Secondary Serotonin Targets**
8-OH-DPAT	agonist	1A	5-HT7
Cyproheptadine	antagonist	2A	2C
Ketanserin	antagonist	5-HT2 receptors - 2A	2C
Ritanserin	antagonist	5-HT2 receptors(2A)	2C
Imipramine		SERT	2A
Citalopram		SERT	

8-hydroxy-DPAT which is an agonist for the 5-HT1A receptor fails to cause cell death in OCI AML2 cells which we would expect if inhibition of the serotonin receptors/transporter is the mechanism through which these cells can die. Antagonists for serotonin receptors used in this study included Cyproheptadine, Ketanserin and Ritanserin. While Cyproheptadine and Ritanserin induce apoptosis in OCI AML2 cells Ketanserin does not. This could be related to the fact that when used at doses above 500nM Ketanserin can affect at least eight different GPCRs from four different families. These include histamine and dopamine receptors. Both Cyproheptadine and Ritanserin are more selective for serotonin receptors. Imipramine and Citalopram can both inhibit the serotonin transporter and also induce apoptosis in OCI AML2 cells.

The outcome for patients with AML is not promising and the treatment regimen for AML has changed little over the last 30 years. There is constantly a need for novel therapeutic targets. This series of experiments, point towards the serotonin receptors

and the serotonin transporter as an important mediator in AML cells survival and at a possible mechanism through which compound 40 may be exerting its transformed cell specific apoptotic effect.

Chapter 5

Conclusions and Future Perspectives

The outcome for patients diagnosed with a haematological malignancy is not optimistic at present. However the recent and rapid development in molecularly targeted therapies has led to a vast improvement in the management of haematological diseases. For example for AML many FLT3 and histone deacetylase inhibitors are now in clinical trials.

In our study we have shown that the NEDDylation inhibitor MLN4924 can induce apoptosis in a number of haematological malignant cell lines. That is, MLN4924 as a single agent can induce apoptosis in these cell lines. MLN4924 is already in clinical trials. Most importantly our study revealed that MLN4924 and TRAIL can in combination induce apoptosis in a synergestic manner. We observed this in particular in AML cell lines but also in MM and DLBCL cell lines. TRAIL has the benefit of being cytotoxic to cancer cells whilst sparing normal healthy cells. However many cancer cells remain resistant to TRAIL-induced apoptosis. In this study we show that MLN4924 can sensitise cells to TRAIL-induced apoptosis. One publication to date has shown that MLN4924 in combination with TRAIL has a synergestic effect in head and neck cancer cells. In our study we additionally observe synergism in AML xenografts treated with MLN4924 and TRAIL. This data is extremely promising and initial studies on primary AML samples have begun. To date six samples have been analysed and it is too small a study to be able to draw conclusions positive or otherwise.

In identifying the mechanism through which synergism between MLN4924 and TRAIL occurs we made the novel discovery that MLN4924 can induce expression levels of the transcription factor c/EBPα. In this manner MLN4924 can sensitise to TRAIL-induced apoptosis. p53 was identified as a possible player in this synerestic effect. It is possible that p53 has a partial effect on the synergism between MLN4923. A functional inhibitor of p53 would be necessary to make this observation conclusive. During this study we also showed that a feedback loop exists between c/EBPα and p53. The induction of p53 also results in the induction of c/EBPα and vice versa.

The future of this study would look at the apoptotic effect of the combination of MLN4924 and TRAIL in a much larger data set of AML patient samples. This would determine if the combination had potential to enter clinical trials.

This thesis also looked at the apoptotic effect of a novel compound on AML cell lines. This compound referred to as compound 40 at present has the ability to induce apoptosis in AML cell lines and had no effect on normal human fibroblasts. We have identified through testing of a series of serotonin receptor agonists and antagonists that this compound may be inducing apoptosis through the serotonin pathway. This would represent a novel mechanism for inducing apoptosis in AML cells. There is increasing interest surrounding leukemic stem cells and targeting them is thought to be the key to improved patient response and relapse rates. It would be interesting to observe if this compound would have an impact on primary cells and in addition on the leukemic stem cell population.

Overall these two novel treatment strategies have resulted in the presentation of data that is optimistic for the future of haematological malignancies, in particular AML.

Chapter 6

Bibliography

Abdouh, M., J. M. Storring, et al. (2001). "Transcriptional mechanisms for induction of 5-HT1A receptor mRNA and protein in activated B and T lymphocytes." J Biol Chem **276**(6): 4382-4388.

Alizadeh, A. A., M. B. Eisen, et al. (2000). "Distinct types of diffuse large B-cell lymphoma identified by gene expression profiling." Nature **403**(6769): 503-511.

Azijli, K., B. Weyhenmeyer, et al. (2013). "Non-canonical kinase signaling by the death ligand TRAIL in cancer cells: discord in the death receptor family." Cell Death Differ **20**(7): 858-868.

Bekes, M. and G. S. Salvesen (2009). "The CULt of caspase-8 ubiquitination." Cell **137**(4): 604-606.

Berko, D., S. Tabachnick-Cherny, et al. (2012). "The direction of protein entry into the proteasome determines the variety of products and depends on the force needed to unfold its two termini." Mol Cell **48**(4): 601-611.

Billard, C. (2013). "BH3 mimetics: status of the field and new developments." Mol Cancer Ther **12**(9): 1691-1700.

Blank, J. L., X. J. Liu, et al. (2013). "Novel DNA damage checkpoints mediating cell death induced by the NEDD8-activating enzyme inhibitor MLN4923." Cancer Res **73**(1): 225-233.

Borner, C. (2003). "The Bcl-2 protein family: sensors and checkpoints for life-or-death decisions." Mol Immunol **39**(11): 615-647.

Brinkmann, K. and H. Kashkar (2014). "Targeting the mitochondrial apoptotic pathway: a preferred approach in hematologic malignancies?" Cell Death Dis **5**: e1098.

Brooks, C. L. and W. Gu (2004). "Dynamics in the p53-Mdm2 ubiquitination pathway." Cell Cycle **3**(7): 895-893.

Burnett, A., M. Wetzler, et al. (2011). "Therapeutic advances in acute myeloid leukemia." J Clin Oncol **29**(5): 487-493.

Cavaletti, G. and A. J. Jakubowiak (2010). "Peripheral neuropathy during bortezomib treatment of multiple myeloma: a review of recent studies." Leuk Lymphoma **51**(7): 1178-1187.

Chinnadurai, G., S. Vijayalingam, et al. (2008). "BIK, the founding member of the BH3-only family proteins: mechanisms of cell death and role in cancer and pathogenic processes." Oncogene **27 Suppl 1**: S20-23.

Chou, T. C. (2010). "Drug combination studies and their synergy quantification using the Chou-Talalay method." Cancer Res **70**(2): 440-446.

Ciechanover, A. (2006). "The ubiquitin proteolytic system: from an idea to the patient bed." Proc Am Thorac Soc **3**(1): 21-31.

Conway O'Brien, E., S. Prideaux, et al. (2014). "The epigenetic landscape of acute myeloid leukemia." Adv Hematol **2014**: 103175.

Crawford, L. J., E. T. Chan, et al. (2014). "Synergistic effects of proteasome inhibitor carfilzomib in combination with tyrosine kinase inhibitors in imatinib-sensitive and -resistant chronic myeloid leukemia models." Oncogenesis **3**: e90.

Crawford, L. J. and A. E. Irvine (2013). "Targeting the ubiquitin proteasome system in haematological malignancies." Blood Rev **27**(6): 297-303.

Cultrera, J. L. and S. M. Dalia (2012). "Diffuse large B-cell lymphoma: current strategies and future directions." Cancer Control **19**(3): 204-213

de Almagro, M. C. and D. Vucic (2012). "The inhibitor of apoptosis (IAP) proteins are critical regulators of signaling pathways and targets for anti-cancer therapy." Exp Oncol **34**(3): 200-211.

de Bie, P. and A. Ciechanover (2011). "Ubiquitination of E3 ligases: self-regulation of the ubiquitin system via proteolytic and non-proteolytic mechanisms." Cell Death Differ **18**(9): 1393-1402.

de la Puente, P., B. Muz, et al. (2014). "Molecularly targeted therapies in multiple myeloma." Leuk Res Treatment **2014**: 976567.

de Wilt, L. H., J. Kroon, et al. (2013). "Bortezomib and TRAIL: a perfect match for apoptotic elimination of tumour cells?" Crit Rev Oncol Hematol **85**(3): 363-372.

Dickens, L. S., I. R. Powley, et al. (2012). "The 'complexities' of life and death: death receptor signalling platforms." Exp Cell Res **318**(11): 1269-1277.

Dikic, I., S. Wakatsuki, et al. (2009). "Ubiquitin-binding domains - from structures to functions." Nat Rev Mol Cell Biol **10**(10): 659-671.

Dikic, I. and M. Robertson (2012). "Ubiquitin ligases and beyond." BMC Biol **10**: 22.

Dimopoulos, M. A. and E. Terpos (2010). "Multiple myeloma." Ann Oncol **21 Suppl 7**: vii143-150.

Driggers, E. M., S. P. Hale, et al. (2008). "The exploration of macrocycles for drug discovery--an underexploited structural class." Nat Rev Drug Discov **7**(7): 608-623.

Falschlehner, C., C. H. Emmerich, et al. (2007). "TRAIL signalling: decisions between life and death." Int J Biochem Cell Biol **39**(7-8): 1462-1475.

Field-Smith, A., G. J. Morgan, et al. (2006). "Bortezomib (Velcadetrade mark) in the Treatment of Multiple Myeloma." Ther Clin Risk Manag **2**(3): 271-273.

Finlay, D., M. Vamos, et al. (2014). "Small-molecule IAP antagonists sensitize cancer cells to TRAIL-induced apoptosis: roles of XIAP and cIAPs." Mol Cancer Ther **13**(1): 5-15.

Friesen, C., M. Roscher, et al. (2008). "Methadone, commonly used as maintenance medication for outpatient treatment of opioid dependence, kills leukemia cells and overcomes chemoresistance." Cancer Res **68**(15): 6059-6063.

Fulda, S. (2009). "Inhibitor of apoptosis proteins in hematological malignancies." Leukemia **23**(3): 467-476.

Fulda, S. and D. Vucic (2012). "Targeting IAP proteins for therapeutic intervention in cancer." Nat Rev Drug Discov **11**(2): 109-123.

Gallastegui, N. and M. Groll (2010). "The 26S proteasome: assembly and function of a destructive machine." Trends Biochem Sci **35**(11): 634-642.

Gilmore, T. D. (2006). "Introduction to NF-kappaB: players, pathways, perspectives." Oncogene **25**(51): 6680-6683.

Godbersen, J. C., L. A. Humphries, et al. (2014). "The Nedd8-activating enzyme inhibitor MLN4924 thwarts microenvironment-driven NF-kappaB activation and induces apoptosis in chronic lymphocytic leukemia B cells." Clin Cancer Res **20**(6): 1576-1583.

Gomez-Bougie, P., E. Menoret, et al. (2011). "Noxa controls Mule-dependent Mcl-1 ubiquitination through the regulation of the Mcl-1/USP9X interaction." Biochem Biophys Res Commun **413**(3): 460-463.

Gonzalvez, F., D. Lawrence, et al. (2012). "TRAF2 Sets a threshold for extrinsic apoptosis by tagging caspase-8 with a ubiquitin shutoff timer." Mol Cell **48**(6): 888-893.

Gounaris-Shannon, S. and T. Chevassut (2013). "The Role of miRNA in Haematological Malignancy." Bone Marrow Res **2013**: 269107.

Green, C. L., K. K. Koo, et al. (2010). "Prognostic significance of CEBPA mutations in a large cohort of younger adult patients with acute myeloid leukemia: impact of double CEBPA mutations and the interaction with FLT3 and NPM1 mutations." J Clin Oncol **28**(16): 2739-2747.

Hardwick, J. M. and R. J. Youle (2009). "SnapShot: BCL-2 proteins." Cell **138**(2): 404, 404 e401.

Hellwig, C. T. and M. Rehm (2012). "TRAIL signaling and synergy mechanisms used in TRAIL-based combination therapies." Mol Cancer Ther **11**(1): 3-13.

Hoogwater, F. J., M. W. Nijkamp, et al. (2010). "Oncogenic K-Ras turns death receptors into metastasis-promoting receptors in human and mouse colorectal cancer cells." Gastroenterology **138**(7): 2357-2367.

Hochstrasser, M. (1996). "Ubiquitin-dependent protein degradation." Annu Rev Genet **30**: 405-433.

Roe, J. S. and C. R. Vakoc (2014). "C/EBPalpha: critical at the origin of leukemic transformation." J Exp Med **211**(1): 1-3.

Herrmann, J., L. O. Lerman, et al. (2007). "Ubiquitin and ubiquitin-like proteins in protein regulation." Circ Res **100**(9): 1276-1291.

Hoeller, D. and I. Dikic (2009). "Targeting the ubiquitin system in cancer therapy." Nature **458**(7237): 438-443.

Hung, A. S., T. Y. Tsui, et al. (2011). "Serotonin and its receptors in the human CNS with new findings - a mini review." Curr Med Chem **18**(34): 5281-5288.

Husnjak, K. and I. Dikic (2012). "Ubiquitin-binding proteins: decoders of ubiquitin-mediated cellular functions." Annu Rev Biochem **81**: 291-322.

Ishimura, N., H. Isomoto, et al. (2006). "Trail induces cell migration and invasion in apoptosis-resistant cholangiocarcinoma cells." Am J Physiol Gastrointest Liver Physiol **290**(1): G129-136.

Jia, L. and Y. Sun (2011). "SCF E3 ubiquitin ligases as anticancer targets." Curr Cancer Drug Targets **11**(3): 347-356.

Jin, Z., Y. Li, et al. (2009). "Cullin3-based polyubiquitination and p62-dependent aggregation of caspase-8 mediate extrinsic apoptosis signaling." Cell **137**(4): 721-735.

Johnstone, R. W., A. A. Ruefli, et al. (2002). "Apoptosis: a link between cancer genetics and chemotherapy." Cell **108**(2): 153-163.

Katsnelson, A. (2012). "Next-generation proteasome inhibitor approved in multiple myeloma." Nat Biotechnol **30**(11): 1011-1012.

Keeshan, K., Y. He, et al. (2006). "Tribbles homolog 2 inactivates C/EBPalpha and causes acute myelogenous leukemia." Cancer Cell **10**(5): 401-411.

Kelly, L. M. and D. G. Gilliland (2002). "Genetics of myeloid leukemias." Annu Rev Genomics Hum Genet **3**: 179-198.

Komander, D., M. J. Clague, et al. (2009). "Breaking the chains: structure and function of the deubiquitinases." Nat Rev Mol Cell Biol **10**(8): 550-563.

Kondo, M. (2010). "Lymphoid and myeloid lineage commitment in multipotent hematopoietic progenitors." Immunol Rev **238**(1): 37-46.

Koschmieder, S., F. D'Alo, et al. (2007). "CDDO induces granulocytic differentiation of myeloid leukemic blasts through translational up-regulation of p42 CCAAT enhancer binding protein alpha." Blood **110**(10): 3695-3705.

Krueger, A., S. Baumann, et al. (2001). "FLICE-inhibitory proteins: regulators of death receptor-mediated apoptosis." Mol Cell Biol **21**(24): 8247-8253.

Kuendgen, A. and U. Germing (2009). "Emerging treatment strategies for acute myeloid leukemia (AML) in the elderly." Cancer Treat Rev **35**(2): 97-120.

Kumar, R., P. E. Herbert, et al. (2005). "An introduction to death receptors in apoptosis." Int J Surg **3**(4): 268-277.

Kumatori, A., K. Tanaka, et al. (1990). "Abnormally high expression of proteasomes in human leukemic cells." Proc Natl Acad Sci U S A **87**(18): 7071-7075.

Laiosa, C. V., M. Stadtfeld, et al. (2006). "Determinants of lymphoid-myeloid lineage diversification." Annu Rev Immunol **24**: 705-738.

Lecker, S. H., A. L. Goldberg, et al. (2006). "Protein degradation by the ubiquitin-proteasome pathway in normal and disease states." J Am Soc Nephrol **17**(7): 1807-1813.

Lemke, J., S. von Karstedt, et al. (2014). "Getting TRAIL back on track for cancer therapy." Cell Death Differ **21**(9): 1350-1363.

Li, M. and Z. G. Xiong (2011). "Ion channels as targets for cancer therapy." Int J Physiol Pathophysiol Pharmacol **3**(2): 156-166.

Lin, L. I., C. Y. Chen, et al. (2005). "Characterization of CEBPA mutations in acute myeloid leukemia: most patients with CEBPA mutations have biallelic mutations and show a distinct immunophenotype of the leukemic cells." Clin Cancer Res **11**(4): 1372-1373.

Lin, J. J., M. A. Milhollen, et al. (2010). "NEDD8-targeting drug MLN4924 elicits DNA rereplication by stabilizing Cdt1 in S phase, triggering checkpoint activation, apoptosis, and senescence in cancer cells." Cancer Res **70**(24): 10310-10320.

Lindqvist, L. M., M. Heinlein, et al. (2014). "Prosurvival Bcl-2 family members affect autophagy only indirectly, by inhibiting Bax and Bak." Proc Natl Acad Sci U S A **111**(23): 8512-8517.

Linkermann, A. and D. R. Green (2014). "Necroptosis." N Engl J Med **370**(5): 455-465.

Lohr, J. G., P. Stojanov, et al. (2014). "Widespread genetic heterogeneity in multiple myeloma: implications for targeted therapy." Cancer Cell **25**(1): 91-101.

Lokody, I. (2014). "Drug resistance: Overcoming resistance in acute myeloid leukaemia treatment." Nat Rev Cancer **14**(7): 452-453.

Lomonosova, E. and G. Chinnadurai (2008). "BH3-only proteins in apoptosis and beyond: an overview." Oncogene **27 Suppl 1**: S2-13.

Mahalingam, D., E. Szegezdi, et al. (2009). "TRAIL receptor signalling and modulation: Are we on the right TRAIL?" Cancer Treat Rev **35**(3): 280-288.

Manier, S., A. Sacco, et al. (2012). "Bone marrow microenvironment in multiple myeloma progression." J Biomed Biotechnol **2012**: 157496.

Martelli, M., A. J. Ferreri, et al. (2013). "Diffuse large B-cell lymphoma." Crit Rev Oncol Hematol **87**(2): 146-171.

Meister, S., U. Schubert, et al. (2007). "Extensive immunoglobulin production sensitizes myeloma cells for proteasome inhibition." Cancer Res **67**(4): 1783-1792.

Milhollen, M. A., M. P. Thomas, et al. (2012). "Treatment-emergent mutations in NAEbeta confer resistance to the NEDD8-activating enzyme inhibitor MLN4923." Cancer Cell **21**(3): 388-401.

Milhollen, M. A., T. Traore, et al. (2010). "MLN4924, a NEDD8-activating enzyme inhibitor, is active in diffuse large B-cell lymphoma models: rationale for treatment of NF-{kappa}B-dependent lymphoma." Blood **116**(9): 1515-1523.

Mitchell, M. J., E. Wayne, et al. (2014). "TRAIL-coated leukocytes that kill cancer cells in the circulation." Proc Natl Acad Sci U S A **111**(3): 930-935.

Mojsa, B., I. Lassot, et al. (2014). "Mcl-1 ubiquitination: unique regulation of an essential survival protein." Cells **3**(2): 418-437.

Mukhopadhyay, D. and H. Riezman (2007). "Proteasome-independent functions of ubiquitin in endocytosis and signaling." Science **315**(5809): 201-205.

Nahi, H., G. Selivanova, et al. (2008). "Mutated and non-mutated TP53 as targets in the treatment of leukaemia." Br J Haematol **141**(4): 445-453.

Nakajima, W., M. A. Hicks, et al. (2014). "Noxa determines localization and stability of MCL-1 and consequently ABT-737 sensitivity in small cell lung cancer." Cell Death Dis **5**: e1052.

Nakayama, K. I. and K. Nakayama (2005). "Regulation of the cell cycle by SCF-type ubiquitin ligases." Semin Cell Dev Biol **16**(3): 323-333.

Nalepa, G., M. Rolfe, et al. (2006). "Drug discovery in the ubiquitin-proteasome system." Nat Rev Drug Discov **5**(7): 596-613.

Nawrocki, S. T., P. Griffin, et al. (2012). "MLN4924: a novel first-in-class inhibitor of NEDD8-activating enzyme for cancer therapy." Expert Opin Investig Drugs **21**(10): 1563-1573.

Ola, M. S., M. Nawaz, et al. (2011). "Role of Bcl-2 family proteins and caspases in the regulation of apoptosis." Mol Cell Biochem **351**(1-2): 41-58.

Özören, N. and W. S. El-Deiry (2003). "Cell surface Death Receptor signaling in normal and cancer cells." Seminars in Cancer Biology **13**(2): 135-147.

Pabst, T., B. U. Mueller, et al. (2001). "Dominant-negative mutations of CEBPA, encoding CCAAT/enhancer binding protein-alpha (C/EBPalpha), in acute myeloid leukemia." Nat Genet **27**(3): 263-270.

Pai, V. P., A. M. Marshall, et al. (2009). "Altered serotonin physiology in human breast cancers favors paradoxical growth and cell survival." Breast Cancer Res **11**(6): R81.

Park, S., N. Chapuis, et al. (2010). "Role of the PI3K/AKT and mTOR signaling pathways in acute myeloid leukemia." Haematologica **95**(5): 819-828.

Pasqualucci, L. and R. Dalla-Favera (2014). "SnapShot: diffuse large B cell lymphoma." Cancer Cell **25**(1): 132-132 e131.

Peirce (2009). "The MDM2 antagonist nutlin-3 sensitizes p53-null neuroblastoma cells to doxorubicin via E2F1 and TAp73." International Journal of Oncology.

Peter, M. E. and P. H. Krammer (2003). "The CD95(APO-1/Fas) DISC and beyond." Cell Death Differ **10**(1): 26-35.

Petros, A. M., E. T. Olejniczak, et al. (2004). "Structural biology of the Bcl-2 family of proteins." Biochim Biophys Acta **1644**(2-3): 83-93.

Petroski, M. D. and R. J. Deshaies (2005). "Function and regulation of cullin-RING ubiquitin ligases." Nat Rev Mol Cell Biol **6**(1): 9-20.

Pierce, N. W., J. E. Lee, et al. (2013). "Cand1 promotes assembly of new SCF complexes through dynamic exchange of F box proteins." Cell **153**(1): 206-215.

Plantivaux, A., E. Szegezdi, et al. (2009). "Is there a role for nuclear factor kappaB in tumor necrosis factor-related apoptosis-inducing ligand resistance?" Ann N Y Acad Sci **1171**: 38-43.

Pulvino, M., Y. Liang, et al. (2012). "Inhibition of proliferation and survival of diffuse large B-cell lymphoma cells by a small-molecule inhibitor of the ubiquitin-conjugating enzyme Ubc13-Uev1A." Blood **120**(8): 1668-1677.

Rajkumar, S. V., A. Dispenzieri, et al. (2006). "Monoclonal gammopathy of undetermined significance, Waldenstrom macroglobulinemia, AL amyloidosis, and related plasma cell disorders: diagnosis and treatment." Mayo Clin Proc **81**(5): 693-703.

Read, M. A., J. E. Brownell, et al. (2000). "Nedd8 modification of cul-1 activates SCF(beta(TrCP))-dependent ubiquitination of IkappaBalpha." Mol Cell Biol **20**(7): 2326-2333.

Reed, J. C. (2008). "Bcl-2-family proteins and hematologic malignancies: history and future prospects." Blood **111**(7): 3322-3330.

Reed, J. C. and M. Pellecchia (2005). "Apoptosis-based therapies for hematologic malignancies." Blood **106**(2): 408-418.

Refaat, A., A. Abd-Rabou, et al. (2014). "TRAIL combinations: The new 'trail' for cancer therapy (Review)." Oncol Lett **7**(5): 1327-1332.

Riedl, S. J. and Y. Shi (2004). "Molecular mechanisms of caspase regulation during apoptosis." Nat Rev Mol Cell Biol **5**(11): 897-907.

Rishi, L., M. Hannon, et al. (2014). "Regulation of Trib2 by an E2F1-C/EBPalpha feedback loop in AML cell proliferation." Blood **123**(15): 2389-2400.

Roboz, G. J., U. Wissa, et al. (2012). "Are low-intensity induction strategies better for older patients with acute myeloid leukemia?" Leuk Res **36**(4): 407-412.

Rushworth, S. A., L. Zaitseva, et al. (2012). "The high Nrf2 expression in human acute myeloid leukemia is driven by NF-kappaB and underlies its chemo-resistance." Blood **120**(26): 5188-5198.

Sadowski, M. and B. Sarcevic (2010). "Mechanisms of mono- and poly-ubiquitination: Ubiquitination specificity depends on compatibility between the E2 catalytic core and amino acid residues proximal to the lysine." Cell Div **5**: 13.

Saha, M. N., L. Qiu, et al. (2013). "Targeting p53 by small molecules in hematological malignancies." J Hematol Oncol **6**: 23.

Saleem, M., M. I. Qadir, et al. (2013). "Inhibitors of apoptotic proteins: new targets for anticancer therapy." Chem Biol Drug Des **82**(3): 243-251.

Sarikas, A., T. Hartmann, et al. (2011). "The cullin protein family." Genome Biol **12**(4): 220.

Serafeim, A. (2002). "5-Hydroxytryptamine drives apoptosis in biopsylike Burkitt lymphoma cells: reversal by selective serotonin reuptake inhibitors." Blood **99**(7): 2545-2553.

Schneider, P. and J. Tschopp (2000). "Apoptosis induced by death receptors." Pharm Acta Helv **74**(2-3): 281-286.

Schuler, M. and D. R. Green (2001). "Mechanisms of p53-dependent apoptosis." Biochem Soc Trans **29**(Pt 6): 684-688.

Sessler, T., S. Healy, et al. (2013). "Structural determinants of DISC function: new insights into death receptor-mediated apoptosis signalling." Pharmacol Ther **140**(2): 186-193.

Sheikh, M. S., Y. Huang, et al. (1999). "The antiapoptotic decoy receptor TRID/TRAIL-R3 is a p53-regulated DNA damage-inducible gene that is overexpressed in primary tumors of the gastrointestinal tract." Oncogene **18**(28): 4153-4153.

Shen, M., S. Schmitt, et al. (2013). "Targeting the ubiquitin-proteasome system for cancer therapy." Expert Opin Ther Targets **17**(9): 1091-1108.

Shiozaki, E. N., J. Chai, et al. (2003). "Mechanism of XIAP-mediated inhibition of caspase-3." Mol Cell **11**(2): 519-527.

Soucy, T. A., L. R. Dick, et al. (2010). "The NEDD8 Conjugation Pathway and Its Relevance in Cancer Biology and Therapy." Genes Cancer **1**(7): 708-716.

Soucy, T. A., P. G. Smith, et al. (2009). "An inhibitor of NEDD8-activating enzyme as a new approach to treat cancer." Nature **458**(7239): 732-736.

Sprick, M. R. and H. Walczak (2004). "The interplay between the Bcl-2 family and death receptor-mediated apoptosis." Biochim Biophys Acta **1644**(2-3): 125-132.

Sprick, M. R., E. Rieser, et al. (2002). "Caspase-10 is recruited to and activated at the native TRAIL and CD95 death-inducing signalling complexes in a FADD-dependent manner but cannot functionally substitute caspase-8." EMBO J **21**(17): 4520-4530.

Steelman, L. S., S. C. Pohnert, et al. (2004). "JAK/STAT, Raf/MEK/ERK, PI3K/Akt and BCR-ABL in cell cycle progression and leukemogenesis." Leukemia **18**(2): 189-218.

Stintzing, S. and H. J. Lenz (2014). "Molecular pathways: turning proteasomal protein degradation into a unique treatment approach." Clin Cancer Res **20**(12): 3064-3070.

Sun, Y. (2003). "Targeting E3 ubiquitin ligases for cancer therapy." Cancer Biol Ther **2**(6): 623-623.

Suzuki, Y., T. Inoue, et al. (2010). "L-type Ca2+ channels: a new player in the regulation of Ca2+ signaling, cell activation and cell survival in immune cells." Mol Immunol **47**(4): 640-648.

Swords, R. T., K. R. Kelly, et al. (2010). "Inhibition of NEDD8-activating enzyme: a novel approach for the treatment of acute myeloid leukemia." Blood **115**(18): 3796-3800.

Taskesen, E., L. Bullinger, et al. (2011). "Prognostic impact, concurrent genetic mutations, and gene expression features of AML with CEBPA mutations in a cohort of 1182 cytogenetically normal AML patients: further evidence for CEBPA double mutant AML as a distinctive disease entity." Blood **117**(8): 2469-2475.

Testa, U. (2010). "TRAIL/TRAIL-R in hematologic malignancies." J Cell Biochem **110**(1): 21-33.

Thieblemont, C. and J. Briere (2013). "MYC, BCL2, BCL6 in DLBCL: impact for clinics in the future?" Blood **121**(12): 2165-2166.

van Wijk, S. J. and H. T. Timmers (2010). "The family of ubiquitin-conjugating enzymes (E2s): deciding between life and death of proteins." FASEB J **24**(4): 981-993.

Vanden Berghe, T., A. Linkermann, et al. (2014). "Regulated necrosis: the expanding network of non-apoptotic cell death pathways." Nat Rev Mol Cell Biol **15**(2): 135-147.

van Meerloo, J., G. J. Kaspers, et al. (2011). "Cell sensitivity assays: the MTT assay." Methods Mol Biol **731**: 237-245.

Walczak, H. and M. R. Sprick (2001). "Biochemistry and function of the DISC." Trends Biochem Sci **26**(7): 452-453.

Walczak, H., K. Iwai, et al. (2012). "Generation and physiological roles of linear ubiquitin chains." BMC Biol **10**: 23.

Walczak, H., R. E. Miller, et al. (1999). "Tumoricidal activity of tumor necrosis factor-related apoptosis-inducing ligand in vivo." Nat Med **5**(2): 157-163.

Wang, L., L. Gao, et al. (2013). "FISH+CD34+CD38- cells detected in newly diagnosed acute myeloid leukemia patients can predict the clinical outcome." J Hematol Oncol **6**(1): 85.

Wang, S. and W. S. El-Deiry (2003). "TRAIL and apoptosis induction by TNF-family death receptors." Oncogene **22**(53): 8628-8633.

Wang, J. and M. A. Maldonado (2006). "The ubiquitin-proteasome system and its role in inflammatory and autoimmune diseases." Cell Mol Immunol **3**(4): 255-261.

Wiley, S. R., K. Schooley, et al. (1995). "Identification and characterization of a new member of the TNF family that induces apoptosis." Immunity **3**(6): 673-682.

Wouters, B. J., B. Lowenberg, et al. (2009). "Double CEBPA mutations, but not single CEBPA mutations, define a subgroup of acute myeloid leukemia with a distinctive gene expression profile that is uniquely associated with a favorable outcome." Blood **113**(13): 3088-3091.

Wu, W., P. Liu, et al. (2012). "Necroptosis: an emerging form of programmed cell death." Crit Rev Oncol Hematol **82**(3): 249-258.

Xie, C. M., W. Wei, et al. (2013). "Role of SKP1-CUL1-F-box-protein (SCF) E3 ubiquitin ligases in skin cancer." J Genet Genomics **40**(3): 97-106.

Xu, G. W., M. Ali, et al. (2010). "The ubiquitin-activating enzyme E1 as a therapeutic target for the treatment of leukemia and multiple myeloma." Blood **115**(11): 2251-2253.

Yang, D., M. Tan, et al. (2012). "The p21-dependent radiosensitization of human breast cancer cells by MLN4924, an investigational inhibitor of NEDD8 activating enzyme." PLoS One **7**(3): e34073.

Yao, W. T., J. F. Wu, et al. (2014). "Suppression of tumor angiogenesis by targeting the protein neddylation pathway." Cell Death Dis **5**: e1053.

Youle, R. J. and A. Strasser (2008). "The BCL-2 protein family: opposing activities that mediate cell death." Nat Rev Mol Cell Biol **9**(1): 47-53.

Zhang, L. and B. Fang (2005). "Mechanisms of resistance to TRAIL-induced apoptosis in cancer." Cancer Gene Ther **12**(3): 228-237.

Zhao, L., P. Yue, et al. (2011). "The NEDD8-activating enzyme inhibitor, MLN4924, cooperates with TRAIL to augment apoptosis through facilitating c-FLIP degradation in head and neck cancer cells." Mol Cancer Ther **10**(12): 2415-2425.

Zhao, Y., X. Xiong, et al. (2012). "Targeting Cullin-RING ligases by MLN4924 induces autophagy via modulating the HIF1-REDD1-TSC1-mTORC1-DEPTOR axis." Cell Death Dis **3**: e386.

Zhao, Y. and Y. Sun (2013). "Cullin-RING Ligases as attractive anti-cancer targets." Curr Pharm Des **19**(18): 3215-3225.

Zhao, Z., J. Zuber, et al. (2010). "p53 loss promotes acute myeloid leukemia by enabling aberrant self-renewal." Genes Dev **24**(13): 1389-1402.

Zong, W. X., T. Lindsten, et al. (2001). "BH3-only proteins that bind pro-survival Bcl-2 family members fail to induce apoptosis in the absence of Bax and Bak." Genes Dev **15**(12): 1481-1486.